Synthetic, electrochemical and kinetic studies of phosphinites and their rhodium(I) complexes

A dissertation submitted in accordance with the requirements for the degree

Magister Scientiae

In the

Faculty of Natural and Agricultural Science

Department of Chemistry

At the

University of the Free State

By

Pholani Sakhile Manana

Supervisor

Dr. E. Erasmus

Acknowledgements

In the beginning was the Word and the Word was with GOD and the Word was GOD, it's by GOD and through GOD that I have come this far. And many more still remains.

To my supervisor and my academic mentor, who took her precious time and academic knowledge to introduce me to the vast world of academia, Dr E. Erasmus, I am greatly thankful and I can never repay your assistance. I hope to make you proud in my academic path. Also in the academic world I would like to appreciate Prof. J.C Swarts who was my first year lecturer and motivator towards pursuing further studies in chemistry, thank you very much. May you continue to explore gems for the academic world.

To the most beautiful, caring and loving Mother, Thulisile Manana, words can never cover your character and personality, GOD bless you. To my Daddy Mvuseleli Manana and my siblings, Lihle, Yenziwe and Mbuyisa thank you for the support.

To the best academic environment Physical Chemistry Group, you rock. Keep the friendships going, one can never feel out in the office or lab.

As for all the crazy people I call family the head-master Thobile; Mamusa, Khanya, Dika, Thembani, Ruswa, Majola, Lefa, Muano and the rest High five.

I am also grateful for the financial support I received from the National Research Fund for making it possible for me fulfil my academic responsibilities.

This is only the beginning….

Mcusi Manana

Table of contents

List of Abbreviations

A	absorbance
pK_a	acid dissociation constant
CH_3CN	acetonitrile
k_B	Boltzmann's constant
CO	carbon monoxide or carbonyl
M	central metal atom
CV	cyclic voltammetry
δ	chemical shift
$ClPPh_2$	Chlorodiphenylphosphine
Δ	delta
ΔS^*	entropy of activation
ΔH^*	enthalpy of activation
E°'	formal reduction potential
FcH	ferrocene
Fc	ferrocenyl
FTIR	Fourier Transformer Infra-red
χ_R	group electronegativity (Gordy scale)
LSV	linear sweep voltammetry
ε	molar extinction coefficient
Me	methyl
MeI	methyl Iodide
K_{obs}	observed rate constant
l	path length
E_{pa}	peak oxidation potential
E_{pc}	peak reduction potential
^1H	NMR Proton Nuclear Magnetic Resonance
^{31}P	NMR Phosphorus Nuclear Magnetic Resonance
h	Planck's constant
Ph	Phenyl
ppm	parts per million
k	rate

υ	stretching frequency/ scan rate
SWV	square wave voltammetry
ΔE_p	separation of anodic and cathodic peak potential
THF	tetrahydrofuran
$[N^nBu_4][PF_6]$	tetrabutylammonium hexafluorophosphate
T	temperature
t	time
UV/vis	ultraviolet-visible
λ	wavelength

1 Introduction and Aim

1.1 Introduction

Phosphorus has the ability to bind to many other elements, with various coordination numbers. Probably the most famous class of phosphorus compounds is the organophosphorus compounds. These are compounds where the phosphorus atom is bound to carbon, including compounds like phosphines (PR_3), phosphinites ($P(OR)R_2$), phosphonites ($P(OR)_2R$), phosphinates ($P{=}O(OR)R_2$) and many more.[1,2]

Organophosphorus compounds are normally used as ligands in coordination chemistry or homogeneous catalysis.[3,4,5] The most commonly used metals in catalysis are the platinum group metals. Organophosphorus-containing rhodium complexes in particular have been studied as homogeneous catalysts for hydroformylation, hydrogenation and carbonylation of methanol in the Monsanto process to liberate acetic acid.[6,7] The reaction mechanism of many catalytic processes including that of the well-known Monsanto process, this process involves the oxidative addition of a suitable substrate to the central metal, migration and insertion of the appropriate ligand (for instance CO in the Monsanto process) between metal and coordinated product. This is subsequently followed by reductive elimination of the final product, making the catalyst ready for the next catalytic cycle. The fundamental steps during the catalytic cycle of the Monsanto process are shown in (**Scheme 1.1.**)

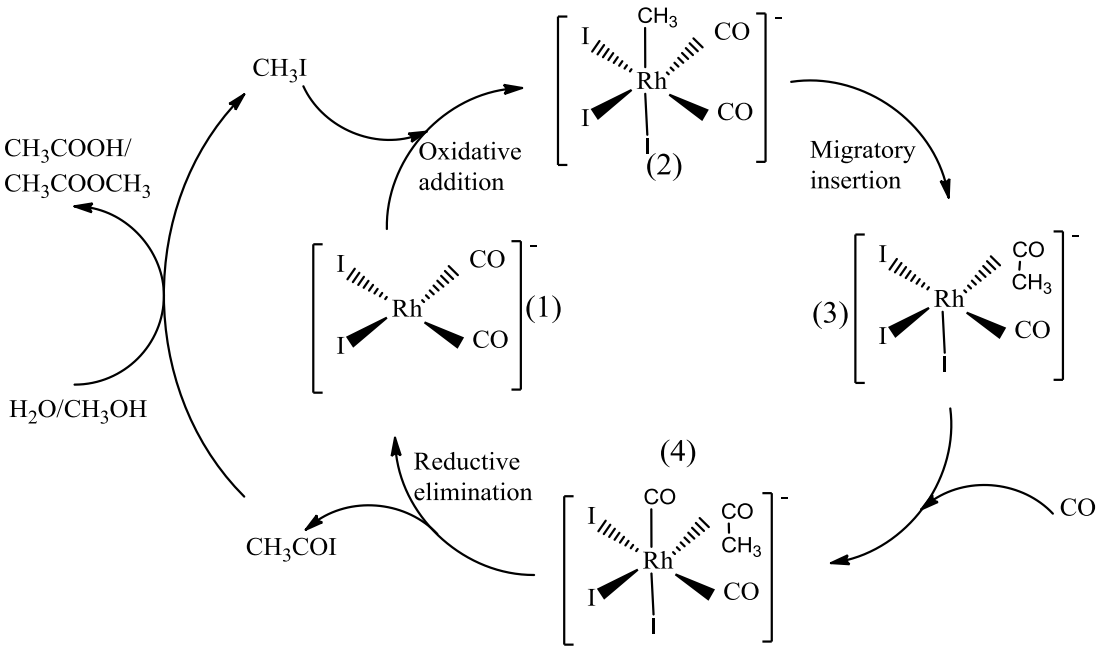

Scheme 1.1. The Monsanto process reaction mechanism.[8] ***Permission granted by American Chemical Society (1976).***

It is well known that the electronic effect of different substituents has a marked influence on the catalytic activity, especially the oxidative addition reaction of the catalyst.[9,10] It has been shown that electron withdrawing groups (like -F) on the ligands can slow down the rate of the oxidative addition, while electron donating groups (like -O) can increase the rate of oxidative addition.

1.2 Aims of this study

With the above background, the following goals were identified for this study:

1. The synthesis and characterisation of a series of different organophosphorus ligands of the types, $C_6H_5XPPh_2$, where X = O, S and NH, as well as *meta*- and *para*-$Ph_2POC_6H_4OPPh_2$.

2. The synthesis and characterisation of a series of organophosphorus-containing rhodium(I) complexes of the type [Rh(acac)CO($C_6H_4XPPh_2$)] where X = O, S and

NH, as well as [(Rh(acac)CO($Ph_2POC_6H_4$-*m*-$OPPh_2$)] and [(Rh(acac)CO($Ph_2POC_6H_4$-*p*-$OPPh_2$)].

3. A kinetic study of the oxidative addition reaction between selected rhodium (I) complexes and methyl iodide by means of UV/Vis and FTIR.

4. An electrochemical study of the organophosphorus ligands and their rhodium (I) complexes.

1.3 Reference

[1] M. M. Rahman, L. Hong-Ye, E. Klaas , P. Alfred, W.P. Giering, *Organometallics.*, 1989, **8**, 1.
2 C. A. Tolman, *J. Amer. Chem. Soc*., 1970, **92**, 2953.
3 R. B. Bedford, S. M. Draper, P .N. Scully, S. L. Welch, *New J. Chem*., 2000, **24**, 745.
4 P. A. Evans, J. D. Nelson, *Tetrahedron Letters*., 1998, **39**, 1725.
5 J. Klosin, C. R. Landis, Acc. Chem. Res., 2007, **40**, 1251.
6 J.J.C. Erasmus, J. Conradie, *Inorganica Chimica Acta.*, 2011, **375**, 128.
7 P. Jaunky, H. W. Schmalle, O. Blacque, T. Fox, H. Berke, J. Organo. Chem., 2005, **690**, 1429.
8 D. Forster, *J. Am. Chem. Soc*., 1976, **98**, 846.
9 J. Rankin, A. D. Poole, A. C. Benyei, D. J. Cole-Hamilton, *Chem. Commun*., 1997, 1835
10 C.M. Thomas, G. Süss-Fink , *Coordination Chemistry Reviews.*, 2003, **243**, 125.

2 Literature Survey

2.1 Introduction

This chapter covers the relevant literature concerning the synthesis of organophosphorus (including phosphinite) ligands and their associated phosphorus-containing rhodium (I) complexes. The chemical and electrochemical behaviour of phosphorus ligands and phosphorus-containing rhodium (I) complexes as well as the kinetic aspects of some rhodium complexes will be reviewed.

2.2 Phosphorus chemistry

2.2.1 Introduction

It is believed that during the seventeenth century Hennig Brandt, an alchemist, discovered phosphorus while trying to make gold. Phosphorus is a Greek word meaning the light bearer. This is due to the fact that in its pure form, phosphorus is a luminous solid that glows in the dark.[11] Since it ignites at 30ºC, it is normally stored under inert conditions or under water. Phosphorus and its derivatives are used in fertilizers, flame retardants, electroplating and in nature, the nucleoside triphosphate ATP,[12] is the energy carrier for metabolic processes in cells. These are but a few of its many uses or applications.

2.2.2 Chemical properties of phosphorus compounds

Phosphorus is an important chemical in both the biological field and in the chemical industry. Our focus will be on its chemical properties which has attracted research in the field of

catalysis. Phosphorus atoms have three lone-pair electrons in the low-lying 3d orbitals,[13] which causes it to behave in a similar manner as a CO ligand. Phosphorus compounds can be present in the following forms: PR_3, PR_2XR, $PR(XR)_2$, $P(XR)_3$ where the R group is an acyl or aryl group and X is a heteroatom such as N or O.[14] These compounds demonstrate different electronic properties (electron donating or electron withdrawing) and each will therefore change the electron-density on the metal center to which it is bound.[15] In terms of the electronic structure, the π-accepting properties of the phosphorus group can be strongly modified via replacement of the P-C bonds with P-O.

2.2.3 Phosphines

Phosphines are a class of phosphorus compounds where the R-group, in the PR_3 compound, is an acyl or alkyl. The general synthesis involves the use of the Grignard reagents or organometallics as shown in (**Scheme 2.1).**[16] The Grignard reaction should be performed under dry and oxygen free conditions, as it reacts with water to form alkanes. Due to the difference of the Pauling electronegativity of the carbon (2.55) to that of the magnesium (1.31), this result in electrons in the C-Mg bond polarized towards the carbon.[17] This makes the Grignard reagents to be strong nucleophiles, which will assist when it react it with a halide such as Cl in chlorodiphenyl phosphine.

For the Grignard reagent

$$PX_3 + 3RMgX \longrightarrow PR_3 + 3MgX_2$$

For the organometallic

$$PX_3 + 3LiR \longrightarrow PR_3 + 3LiX$$

For halo organo species and the alkyl and alkyl substituted species

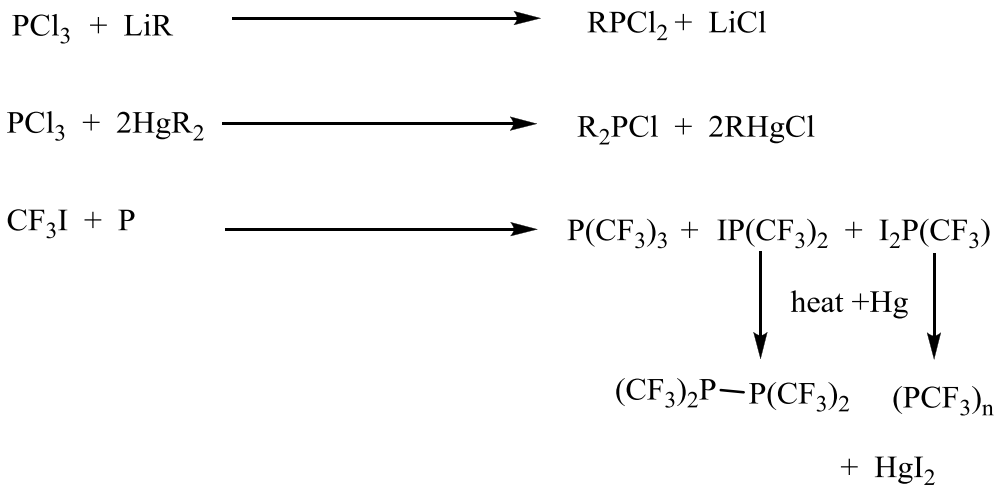

Scheme 2.1. Different methods of Phosphine synthesis (adopted sketch from reference[16]).

Phosphine ligands are excellent soft-donor ligands with a wide variety of adjustable electronic and steric properties. These electronic and steric properties are determined by the R-substituents on the PR_3 phosphine. Usually phosphines, are weak π-acceptors and strong σ-donors, however when the R-groups are electron-withdrawing the π-acceptor property will be favoured while electron-donating R-groups will favour the σ-donating properties.[18] To further explain the donor/acceptor ability of the phosphorus ligand, assume that a series of PR_3 ligands has constant σ-donation to a metal and that R becomes more electronegative, the phosphorus empty d orbital becomes more electronegative, which will enhance the dπ-dπ back bonding.[19] This makes ligands such as PF_3, PCl_3 and $P(OR)_3$ strong electron acceptors while ligands such as $P(CH_3)_3$ would be more electron donating.[20,21] **Figure 2.1** illustrates both the σ-donation and π-back donation.

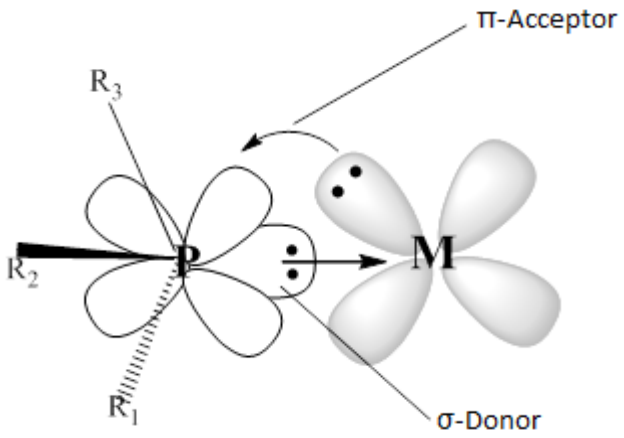

Figure 2.1. Orbital depiction of both the σ-donation and π-back donation.

2.2.4 Phosphinite

Phosphinites are organophosphorus compounds with the general formula $P(OR)R_2$.[22] These are stronger π-accepting and weaker σ-donating than their corresponding phosphines.[23,24,25] The synthesis of phosphinites involves the use of phosphorus halides, such as chloro dialkyl phosphine, with an alcohol, ROH, in the presence of a base such as triethylamine. An acid forms as a by-product, which is trapped by the base, triethylamine as the $Et_3N^+HCl^-$ salt. (**Scheme 2.2)** below shows a typical synthesis process for a diphosphinite with the use of pyridine and the resultant pyridine hydrochloride is filtered off.

There are a few examples of phosphinites being used as ligands in various catalytic systems e.g. Bedford *et al.* used a biphosphinite 'PCP' pincer ligand (*meta*-$Ph_2POC_6H_4OPPh_2$, *m eta*-$Ph_2POCH_3C_6H_3OPPh_2$) for a palladium catalyst in Suzuki reactions,[26] while van der Slot *et al.* used both mono- and bidentate phosphinites as ligands for rhodium catalysts used in hydroformylation reactions, (**Figure 2.2).**[27]

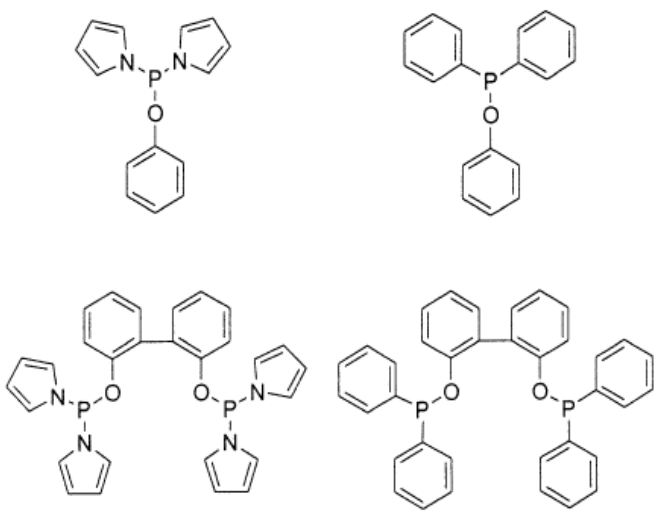

Figure 2.2. Showing both the monodentate and bidentate organophosphorus ligands.[16] ***Permission has been granted by American Chemical Society (2002).***

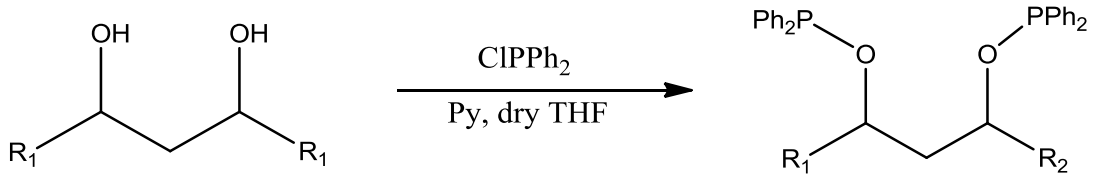

Scheme 2.2. Schematic representation of diphosphinite synthesis.[28] ***Permission has been granted by John Wiley & Sons (2013).***

2.2.5 Determining the electronic and steric properties

The electronic effect of a phosphorus compound can be altered by introducing R-groups with different electron donating and withdrawing abilities, which will transmit their electronic effects along the chemical bonds. The electron donating effect of the CH_3 group in $P(C_6H_4$-*p*-$CH_3)_3$ will increase the σ-donor ability of the ligand compared to $P(C_6H_4$-*p*-$Cl)_3$, whereas R = Cl, which is electron withdrawing which causes the phosphine to be a weaker σ-donor.[29]

A steric effect is observed when the R groups spatially "interfere" with each other due to electron clouds that may overlap. The forces, usually nonbonding, between different groups within the molecule cause repulsion or steric strain on bonds. There is an increase in bulkiness when moving from the $P(Me)_3$ to the $P(t$-$Bu)_3$ ligand, which will result in steric

strain, for which the binding ability decreases from the $P(Me)_3$ to the $P(t\text{-}Bu)_3$ ligand.[30] It has also been reported that the steric effect of the phosphorus ligand has an influence on the regioselectivity of the product formed by the phosphorus-containing metal catalyst.[31,32]

By varying the R-groups within a phosphorus compound it is possible to tune the properties of the ligand in terms of electronic and steric effect as desired. These two parameters have a significant effect on the properties, reactivity and catalytic ability of the transition metal to which they are bound. Due to this flexibility in properties, phosphorus systems are considered as some of the most versatile ligands in organometallic and inorganic chemistry.

The electronic properties of the coordinated phosphorus ligand can be determined amongst others using Fourier transformed Infrared (FTIR). The shift in carbonyl stretching frequency of the phosphine- and carbonyl containing metal complex is an indication of the electronic effect of the R groups on the phosphine. More electron withdrawing R-groups will cause the CO stretching frequency to shift to more positive wavenumbers, whereas electron donating R-groups will cause a negative shift of the CO stretching frequency.[33,34,35] One of these FTIR methods of determining the electronic effect is the Tolman's electronic parameter (TEP), which is an observed quantity of a particular PR_3 ligand, which is obtained by measuring the FTIR spectrum of its $[Ni(CO)_3PR_3]$ complex. Because the carbonyl stretching frequency value of the metal-carbonyl can be used as the indicator of the metal center electron density, the TEP can be used to determine the electron properties of the phosphine.[36] The stretching frequency of the coordinated CO is an indication of back donation, e.g. an increase in the electron density on the metal center, due to an electron donating phosphorus ligand, will lead to the increase in the back donation into the CO ligand π^* orbital, which will lower the CO stretching frequency, and with weak back donation the result leads to higher CO stretching frequency.[37]

The steric property analysis was introduced by Tolman since it became clear that the ability of the phosphorus ligands to compete for coordination positions on the zero valent nickel could not be explained by their electronic characteristics.[38] (**Figure 2.3)** depicts how both the symmetric and non-symmetric ligands' cone-angles are defined. For the symmetric ligands the steric parameter is the apex angle of the cylindrical cone, which is centered 2.28 Å from the center of P atom, which just touches the van der Waals radii of the outermost atoms of the model.

For the non-symmetric ligands (**Figure 2.3) (b)** $PX_1X_2X_3$ the effective cone angle can be defined by a model which minimizes the sum of the cone half angles using the following **Equation 2.1**:

$$\theta = (2|3)\sum_{i=1}^{3}\theta_i\,/2 \qquad 2.1$$

With the work done by Van Rooy *et al.* on the rhodium-catalysed hydroformylation with the use of bulky phosphite, it was concluded that the structure of the catalyst has a large influence on both the activity and the selectivity of the rhodium carbonyl hydroformylation catalyst. They observed that with the PPh_3-modified catalyst, the rate decreases with increasing steric hindrance by the substituents.[39]

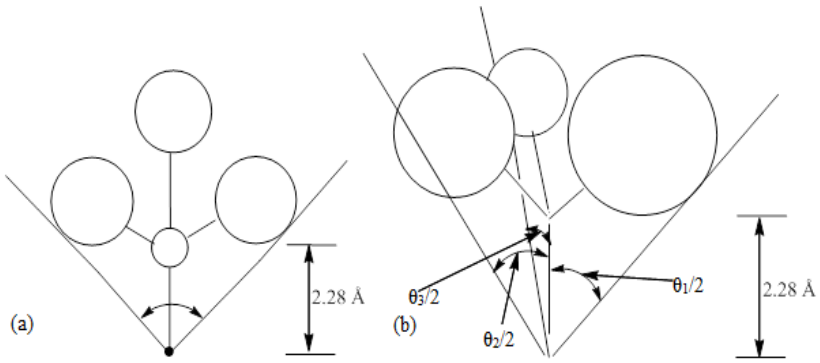

Figure 2.3. (a) Symmetrical ligands cone-angle measurement, (b) non-symmetrical ligands cone-angle measurements.[26] ***Permission American Chemical Society (1970).***

2.3 Rhodium

2.3.1 Introduction

Rhodium metal is part of the platinum group metals, which was discovered in 1803 by W.H. Wollaston and he named it "Rhodes", which is Greek for rose, owing to the rose red colour of its salt solution.[40] It is approximated that 70 % of the rhodium is used as catalysts in vehicle exhausts, as well as in the chemical- and pharmaceutical industry. Some of its chemical properties include resistance to halogen attack and it is more resistant to air oxidation.[41]

2.3.2 Catalytic properties

Organometallic compounds of rhodium have shown good catalytic results for carbonylation,[42,43] hydrogenation,[44] and hydroformylation reactions,[45,46] which will be discussed below.

2.3.2.1 Carbonylation reaction

A catalytic carbonylation reaction is where carbon monoxide is introduced into an organic or inorganic compound. For example, the Monsanto process,[47,48,49] involves the carbonylation of methanol to produce acetic acid. In the reaction (**Scheme 2.3**) the first step is where methyl iodide is oxidatively added to $[Rh(CO)_2I_2]^-$ (**1**), which is the rate-determining step of the cycle. The resultant hexacoordinated alkyl rhodium(III) intermediate (**2**) undergoes carbonyl migratory-insertion to form the acyl $[(MeCO)Rh(CO)I_3]^-$ (**3**) complex. This is followed by addition of another carbon monoxide group, which leads to the formation of the six-coordinated dicarbonyl $[(MeCO)Rh(CO)_2I_3]^-$ (**4**) complex. Finally the reductive elimination of acetyl iodide, CH_3COI, which results in the regeneration of the starting $[Rh(CO)_2I_2]^-$(**1**) complex takes place. The oxidative addition and the migratory insertion steps are important for this study and these steps will be discussed in detail.

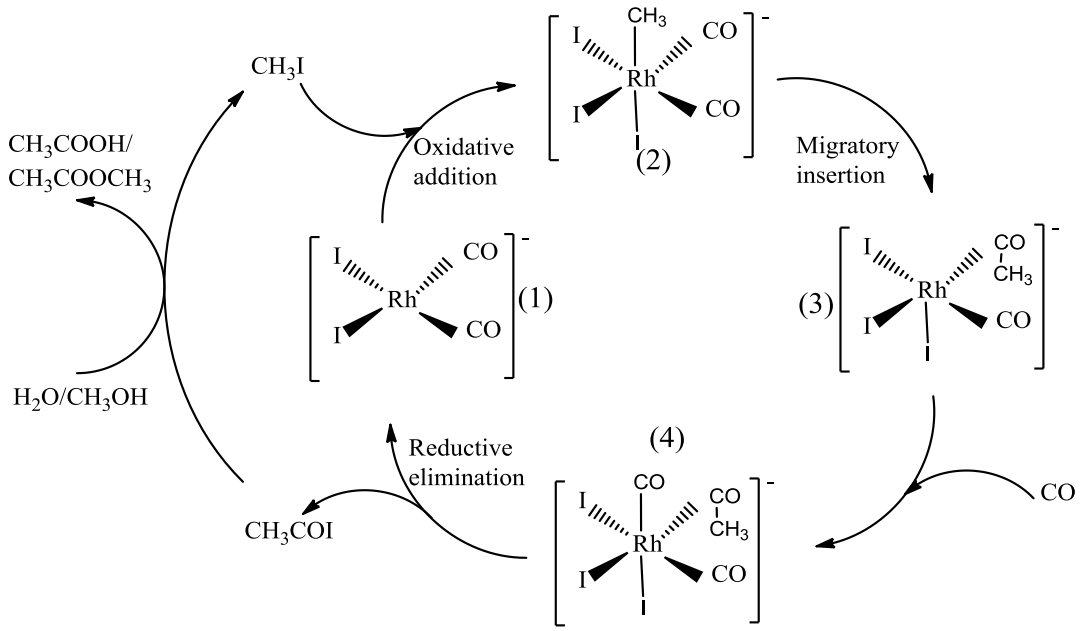

Scheme 2.3. The Monsanto process reaction mechanism.[50] ***Permission granted by American Chemical Society (1976).***

Oxidative addition

Oxidative addition reaction of an alkyl halide, such as methyl iodide onto a coordinatively unsaturated transitional metal, results in the increase of both the oxidation and coordination number of the metal complex.

$$L_mM^n + XY \rightleftharpoons L_mM^{n+2}XY$$

The dominant metal between the reduced and oxidised side of the equilibrium is dependent on three things, firstly the nature of the metal and its ligands, secondly on the incoming compound XY and thirdly the solvent in which the reaction takes place.[51] With the rhodium based complexes the rate determining step for the catalytic cycle is oxidative addition of iodomethane to $[Rh(CO)_2I_2]^-$. It has been shown that the increase of the electron density on the metal centre, by an electron donating ligand such as (PEt_3), will result in the doubling of the reaction rate compared to the reaction rate of the $[Rh(CO)_2Cl]_2$ complex under the same reaction conditions.[52,53,54]

Migratory insertion

Migratory insertion involving CO is where the CO first migrates to the alkyl group bonded onto the metal and secondly insert between the metal and the alkyl group.[55] It has been experimentally reported that π-acceptor ligands such as CO and isonitriles which are trans to the migrating methyl ligand does indeed promote migratory insertion and that the σ-donor ligands trans to the migrating methyl ligand do not promote migration.[56] Theoretical calculations done by P. Margl *et al*. has suggested similar results, that the increase of the number of π-acceptor ligands will promote methyl migration by reducing the activation energy for the migration step.[57] In other studies it was reported that the rate of migration may be enhanced by the use of less polar solvents, as it was shown that the rate constant is four times larger in mesitylene than in *n*-hexane, in mesitylene, 1.11 $x10^{-4}$ $M^{-1}sec^{-1}$ and in *n*-hexane, 2.7 $x10^{-5}$ $M^{-1}sec^{-1}$.[58] Steric effect of the ligands has also been shown to have a dramatic influence on the migratory insertion on rhodium, given the fact that $Ph_2PCH_2P(S)Ph_2$ (dppms) ligand is able to promote both oxidative addition and migratory insertion. This strong electron donor ligand, which accelerates oxidative addition, would normally be expected to inhibit CO insertion, but rather steric effect of the dppms ligand seems to dominate.[59]

2.3.2. 2 Hydrogenation

A hydrogenation reaction involves the reaction of an alkene (double bond) with H_2 to yield an alkane (single bonds) in the presence of a catalyst.[60] Wilkinson was the first to introduce the use of rhodium metal for the hydrogenation of alkene and alkane compounds. **(Scheme 2.4)** below shows the reaction mechanism of the alkene hydrogenation using Wilkinson's catalyst. The fluoro analogue of Wilkinson's catalyst has been synthesised and characterised and was found to be exceptionally reactive towards non-activated chloroarenes.[61] Modified Wilkinsons catalysts with triorganophosphite additives, such as triphenylphosphite, triisopropylphosphite and trimethylphosphite, have also been used as allylic alkylation reactions. This resulted in an increase in turnover rate and excellent regioselectivity.[62] Immobilisation of the Wilkinson's catalyst to combine the advantages of homogeneous and heterogeneous catalysts like easy separation of reactants, products, and catalysts, as well as high activity and selectivity has been studied. From the results obtained it was concluded that

the catalyst was still very active with respect to the hydrogenation of different substrates, and the chemoselectivities were not changed by the immobilization.[63]

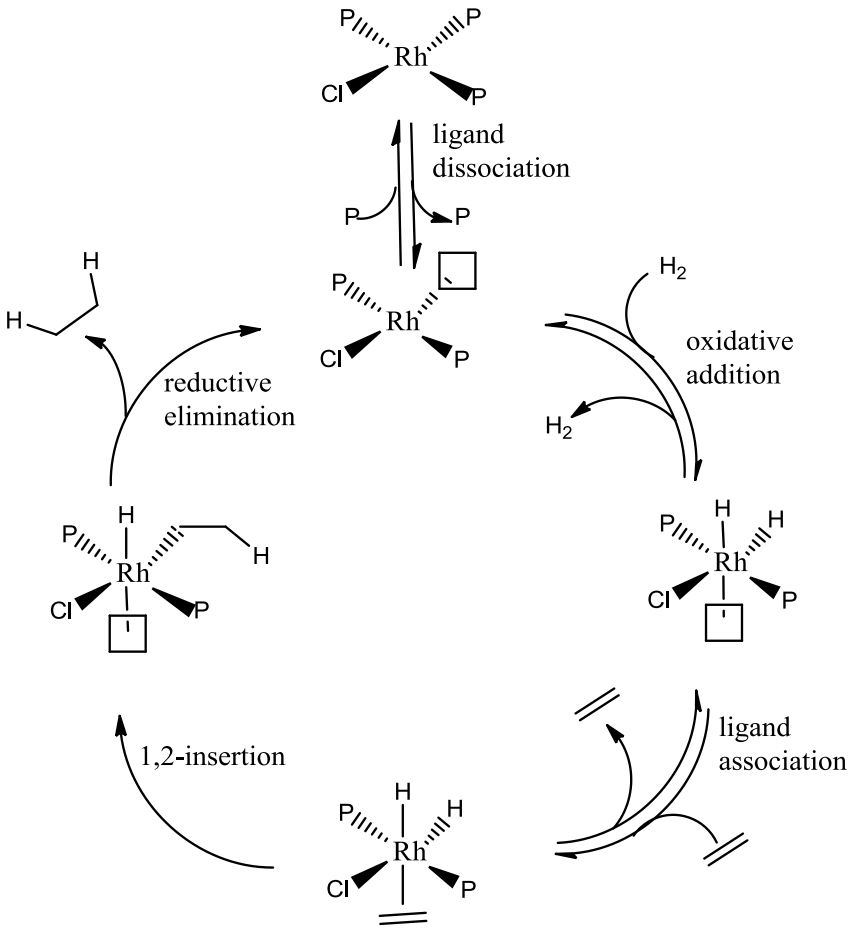

Scheme 2.4. Alkene hydrogenation mechanism using the Wilkinson's catalyst.[64]
Permission granted by Royal Society of Chemistry (2013).

2.3.2.3 Hydroformylation

Hydroformylation is a transitional metal catalysed conversion of alkenes to aldehydes in the presence of CO and H_2. This reaction involves the addition of the formyl (CHO) group and a hydrogen atom to a carbon-carbon double bond as illustrated in the (**Scheme 2.5)** below.

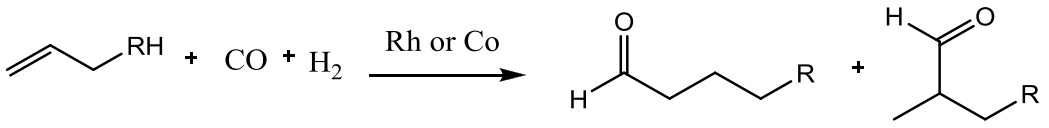

Scheme 2.5. Hydroformylation of the alkene to the linear and the branched aldehyde product.

From kinetic data obtained in reported studies,[65] using $HRh(CO)L_2$ it was shown that the rate-determining step of the hydroformylation reaction cannot be reduced to one single step of the hydroformylation mechanism, see (**Scheme 2.6)** below. It has also been reported that the structure of the modified rhodium carbonyl catalyst has a large influence on both the activity and selectivity of the product that formed. When triphenylphosphine is used it makes the coordination of the alkene the rate determining step.[66]

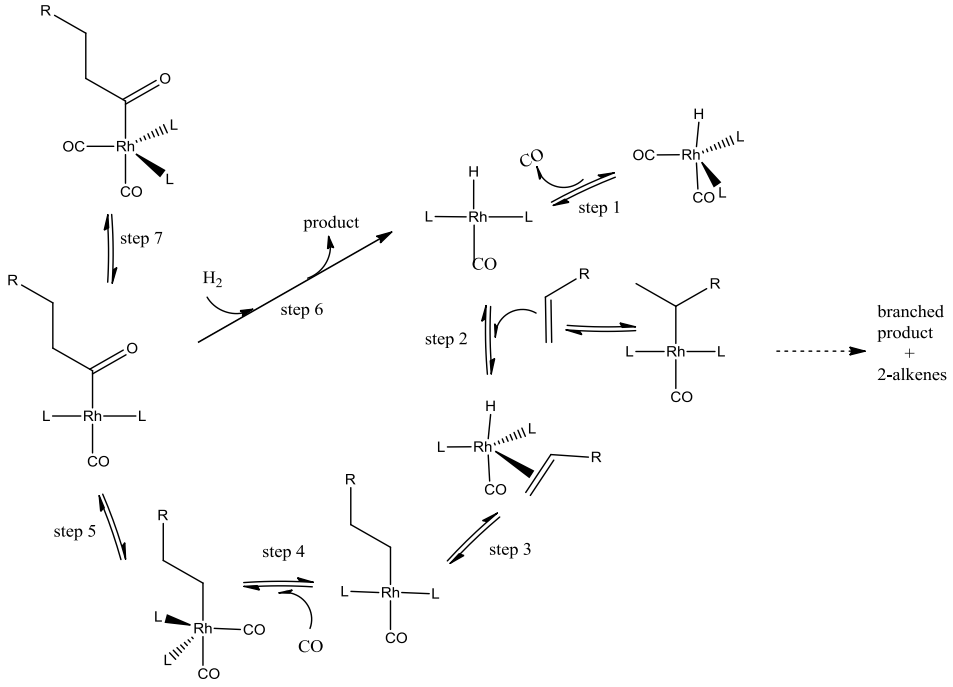

Scheme 2.6. Hydroformylation of the alkene reaction mechanism.[54] ***Permission granted by Elsevier (2004.).***

2.4 Electrochemistry

2.4.1 Introduction

Electrochemistry studies the interrelation of electrical and chemical effects of chemical systems. Electrochemical analysis has found use in inorganic chemistry to study the ligand effect on the oxidation/reduction of the central metal,[67] in enzymatic catalysis model studies, while organic chemists apply it to study biosynthetic reaction pathways.[68]

Voltammetry employs potential that vary with time to a working electrode in a solution containing the electroactive species and measures the current that flows between the working

and counter electrode.[69] The working electrode potential is controlled versus a reference electrode, while an auxiliary (or counter) electrode completes the electrical circuit. There are several different excitation signals that can be applied to the working electrode; these are dependent on the voltammetry experiment being done. **Table 2. 1** below shows the voltage versus time excitation signals in voltammetry and the corresponding voltammogram of cyclic, square-wave and linear-sweep voltammetry. In **Table 2. 1,** (**a**) represent cyclic voltammetry with the triangular waveform, where the potential is varied between the maximum and minimum values. The current response is then recorded as a function of applied potential. For square-wave voltammetry (**b**) with a pulsed wave-form, makes use of a pulse-type excitation signal and the current is measured at various times during the life-time of the pulse. Lastly in the **Table 2. 1**, is linear-sweep voltammetry (**c**), with this one there is a linear increase to the potential at a very slow rate of not more than 2 mVs^{-1}.[70] This is a useful technique to determine the number of electrons transferred.

Type of Voltammetry	Potential waveform	Typical Voltammogram
a **Cyclic Voltammetry**	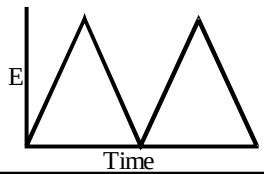	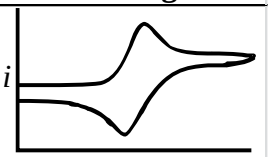
b **Square-wave Voltammetry**	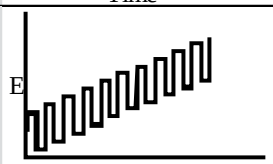	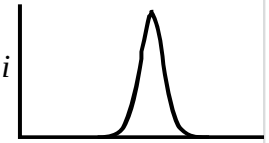
c **Linear-sweep Voltammetry**	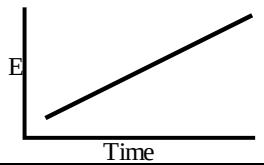	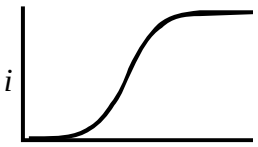

Table 2. 1. The voltage versus time excitation signals in voltammetry and their corresponding voltammograms.

2.4.2 Solvents, electrolytes and internal standards

The solvent of choice has certain important electrochemical implications, which should be taken into consideration such as (1) its ability to dissolve both the analyte of interest and the

supporting electrolyte; (2) its voltage limits should be compatible to the system and (3) its viscosity as this will affect mass transport by diffusion. A study was conducted that showed that there was an increase in viscosity or solution resistance of quaternary ammonium salt electrolyte dissolved in hexamethylphosphoramide, which resulted in a resistance four times than that of solution in acetonitrile or dimethylformamide at the same concentration.[71] It is important that the solvent must not coordinate to the electroactive species as well.

The supporting electrolyte is added so that it decreases the solution resistance, therefore the supporting electrolyte acts as a conducting medium. The supporting electrolyte must be inert and it must dissolve in the solvent of choice. Tetrabutylammonium hexafluorophosphate, $[N^nBu_4][PF_6]$,[72,73] is one of the most commonly used electrolyte in comparison to the less used tetrabutylammonium(tetrakispentafluorophenyl)borate, $[N^nBu_4][B(C_6F_5)_4]$,[74] which is non-coordinating but it is very costly.

Due to the use of a variety of reference electrodes, the literature contains numerous reduction potentials, which cannot be related to each other and which are also difficult to reproduce. To combat this potential drifts the potential of the oxidation of ferrocene as an internal standard is used according to IUPAC.[75] The ferrocene is usually added to the solution once the electrochemistry of the compound of interest is complete. Thereafter the electrochemistry experiment is repeated, now in the presence of the internal standard. The position of the redox waves can now be compared directly to the ferrocene/ferrocenium (FcH/FcH^+) couple potential, which is set to be at 0mV.[75] In cases where the FcH/FcH^+ couple potential interferes with the analyte another internal standard in the form of decamethylferrocene/decamethylferrocenium (Fc^*/Fc^{*+}) couple potential can be employed.[76]

2.4.3 Cyclic Voltammetry

Cyclic voltammetry (CV) is a widely applied electroanalytical technique used to study redox systems. This is often the first experiment performed in an electrochemical study. The potential of the working electrode is swept back and forth by the triangular excitation signal; this can lead to one or more cycles. The potential is ramped from an initial potential and at the end of the linear sweep, the potential scan is reversed, it can be reversed back to the initial potential and the cycle could be repeated. The potential at which the scan direction is changed is called the switch potential. The voltammogram is obtained from the current of the working

electrode during the potential scan. The important parameters in the cyclic voltammogram are the magnitude of the peak currents (anodic and cathodic), i_{pa} and i_{pc} as well as the peak potentials (anodic and cathodic) E_{pa} and E_{pc}, at which the peaks appear. The use of the correct base line for the determination of the peak current is of importance as this will determine whether the sample is electrochemically or chemically reversible.

An electrochemically reversible couple is a redox couple where both the oxidised and reduced form of the electroactive species under investigation, exchange electrons with the working electrode more rapid than the diffusion rate.[77] Such a couple can be identified from the cyclic voltammogram, as shown in (**Figure 2.4)**, by measuring the potential deference between the two peak potential, using the **Equation 2.3** below:

$$\Delta E_p = E_{pa} - E_{pc} \approx \frac{0.059}{n} \qquad 2.3$$

E_{pa} and E_{pc} anodic and cathodic peak potential in volts respectively. In the equation 0.059mV/n, *n* is the number of transferred electrons and it is independent on the scan rate. For an ideal system for a one electron process the separation should be 59 mV for electrochemical reversibility, however due to cell internal resistance, ΔE_p of up to 90 mV is considered an electrochemically reversible system.[78] The ΔE_p -values which are between 90 mV and 150 mV are said to be electrochemically quasi-reversible and above 150 mV electrochemically irreversible. The redox couple is reported as the formal reduction potential, $E^{o'}$, in electrochemically reversible system given by **Equation 2.4**:

$$E^{o'} = \frac{E_{pc} + E_{pa}}{2} \qquad 2.4$$

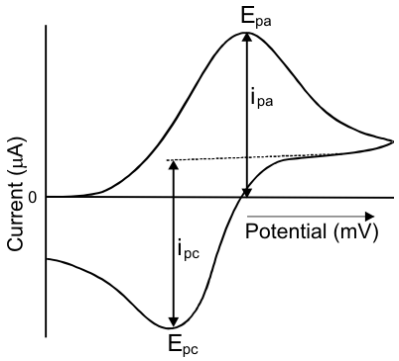

Figure 2.4. Cyclic voltammogram, with the potential peaks and the peak currents.

Chemical reversibility on the other hand is determined by the peak current ratio (i_{pa}/i_{pc}). A system is said to be chemically reversible if the ratio approaches one, meaning that after oxidation or reduction the species does not undergo further reaction before it is reduced or oxidised in the reverse scan. Both the i_{pa} and i_{pc} values are influenced by the scan rate.

2.4.4 Electrochemistry of rhodium complexes

There are a few examples in literature on the electrochemistry of rhodium based complexes.[79,80] One of these studies used the technique to determine the electron density on the rhodium metal in complexes of the type [Rh(I)(β-diketonato)(CO)(PPh_3)] by measuring its oxidation potential.[81] It was concluded that the higher the pK_a values of the β-diketones, meaning the more electron rich the Rh(I) metal center will be, the less positive the oxidation potential and the more negative the reduction potential will be as shown in **(Figure 2.5).**

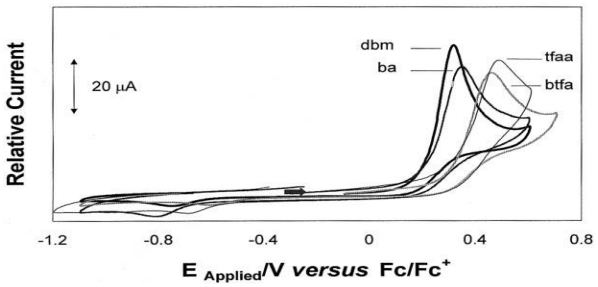

Figure 2.5. cyclic voltammetry of the metal complexes with the various ligands.[69] ***Permission granted by Elsevier (2000).***

In the same study the solvent effect on the metal complex revealed that solvents with better coordination properties made it more difficult to reduce the rhodium(III) species to rhodium(I) see (**Figure 2.6**).

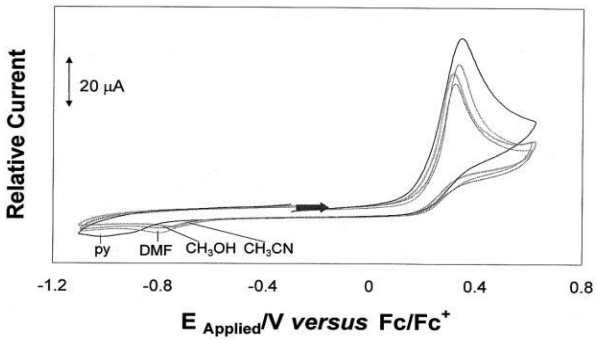

Figure 2.6. Cyclic voltammetry showing the solvent effect on the reduction potential of the rhodium complex.[69] *Permission granted by Elsevier (2000).*

In another study,[82] similar results were obtained with the ferrocene-containing rhodium (I) dicarbonyl complexes of the type [Rh(I)(FcCOCHCOR)$(CO)_2$], studied in CH_3CN/0.1 M [N*n*Bu_4][PF_6], see (**Figure 2.7**). **Table 2. 2** shows the influence of the electronegativity of the R group on the electrochemistry of the metal complex, the higher the electronegativity value is, the lower the oxidation peak potential of the metal center in the complex will be, due to the lower electron density around the metal center making it more difficult to oxidise. The same authors found a linear relationship between the electron density on the metal center and the R-group electronegativity.[83]

Table 2. 2. Peak potential of the metal complex and the R-group electronegativity

R	$E^{o'}$(mV)	$E_{pa,Fc}$ (mV)	$E_{pa,Rh}$(mV)	χ_R
CF_3	304	345, 457	901	3.01
CH_3	190	224	844	2.34
Ph	199	235	718	2.21
Fc	172	207, 312	1022	1.87, (2.28)

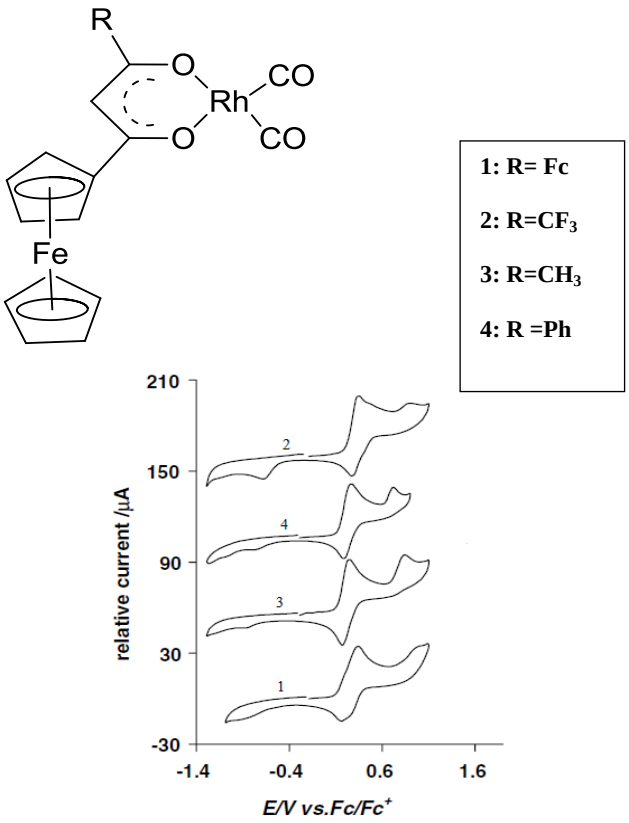

Figure 2.7. Rhodium (I) dicarbonyl complexes with their respective cyclic voltammetry.[70] *Permission granted by Elsevier (2005).*

2.5 Kinetics

2.5.1 Introduction

Kinetics is the scientific study that deals with motion. Chemical kinetics studies the rate of chemical reactions, including the factors that influence the rate of the reaction as well as the reaction mechanism.[84] Some of the factors to be considered in kinetic studies are the pressure, temperature, concentration of the reactants, thermal state, homogeneity of the system and to determine if the system is closed or open, which will influence the volume of the system amongst many others. Solvent properties also influence the rate of chemical reaction,[85] thus the choice of solvent in which the reaction will be studied is also important.

The importance of studying and understanding chemical kinetics is to optimise industrial process, which will have an impact on the commercial products.

2.5.2. Oxidative addition reactions

In transition metal chemistry the process of oxidative addition is used to describe the addition of a neutral molecule to the metal complex, which has 16 valence electrons or less. The schematic representation of an oxidative addition reaction is presented in **(Scheme 2.7).** The forward reaction represents the oxidative addition of XY, while the backward reaction is the reductive elimination of XY.

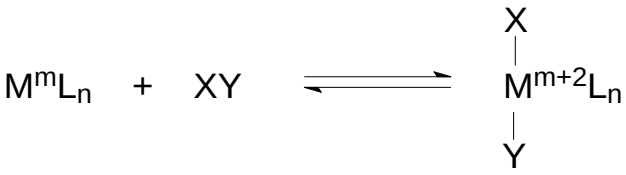

Scheme 2.7. The oxidative addition of a neutral molecule XY to transition metal complexes M^mL_n, with m = the oxidation state and n = the number of ligands bonded to the metal center.

During the forward reaction in **(Scheme 2.7),** the oxidative addition of XY increases the oxidation state of the metal complex by two as well as increasing the coordination number by two. This implies that a transition metal complex can behave like a Lewis acid and a Lewis base.

The mechanism of the oxidative addition of an organic halide onto a transition metal complex can proceed either by a one-step concerted three center mechanism or an S_N2 mechanism. The concerted three centerd mechanism involves a three centerd transition state, see **(Scheme 2.8).** This type of mechanism leads to the formation of a *cis*-addition of the alkyl halide

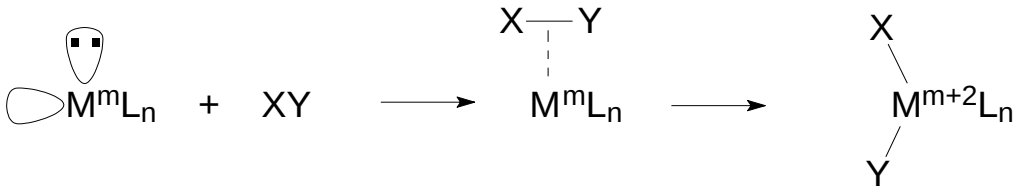

Scheme 2.8. A representation of a concerted three centerd mechanism of oxidative addition.

The other common mechanism is the S_N2 mechanism, which involves the nucleophilic attack of an electron-rich metal center on an electropositive alkyl-group, see **(Scheme 2.9).** This type of mechanism leads to the formation of a linear transition state and ultimately to *trans*-addition of the alkyl halide.

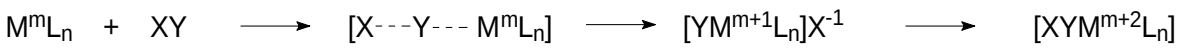

Scheme 2.9. A representation of an S_N2 mechanism of oxidative addition.

Other possible mechanisms of oxidative addition is the radical mechanism,[86] or the ionic mechanism.[87]

2.5.3. Oxidative addition onto rhodium complexes

The square planar rhodium catalyst, $[Rh(CO)_2I_2]^-$, is the original anionic catalyst for the Monsanto process. An increase in the rate of oxidative addition on the rhodium center is observed when the electron density on the rhodium center is increased.

Many rhodium complexes which is bound to different ligands have also been investigated for the rate of oxidative addition reactions. Among these are the diphosphine-containing rhodium complexes, $[Rh(CO)X(PR_3)_2]$, where X = Cl or I. When using trialkylphosphines as ligands, the catalyst showed high activity and selectivity, which was attributed to the short lifetimes of the metal-containing intermediates. Due to the high electrondonating ability of the triethylphosphine, the catalyst was found to be the most effective phosphine. The longer the alkyl chain becomes, the slower the rate of oxidative addition became, which could possibly attributed to steric interference. The reaction was found to proceed according to an S_N2 mechanism, with *trans*-addition.

Probably the most important other ligand that has been explored in the oxidative addition reactions is the bidentate β-diketone ligand. The reaction also proceeds according to an ionic S_N2 mechanism, with the final product showing *trans*-addition. Again, an increase in electrondonating ability of the ligand increases the rate of oxidative addition onto the rhodium center.

2.5.4. Activation parameters

The rate of chemical reactions increases with temperature. Generally, the dependence of the rate constant k on temperature follows the Arrhenius equation **Equation 2.5**.[88]

$$k = Ae^{(-Ea/RT)} \qquad 2.5$$

Here E_a is the activation energy and is useful in determining the mechanism of the reaction. The higher the activation energy the slower the reaction at any given temperature.

Other activation parameters include ΔH^*, ΔS^* and ΔG^*. The sign and magnitude of these thermodynamic parameters also often indicate the mechanism of a reaction. The transition state theory postulates that an activated complex is in equilibrium with the reagent before the reaction takes place and that the reaction rate is given by the rate of decomposition of the activated complex to form the products **(Scheme 2.10)** and the rate constant is given by **Equation 2.6**

$$A + B \underset{}{\overset{K_c^*}{\rightleftharpoons}} [A \cdot B]^* \xrightarrow{k} \text{products}$$

Scheme 2.10. General scheme illustrating the transition state theory.

$$k = (RT/Nh)K_c^* \qquad 2.6$$

Here K_c^* = equilibrium constant, R = gas constant, h = Planck's constant, N = Avogadro's number and T = absolute temperature.

The information of this activated complex is governed by thermodynamic considerations similar to those of ordinary chemical equilibria. The free energy of activation is thus defined thermodynamically as shown in **Equation 2.7**.

$$\Delta G^* = -RT \ln K_c^*$$
$$= \Delta H^* - T\Delta S^* \qquad 2.7$$

Combination of **Equations 2.6** and **2.7** gives **Equation 2.8.**

$$\ln k = \ln [(RT)/(Nh)] + \Delta S^{*}/R - \Delta H^{*}/ RT \qquad 2.8$$

The magnitude of ΔS^{*}, can be used to determine whether the mechanism of substitution is associative or dissociative of nature. A small negative or positive ΔS^{*} value indicates a dissociative mechanism and a large negative ΔS^{*} value indicates an associative mechanism of substitution.

This concludes the literature survey for this study.

2.6 References

[11] M. E. Weeks, Discovery of the elements, Journal of chemical education Publ., Easton. PA. 1945.pg 34.
[12] A.D. F. Toy, Phosphorus chemistry in everyday life, Washington D.C: American chemical society, 1976.
[13] R. H. Crabtree, The organometallic chemistry of the transition metals, New York: John Wiley & Sons Inc, 1948.pg 71.
[14] N. N. Greenwood, A. Earnshaw, *Chemistry of the elements*, 1st Ed., Oxford: Pergamon press Ltd, 1984.pg 566.
[15] B. Nhat-Nguyen, H. Jong-Tai, H. Xuan-Huong, Mho. Sun-il, J. Hye-Young, *Bull. Korean Chem. Soc*., 2008, **29**, 1624.
[16] A.G. Sharpe, Inorganic Chemistry, Longman, 1981.
[17] L. Pauling, *The Chemical Bond*, Cornell University Press, Ithaca, New York, 1967.
[18] A. Richel, A. Demonceau, A.F. Noels, *Tet. Let.* 2006, **47**, 2077-2078.
[19] C.M. Lukehart, fundamental Transition Metal Organometallic Chemistry, Brooks/Cole Publishing Company, 1985.
[20] C.H. Suresh, N. Koga, *Inorg. Chem*., 2002, **41**, 1573.
[21] I.S Butler, F. Basolo, R. . Pearson, *Inorg. Chem*., 1967, **6**, 2074.
[22] H. Fernández-Pérez, P. Etayo, A. Panossian, A. Vidal-Ferran., *Chem. Rev*. 2011, **111**, 2119.
[23] M. S. Davies, M. J. Aroney, I. E. Buys, T. W. Hambley, *Inorg. Chem*., 1995, **34**, 330.
[24] M.P. Mitoraj, A. Michalak, *Inorg. Chem*., 2010, **49**, 578.
[25] I. Odinets, T. Kégl, Elena. Sharova, O. Artyushin, E. Goryunov, G. Molchanova, K. Lyssenko, T. Mastryukova, G. Röschenthaler, G. Keglevich, L. Kollár, *J. Organomet. Chem*., 2005, **690**, 3456.
[26] R. B. Bedford, S. M. Draper, P. N. Scully, S. L. Welch, *New J. Chem*., 2000, **24**, 745.
[27] S.C. van der Slot, J. Duran, J. Luten, P.C.J. Kamer, P.W.N.M. van Leeuwen, *Organomet.*, 2002, **21**, 3873.
[28] S. R. Khan, B. M. Bhanage, *Appl. Organometal. Chem*., 2013, **27**, 313.
[29] C. A. Tolman, *J. Am. Chem. Soc.*, 1970, **92**, 2953.
[30] C.A. Tolman, *Chem. Rev*., 1977, **77**, 313.
[31] B. Breit, R. Winde, K. Harms, *J. Chem. Soc., Perkin Trans*., 1997, **1**, 2681.
[32] A. van Rooy, P.C.J. Kamer, P.W.N.M. van Leeuwen, K. Goubitz, J. Fraanje, N. Veldman, A.L. Spek, *Organomet.* 1996**, 15**, 835.
[33] Y.S. Varshavskii, T.G. Cherkasova, I.S. Podkorytov, A.A. Korlyukov, V.N. Khrustalev, A.B. Nikol'skii, *Rus. J. Coord. Chem*.. 2005, **31**, 124.
[34] O. Kühl, *Coord. Chem. Rev*., 2005, **249**, 693-695.
[35] D.R. Anton, R.H. Crabtree, *Organomet*., 1983, **2**, 621.
[36] C.M. Thomas, G. Süss-Fink, *Coord. Chem. Rev.*, 2003, **243**, 131.

[37] A.M. Trzeciak, T. Glowiak, R. Grzybek, J.J Ziólkowski, *J. Chem, Soc*., 1997, 1831.
[38] C.A. Tolman, *J. Amer. Chem. Soc*., 1970, **92**, 2956.
[39] A. Van Rooy, J. N. H. de Bruijn, K. F. Roobeek, P. C. J. Kamer, P. W. N. M. Van Leeuwen, *J. Organomet. Chem*., 1996, **507**, 69.
[40] W. H. Wollaston, Phil. *Trans. R. Soc. Lond*., 1804, **94**, 419.
[41] F.R. Hartly, Chemistry of the platinum group metals, New York: Elsevier 1991.chapter 1.
[42] J. Zakzeski, S. Burton, A. Behn, M. Head-Gordon, A. T. *Bell, Phys. Chem*., 2009, **11**, 9903.
[43] N. Lassauque, T. Davin, D. Hanh, R. J. Adcock, Y. Coppel, C. Le Berre, P. Serp, L. Maron, P. Kalck, *Inorg. Chem*., 2012, **51**, 4.
[44] J. Luo, A. G. Oliver, J. S. Mclndoe, *Dalton Trans.*, 2013, **42**, 11312.
[45] A. Van Rooy, J. N. H. de Bruijn, K.F. Roobeek, P. C. J. Kamer, *J. Organomet. Chem*., 1996, **507**, 69.
[46] H. You, Y. Wang, X. Zhao, S. Chen, Y. Liu, *Organomet.*, 2013, **32**, 2698.
[47] G. W. Parshall, *Science.*, 1980, **208**, 1223.
[48] A. Haynes, P.M. Maitlis, G.E. Morris, G.J. Sunley, H. Adams, P.W. Badger, C.M. Bowers, D.B. Cook, P.I.P. Elliot, T. Ghaffer, H. Green, T.R. Griffin, M. Payne, J.M. Pearson, M.J. Taylor, P.W. Vickers and R.J. Watt, *J. Am.*
Chem. Soc., 2004, **126**, 2847.
[49] P.M. Maitlis, A. Haynes, G.J Sunley and M.J. Howard, *J. Chem. Soc. Dalton Trans*., 1996, 2187.
[50] D. Forster, *J. Am. Chem. Soc*., 1976, **98**, 846.
[51] F.A. Cotton, G. Xilkinson, P.L. Gaus, Basic Inorganic Chemistry, 3rd Ed., New York: John Wiley & Sons, Inc 1976
[52] J. Rankin, A. D. Poole, A. C. Benyei, D. J. Cole-Hamilton, Chem. Commun., 1997, 1835, 1836.
[53] K. G. Moloy, R.W. Wegman, Organometallics., 1989, **8**, 2883.
[54] C. M. Thomas, R. Mafua, B. Therrien, E. Rusanov, H. Stoeckli-Evans, G. Süss-Fink, Chem. Eur. J., 2002, **8**, 3343-3352.
[55] R. H. Crabtree, The organometallic chemistry of the transition metals, New York: John Wiley & Sons Inc, 1948.
[56] M. Kubota, T. M. McClesky, R. K. Hayashi, C. G. Webb, J. Am. Chem. Soc., 1987, **109**, 7569-7570
[57] P. Margl, T. Ziegler, P. E. Blöchl, J. Am. Chem. Soc., 1996, **118**, 5412-5419.
[58] R. J. Mawby, F. Basolo, R. G. Pearson, J. Am. Chem Soc., 1964, **86**, 3996.
[59] L. Gonsalvi, H. Adams, G. J. Sunley, E. Ditzel, A. Haynes, J. Am. Chem. Soc., 1999**, 121**, 11233-11234
[60] J. F. Young, J. A. Osborn, F. H. Jardine, G. Wilkinson, *Chem. Commun*., 1965, 131.
[61] V. V. Grushin, W. J. Marshall, *J. Am. Chem. Soc*., 2004, **126**, 3069.
[62] P.A. Evans. J. D. Nelson, *Tet. Let.*, 1998, **39**, 1725.
[63] C. Merckle, S. Haubrich, J. Blümel, *J. Organomet. Chem.*, 2001, **627**, 44.
[64] J. Luo, A. G. Oliver, J. S Mclndoe, Dalton Trans., 2013, **42**, 11314.
[65] P.C.J. Kamer, A. van Rooy, G.C. Schoemaker, P.W.N.M. van Leeuwen, Coordination Chemistry Reviews., 2004, **248**, 2412.
[66] A. van Rooy, J.N.H. Bruijn, K.F. Roobeek, P.C.J. Kamer, P.W.N.M. van Leeuwen, *J. Organomet. Chem.*, 1996, **507**, 69.
[67] R.R. Gagnĕ; J.L. Allison; G.C. Lisensky, *Inorg. Chem*., 1978, **17**, 3569.
[68] G.A. Mabbott, *J. Chem. Edu*., 1983, **60**, 697.
[69] A.J. Bard, C.G. Zoski, *Anal. Chem*., 2000, **72**, 346A.
[70] D.A. Skoog, D.M. West, F.J. Holler, S.R. Crouch, Fundamentals of analytical chemistry, 8th Ed, THOMSON publishers, 2004.
[71] H.O. House, E. Feng, N.P. Peet, *J. Org. Chem*., 1971, **36**, 2371.
[72] D. Lamprecht and G.J. Lamprecht, *Inorg. Chim. Acta.*, 2000, **309**, 72.
[73] J. Conradie and J.C. Swarts, *Dalton. Trans.*, 2011, **40**, 5844.
[74] C. Ohrenberg and W.E. Geiger, *Inorg. Chem*., 2000, **39**, 2947.
[75] R.R. Gagne, C.A. Koval and G.C. Lisensky, *Inorg. Chem*., 1980, **19**, 2854.
[76] I. Noviandri, K.N. Brown, D.S. Fleming, P.T. Gulyas, P.A. Lay, A.F. Masters and L. Phillips, *J. Phys. Chem*., 1999, **103**, 6713.
[77] P.T. Kissinger, W.R. Heineman, Laboratory techniques in electrochemical chemistry, MARCEL DEKKER, New York, 1984.
[78] A. Auger, J.C. Swarts, *Organomet.*, 2007, **26**, 105.
[79] M. Fátima, C.G. da Silva, A.M. Trzeciak, J.J. Ziólkowski and A.J.L. Pombeiro, *J. Organomet. Chem*., 2001, **620**,174.
[80] J. Conradie and J.C. Swarts, *Eur. J. Inorg. Chem*., 2011, 2439.
[81] D. Lamprecht and G.J. Lamprecht, *Inorg. Chim. Acta.*, 2000, **309**, 72.

[82] J. Conradie, T.S. Cameron, M.A.S. Aquino, G.J. Lamprecht and J.C. Swarts, *Inorg. Chim. Acta*., 2005, **358**, 2530.
[83] J. Conradie and J.C. Swarts, *Dalton Trans*., 2011, **40**, 5847.
[84] J. W. Moore, R. G. Pearson, Kinetics and Mechanism, 3rd Ed., Wiley-Interscience publishers, 1961.
[85] K. A. Connors, Chemical Kinetics: the study of reaction rates in solution, VCH publishers, 1932.
[86] R.S. Dickson, *Organometallic chemistry of rhodium and iridium,* Academic Press, London, 1983, p 70-79.
[87] R.J. Cross, *Chem. Soc. Rev.*, 1985, **14**, 197.
[88] S. Arrhenius, *Z. Phys. Chem.*, 1889, **4**, 226.

3 Results and Discussion

3.1 Introduction

This section deals with the synthesis and characterisation of new and known phosphorus-containing ligands and their rhodium(I) complexes. The phosphorus based ligands are of the type $C_6H_5OPPh_2$ **(6)**, *para*-$Ph_2POC_6H_4OPPh_2$ **(7)**, *meta*-$Ph_2POC_6H_4OPPh_2$ **(8)**, $C_6H_5SPPh_2$ **(9)**, $C_6H_5NHPPh_2$ **(10)** while the rhodium complex are of the form [Rh(acac)CO($C_6H_4OPPh_2$)] **(11)**, [(Rh(acac)CO($Ph_2POC_6H_4$*p*-$OPPh_2$)] **(12)**, [(Rh(acac)CO($Ph_2POC_6H_4$*m*-$OPPh_2$)] **(13)**, [Rh(acac)CO($C_6H_4SPPh_2$)] **(14)**, [Rh(acac)CO($C_6H_4NHPPh_2$)] **(15)**.

Spectroscopic characterization of these complexes was performed by proton (^{1}H NMR) and phosphorus (^{31}P NMR) Nuclear Magnetic Resonance, Attenuated Total Reflectance Fourier Transformed Infrared (ATR FTIR) and Ultra Violet (UV/Vis) spectroscopy.

Oxidative addition of methyl iodide onto the Rh(I) center, as well as the electrochemical study with cyclic voltammetry (CV) of these complexes are described.

3.2 Synthesis

3.2.1 Synthesis of the organophosphorus ligands

The organophosphorus ligands **6-10** have been prepared by the reaction between the desired oxygen-, sulphur- or nitrogen-containing phenyl substituent (namely phenol, hydroquinone, resorcinol, thiophenol or aniline) and chlorophenylphosphine, in the presence of triethylamine see (**Scheme 3. 1)** for the synthesis of phenyl diphenylphosphinite, **6**, as an example. During the reaction, HCl formed, which was trapped by the triethylamine as the $Et_3N^+HCl^-$ salt, which was filtered off to produce the crude product. The crude product was

purified by chromatography or recrystallisation. The organophosphorus ligands were synthesised in 20-60% yields.

Care had to be taken to avoid oxidation since during the synthesis of the ligands **6-10**, the phosphrous atom can easily be oxidized, which will prevent the compound to act as a ligand. This was achieved by using dry degased solvents under oxygen free atmosphere.

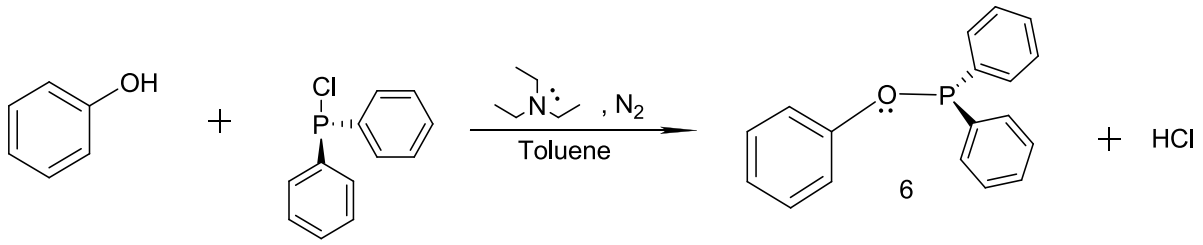

Scheme 3. 1. Schematic representation of the synthesis of phenyl diphenylphosphinite (6).

The organophosphorus ligands **6-8** were synthesised using toluene as the solvent, while ligands **9** and **10** were synthesised using diethyl ether as the solvent. When toluene is used as solvent for the preparation of ligands **9** and **10**, only the oxidised form of ligands **9** and **10** could be isolated see (**Figure 3. 1**), oxidation did not occur in diethyl ether.

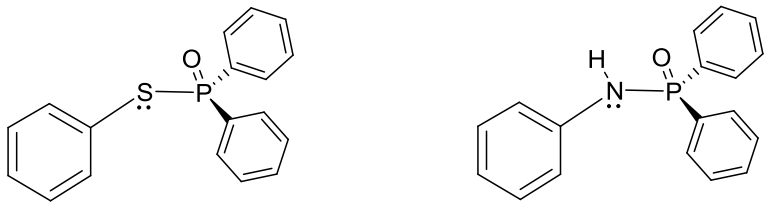

Figure 3. 1. The oxidised form of ligands 9 and 10.

The ^{1}H NMR and ^{31}P NMR spectra of ligand **10** are shown as an example in (**Figure 3. 2)** and selected ^{1}H NMR and ^{31}P NMR data of **6-10** are tabulated in **Table 3. 1.** The ^{31}P NMR shifts of compounds **6, 9-10** were compared with the Pauling electronegativity scale of O (χ_O = 3.44), S (χ_S = 2.58) and N (χ_O =3.04) see (**Figure 3. 3**).

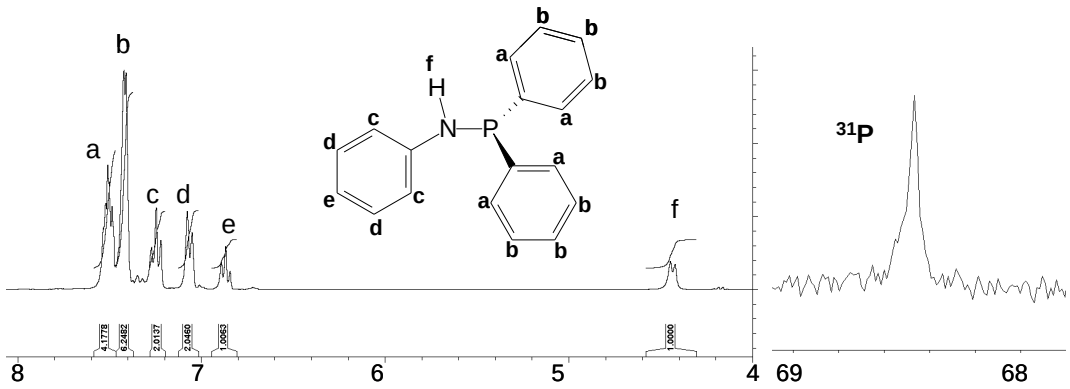

Figure 3. 2. ^{1}H NMR (left) and ^{31}P NMR (right) of ligand 10 as an example

Table 3. 1 Pauling electronegativity scale[80] χ_R, and selected ^{1}H and ^{31}P NMR data, for the organophosphorus ligands (6-10). ^{1}H NMR data is given for the *ortho* and *meta-para* positions of the two diphenyl rings (directly connected to the P-atom).

No.	Name	χ_R	^{31}P NMR (ppm)	^{1}H NMR shifts of Diphenyl rings connected to P (ppm)	
				^{1}H *ortho*	^{1}H *meta* + *para*
6	$C_6H_5OPPh_2$	3.44	110.67	7.68	7.48
7	*para*-$Ph_2POC_6H_4OPPh_2$	3.44	112.38	7.60	7.42
8	*meta*-$Ph_2POC_6H_4OPPh_2$	3.44	110.76	7.61	7.41
9	$C_6H_5SPPh_2$	2.58	41.60	7.65	7.56
10	$C_6H_5NHPPh_2$	3.04	68.54	7.57	7.43

A linear correlation is observed between the Pauling electronegativity scale, χ_R, of O, S, N and the ^{31}P NMR shift of the respective organophosphorus ligands, **6, 9-10**. A shift of the ^{31}P NMR signal towards a higher field is observed with increasing χ_R. The effect observed for **6, 9-10,** shows that, when changing X in $C_6H_5XPPh_2$ with more electron withdrawing substituents (*i.e.* increasing χ_R), more electron density is moved away from the phosphorous atom, deshielding the P and causing a down field shift see (**Figure 3. 3**). The oxidised form the ligand showed a ^{31}P NMR shift at *ca*. 32 ppm for all complexes.

From the NMR data (**Table 3. 1**), it clear that the phosphorus ligands containing oxygen **6-8** all have ^{31}P NMR shifts at *ca.*110.7-112.4 ppm, while the ligands containing S and N have shifted down field as explained above. This shows that the structure of the ligand does not play as big a role in the ^{31}P NMR shifts as the electronic influence of molecules within the structure of the ligand. The ^{1}H NMR data (**Table 3. 1**) of diphenyl rings connected to P showed that the position of the second diphenylphosphine in **7** and **8** does not influence that NMR shifts. However, changing X in $C_6H_5XPPh_2$ (where X = O, S or N) does cause a shift in the ^{1}H NMR shifts of the diphenyl rings connected to P. There are however no direct correlation found between the Pauling electronegativity scale and the ^{1}H NMR shifts.

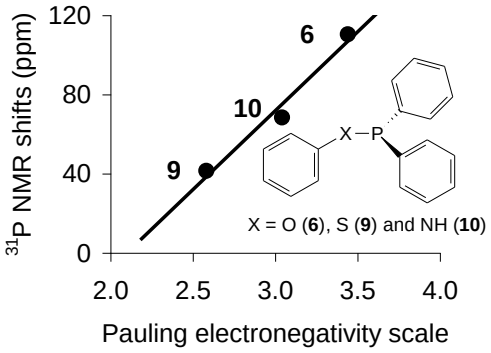

Figure 3. 3. Correlation graphs of ^{31}P NMR shifts of 6, 9-10 *vs* the Pauling electronegativity scale of the O, S and N.

3.2.2 Synthesis of the rhodium complexes

The organophosphorus-containing rhodium(I) complexes (**11-15**) were prepared by the addition of an equivalent amount of the organophosphorus ligand (**5-10**) in hot dry *n*-hexane to a hot solution of [$Rh(CO)_2(acac)$] in dry *n*-hexane while stirring under Schlenck conditions, to prevent oxidation of the phosphorus moiety of the ligand (see **Scheme 3. 2**). In the case of complexes **12-15**, the ligands were dissolved in THF, as the solid product did not dissolve in the *n*-hexane. Normally when using triphenyl phosphine the reaction is immediately finished, however for these organophosphorus ligands (**5-10**) the reaction required longer times of up to 5 min while boiling. Good yields were obtained for the phosphinite ligands **6-8**, however, the sulphur (**9**) and nitrogen (**10**) containing ligand gave

poor yields of 58 and 44% respectively. The poor yields obtained by **9** and **10** could be explained by the different electronic properties of S and NH, longer reactions times might have increased the yields.

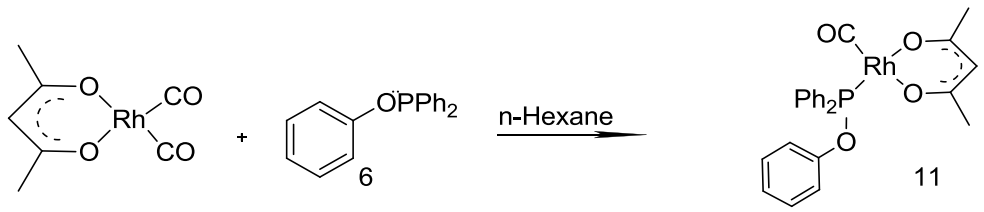

Scheme 3. 2. Schematic representation of the synthesis [Rh(acac)CO($C_6H_4OPPh_2$)], 11

Selected ^{1}H NMR and ^{31}P NMR data of **6-10** are tabulated in **Table 3. 2** and the ^{1}H NMR and ^{31}P NMR spectra of [Rh(acac)CO($C_6H_4OPPh_2$)] **11** are shown as an example in (**Figure 3. 4)**. The ^{1}H NMR spectra of all the rhodium(I) complexes (**11-15**) show the characteristic peaks of the ß-diketonato ligand of the methine proton at *ca.* 5.4-5.6 ppm. Upfield from this are the two peaks belonging to the methyl protons. Above 6 ppm the characteristic peaks of the specific organophosphorus ligand is observed. The ^{31}P NMR shifts of compounds **11, 14-15** were compared with the Pauling electronegativity scale[89] of O (χ_O = 3.44), S (χ_S = 2.58) and N (χ_O =3.04) see (**Figure 3. 5**). Similar to the trend observed with the ligands (**5, 9-10**) an increasing χ_R of the X on the ligands caused a shift of the ^{31}P NMR signal towards a higher field, due to more of the electron density which is moved away from the phosphorous atom, deshielding the P and causing a down field shift see (**Figure 3. 5**).

The rhodium(I) complexes bonded to the ligand containing oxygen **11-13** all have ^{31}P NMR shifts at *ca.*137.2 – 139.9 ppm, while the ligands containing S and N showed a down field shift. The methine and methyl protons on the ß-diketonato ligand are also influenced by the Pauling electronegativity of the organophosphorus ligands **11, 14-15** (see **Table 3. 2** and Experimental section).

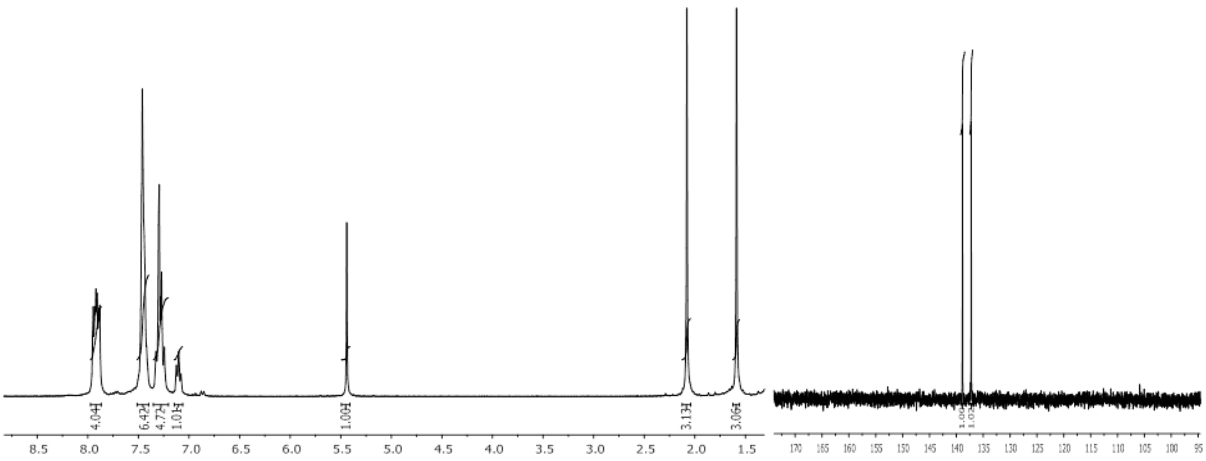

Figure 3. 4. ^{1}H NMR (left) and ^{31}P NMR (right) of [Rh(acac)CO($C_6H_4OPPh_2$)] 11 is shown as as an example.

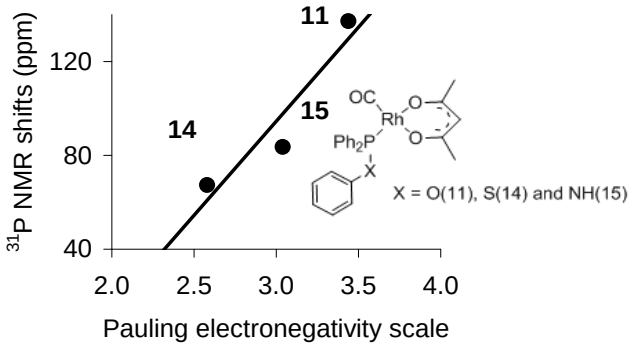

Figure 3. 5. Correlation graphs of ^{31}P NMR shifts of 6, 9-10 *vs* the Pauling electronegativity scale of the O, S and N of [Rh(acac)CO($C_6H_4XPPh_2$)].

The ATR FTIR spectra of the rhodium starting material, [Rh(acac)$(CO)_2$], showed two distinct separate carbonyl stretching frequencies at 2060 and 1993 cm^{-1}. Upon substitution of one of the carbonyl ligands with one of organophosphorus ligands (**6-10**) the monocarbonylrhodium(I) complexes (**11-15**) are obtained.

Table 3. 2. Pauling electronegativity scale[80] χ_R, % yields and selected ^1H and ^{31}P NMR data, for the rhodium(I) complexes (11-15). ^1H NMR data is given for the methine proton of the ß-diketonato ligand.

No.	Name	χ_R	% Yield	^{31}P NMR (ppm)	^1H NMR (ppm)
11	[Rh(acac)CO($C_6H_4OPPh_2$)]	3.44	85	137.26 - 138.87	5.44
12	[(Rh(acac)CO($Ph_2POC_6H_4$*p*-$OPPh_2$)]	3.44	84	138.31 - 139.94	5.44
13	[(Rh(acac)CO($Ph_2POC_6H_4$*m*-$OPPh_2$)]	3.44	76	137.26 - 138.87	5.45
14	[Rh(acac)CO($C_6H_4SPh_2$)]	2.58	58	83.59 - 85.15	5.41
15	[Rh(acac)CO($C_6H_4NHPPh_2$)]	3.04	44	67.31 - 68.72	5.59

These compounds only show a single carbonyl stretching frequency in the region of 1994 - 1982 cm^{-1} (see **Table 3. 3** and **Figure 3. 6)**. The lower carbonyl stretching frequency observed for the monocarbonyl species is in agreement with increased electron density on the rhodium metal center due to the electron σ-donating ability of the phosphorus in the organophosphorus ligands through a σ bond.

Table 3. 3. The ATR FTIR carbonyl stretching frequency for the rhodium(I) complexes.

No	**Compound**	**υ(CO) cm^{-1}**
-	Rhodium(acac)$(CO)_2$	2060, 1993
11	[Rh(acac)CO($C_6H_4OPPh_2$)]	1994
12	[(Rh(acac)CO($Ph_2POC_6H_4$*p*-$OPPh_2$)]	1989
13	[(Rh(acac)CO($Ph_2POC_6H_4$*m*-$OPPh_2$)]	1991
14	[Rh(acac)CO($C_6H_4SPPh_2$)]	1982
15	[Rh(acac)CO($C_6H_4NHPPh_2$)]	1985

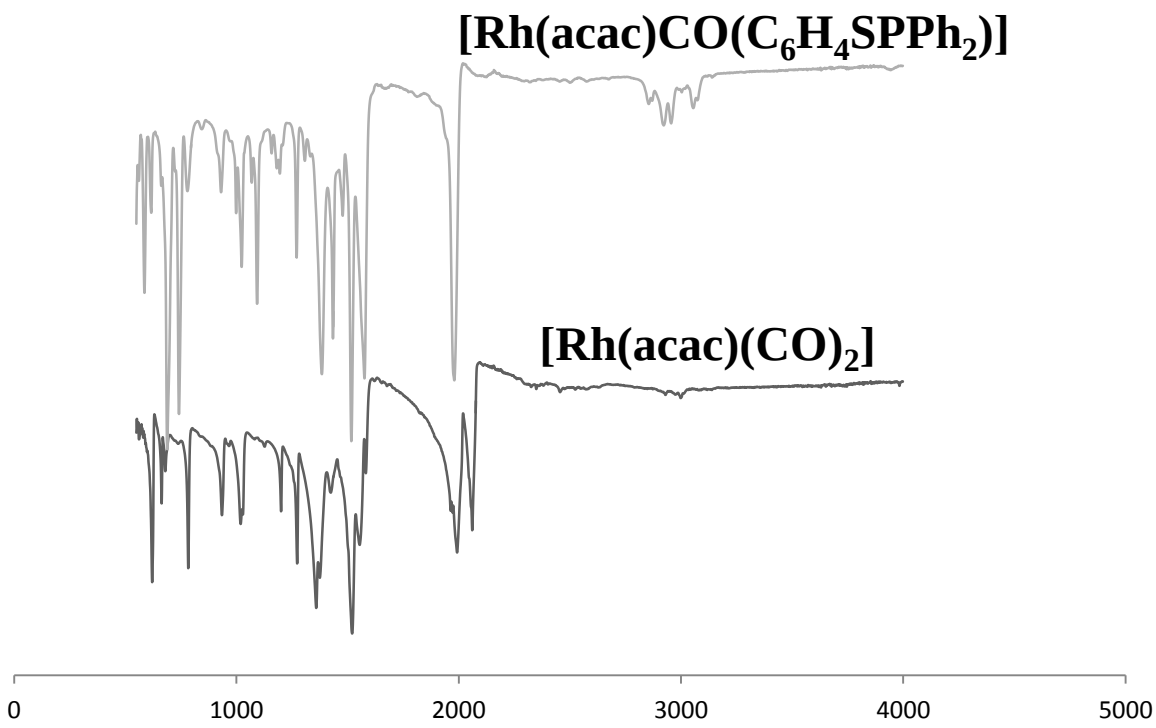

Figure 3. 6. The ATR FTIR spectra for the complexes (a) [Rhodium(acac)$(CO)_2$] and (b) [Rh(acac)CO($C_6H_4SPPh_2$)].

3.3 Electrochemistry

An electrochemistry study was conducted on all the phosphorus containing ligands **6-10** and their rhodium(I) complexes **11-15**. The cyclic voltammetry (CV) experiments were conducted in CH_3CN as the solvent with 0.1 mol dm^{-3} $[NBu_4][PF_6]$ as the supporting electrolyte on a glassy carbon working-electrode, at 25°C.

3.3.1. Electrochemistry of the organophosphorus ligands, 6-11

The cyclic voltammograms of the various organophosphorus ligands **6-10** were recorded in CH_3CN/0.1 mol dm^{-3} $[NBu_4][PF_6]$, on a glassy carbon working-electrode, at 25ºC and the comparative voltammograms at a scan rate of 100 mV s^{-1}, are shown in **Figure 3. 7** (Left). The comparative electrochemical data for these voltammograms are summarised

in **Table 3. 4**. The oxidation and reduction peaks of the phosphorous are observed at the potential limits of the solvent system used.

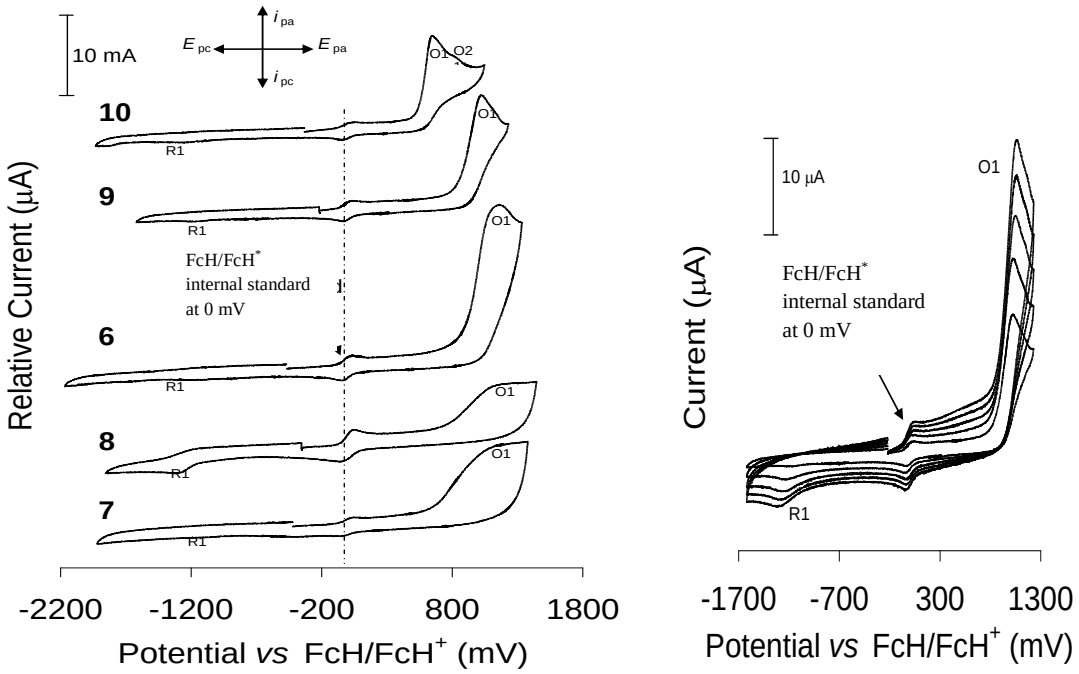

Figure 3. 7. Left: A comparative graph of the cyclic voltammograms of 0.2 mmol dm^{-3} of the organophosphorus ligands (6-10) in CH_3CN/0.1 mol dm^{-3} $[NBu_4][PF_6]$, on a glassy carbon working-electrode, at 25ºC, and a scan rate of 100 mV s^{-1}. Right: Cyclic voltammogram of diphenylphosphinothious acid, compound 9, in acetonitrile on a glassy carbon working electrode at 25˚C and at scan rates of 100-500 mV s^{-1} (100 mV s^{-1} increments).

The redox activity of organophosphorus ligands **6-10** is chemically and electrochemically irreversible and shows one oxidation and one reduction peak, with the exception of ligand **10**, which shows two oxidation peaks. In agreement with the interpretation of Fourie *et al.*[90] and Hall *et al.*[91] the oxidation peak (labelled O1) is allocated to the one-electron oxidation of the free electron-pair on the phosphorous moiety. This one-electron oxidation of the phosphorous moiety liberates a radical cation, according to the proposed reaction in (**Scheme 3. 3)**, using **6** as an example.

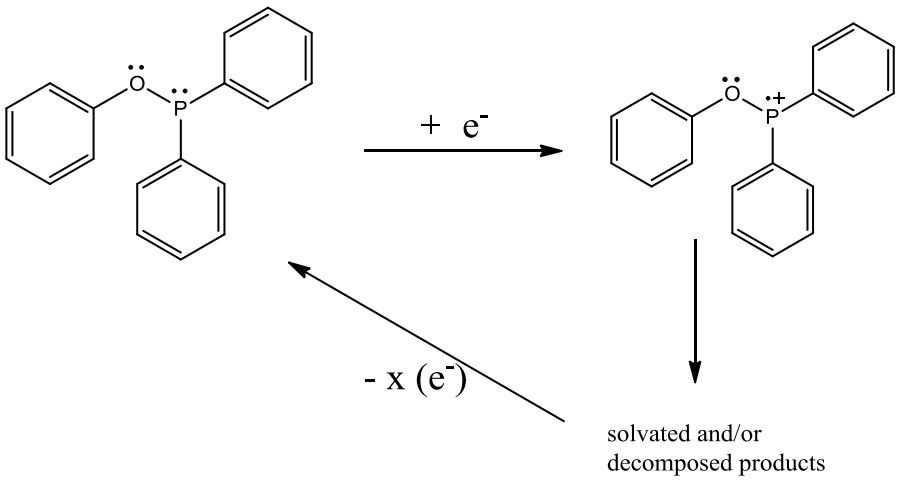

Scheme 3. 3. The proposed one-electron oxidation/reduction of 6, as a representation of the oxidation of ligands 6-10. X<0.1 from Figure 3.7.

The second oxidation peak observed for **10**, marked as O2 see (**Figure 3. 7**), is allocated to either the further oxidation of the radical cation or the oxidation of chemically decomposed products that formed. The decomposition products could be a mixture of many different compounds. A few proposed compounds include the oxidised specie namely the phosphinate, where the phosphorus moiety is oxidised ($O=P(Ph)_2$-R), another possible decomposed product could be a radical $Ph_2P^{\bullet}$ which was proposed by Hall *et al.* or a solvent-coordinated species, $[Ph_2\ P\bullet(CH_3CN)\text{-}R]^+$. These types of solvent-coordinated species that form during the oxidation of compounds in CH_3CN, are well-known.[92,93]

Comparison of the E_{pa} of organophosphorus ligands **6-8**, which is the phenyl diphenylphosphine derivatives with the basic structure of Ph_2POPh-R, where R = H (**6**), *p*-OPh_2 (**7**) and *o*-OPh_2 (**8**), showed that the additional R-groups did not have a big influence on the oxidation of the phosphorus moiety.

Table 3. 4. The data obtained for a 0.2 mM solution of the organophosphorus ligands (6-10) in CH_3CN/0.1 mol dm^{-3} $[NBu_4][PF_6]$ at 25º C, at different scan rates and reference against FcH/FcH^+ as the internal standard. The diffusion coefficient, D, E_{pa} (anodic peak potential) as well as i_{pa} (anodic peak current and, E_{pc} (cathodic peak potential) peak for each compound is shown.

name	no	D for i_{pa} and i_{pc} ($cm^2.s^{-1}$)	υ/mVs^{-1}	E_{pa}/mV	i_{pa}/μA	E_{pc}/mV
$C_6H_5OPPh_2$	**6**		100	1166	16.9	-1257
		6.07×10^{-5}	200	1179	22.0	-1570
		2.8×10^{-11}	300	1192	24.1	-1737
			400	1205	24.6	-1765
			500	1216	26.2	-1778
para-$Ph_2POC_6H_4OPPh_2$	**7**		100	1173	7.8	-1121
		2.37×10^{-5}	200	1225	13.9	-1177
		2.8×10^{-11}	300	1277	18.7	-1233
			400	1329	22.8	-1289
			500	1380	32.0	-1347
meta-$Ph_2POC_6H_4OPPh_2$	**8**		100	1187	5.0	-1340
		1.17×10^{-5}	200	1199	7.1	-1372
		2.5×10^{-12}	300	1212	9.6	-1405
			400	1224	10.7	-1437
			500	1237	12.8	-1470
$C_6H_5SPPh_2$	**9**		100	1030	12.2	-1199
		5.01×10^{-5}	200	1043	17.2	-1237
		1.52×10^{-7}	300	1056	20.8	-1275
			400	1069	23.9	-1313
			500	1083	26.2	-1350
$C_6H_5NHPPh_2$	**10**		100	652	10.4	-1272
		3.24×10^{-5}	200	657	14.6	-1304
		1.3×10^{-11}	300	662	17.9	-1307
			400	667	21.0	-1315
			500	674	23.2	-1323

When X in $C_6H_5XPPh_2$ is substituted with different atoms, X = O, S or NH, there is a drastic change in the oxidation potential of the phosphorus moiety. Even though no correlation between the E_{pa} and the Pauling electronegativity scale could be obtained, the drastic change in E_{pa} still showed that there is electronic communication between the X and the P in the X-P bond, which influences the potential at which the phosphorus moiety is being oxidised.

The reduction peak marked R1 see (**Figure 3. 7**), is observed at the negative limit of the solvent window. This reduction peak is associated with the oxidation peak, O1, which is the reduction of the decomposed oxidised species back to the neutral form (with the free electron-pair on the phosphorous moiety), according to the schematic representation in **Scheme 3. 3**.

The peak current for the oxidation and reduction of the phosphorus moiety in the organophosphorus ligand **6-10** is described by the Randles-Sevcik equation:

$$i_p = (2.69x10^5)n^{\frac{3}{2}}AD^{\frac{1}{2}}C\upsilon^{\frac{1}{2}}$$

where n is the amount of electrons transfered (one electron per phosphorus moiety), A is the area of the electrode in cm^2, D is the diffusion coefficient in $cm^2.s^{-1}$, C is the concentration of the analyte and υ is the scan rate measured in $V.s^{-1}$. Even though the organophophorus ligand system was chemical and electrochemical irreversible, a linear relationship was obtained between i_p and $\upsilon^{1/2}$ (see **Figure 3. 8**). This showed that no major structural changes occurred in the analyte. As an example ligand **9** will be discussed further, the slope of the graph for the anodic peak vs (scan rate)$^{1/2}$ = 1.197 μA.(mV.s^{-1})$^{1/2}$. Using the Randles-Sevcik equation, the diffusion coefficient for the oxidation of the phosphorus moiety is calculated to be 5.01 x 10^{-5} $cm^2.s^{-1}$. For all the ligands **6-10** the diffusion coefficient for the oxidation of the phosphorus moiety is ca. 10^{-5} $cm^2.s^{-1}$ whereas for the reduction the diffusion coefficient is between 10^{-7} and 10^{-12} $cm^2.s^{-1}$.

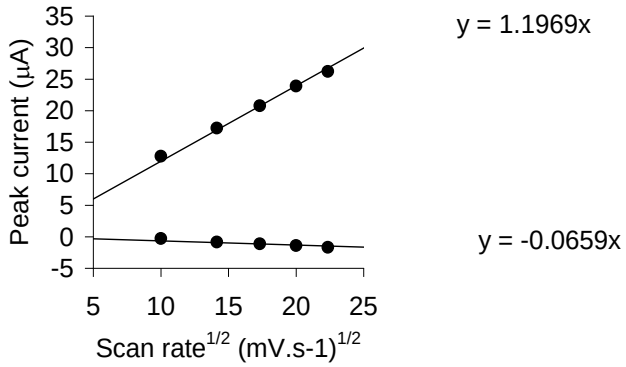

Figure 3. 8. Graph illustrating the linear relationship between the anodic and cathodic peak currents and (scan rate)$^{1/2}$ for ligand 9 as an example.

3.3.2 Electrochemistry of the rhodium complexes

One of the main focus areas of this dissertation was to investigate the electrochemical behaviour of the phosphorus ligand, the rhodium complex and to find the influence of the ligand on the rhodium and a correlation of the influence of the ligand on the rhodium, if any.

The cyclic voltammograms of the various rhodium complexes (**11-15**) were measured in CH_3CN/0.1 mol dm^{-3} $[NBu_4][PF_6]$, on a glassy carbon working-electrode, at 25ºC and the comparative voltammograms at a scan rate of 100 mV s^{-1}, are shown in **Figure 3. 9.** The electrochemical data for these voltammograms are summarised in **Table 3. 5**.

The cyclic voltammogram of the rhodium(I) complexes (**11-15**) show two oxidation and two reduction peaks.

Table 3. 5. The data obtained for a 0.2 mM solution of the rhodium (I) complexes(11-15) in CH_3CN/0.1 mol dm^{-3} $[NBu_4][PF_6]$ at 25° C, reference against FcH/FcH^+ as the internal standard.

no	E_{pa} (O1) /mV	i_{pa}/µA	E_{pa} (O2) /mV	i_{pa}/µA	E_{pc} (R1) /mV	E_{pc} (R2) /mV
11	506	11.8	1009	5.1	-391	-1316
12	437	23.9	776	-	-620	-956
13	472	3.6	773	8.2	-687	-1026
14	527	13.2	1148	9.4	-555	-891
15	375 (676)	1.2 (1.1)	1179	10.1	-676	-1318

From the data obtained by the organophosphorus ligands (in section 3.3.1.) and a previously published article on similar rhodium (I) complexes.[94] The assignment of the peaks were made as follows: The peak obtained at O1 is assigned to the two electron oxidation of the Rh(I) to Rh(III), while the peak labelled O2 is assigned to the one electron oxidation of the free electron-pair on the phosphorous moiety. This assignment was further confirmed by the linear square wave (see Figure 3. 9), which shows that oxidation peak O1 is doubled that of O2. Thus O1 is the two electron oxidation of Rh(I) to Rh(III), while O2 is the one electron oxidation of the lone pair electron on the phosphorus atom. No further oxidation or decomposition of the compound could be observed within the solvent window of the solvent system used.

The reduction peaks labelled R1 and R2 see (**Figure 3. 9**), was assigned to the reduction of the Rh(III) back to Rh(I) in a two electron process and the second reduction peak (R2) is associated with the oxidation peak, O2, which is the reduction of the radical cation of the organophosphorus ligand back to the neutral form (with the free electron-pair on the phosphorous moiety), respectively. These assignments was again made in correlation with the data obtained from the neat organophosphorus ligands (in section 3.3.1.) and published results of similar rhodium complexes.[95]

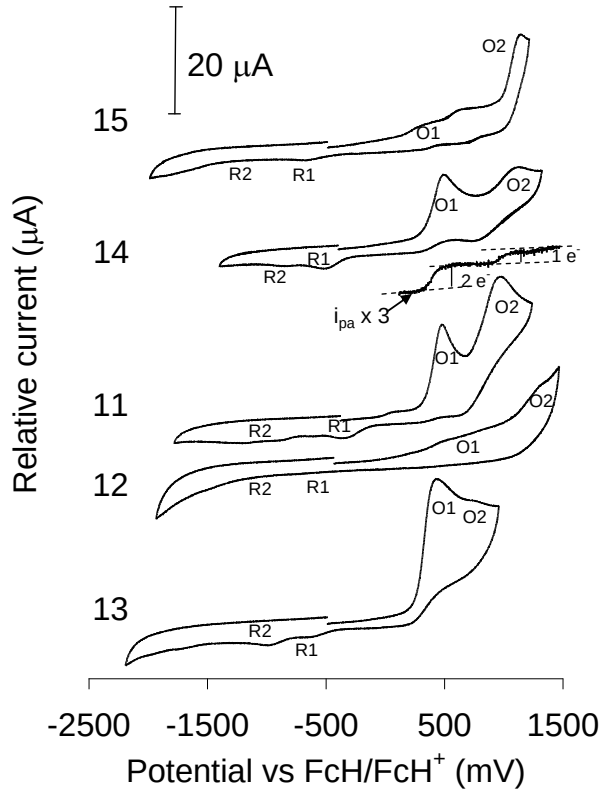

Figure 3. 9. A comparative graph of the cyclic voltammograms of 0.2 mmol dm^{-3} of therhodium (I) complexes(11-15) in CH_3CN/0.1 mol dm^{-3} $[NBu_4][PF_6]$, on a glassy carbon working-electrode, at 25ºC, and a scan rate of 100 mV s^{-1}. The linear square wave of 11 is also shown just above the CV of 11.

3.4 Kinetics

The oxidative addition of methyl iodide onto the Rh(I) center of complexes **11, 14-15**, of the form $[Rh(H_3CCOCHCOCH_3)CO(C_6H_5XPPh_2)$, where X = O, S and NH were investigated using chloroform as the solvent under pseudo first-order kinetic conditions, utilizing an excess of 25-2000 methyl iodide over the rhodium concentration (48 x 10^{-5} M). Kinetic rate constants were determined by UV/Vis and IR spectroscopy. From many previously conducted studies on the oxidative addition of methyl iodide onto the Rh (I) center, a variety of different mechanisms was proposed,[88, 89, 90, 91] all of which are dependent on the type of rhodium complexes studied. Some of these mechanisms are depicted in (**Scheme 3. 4**.)

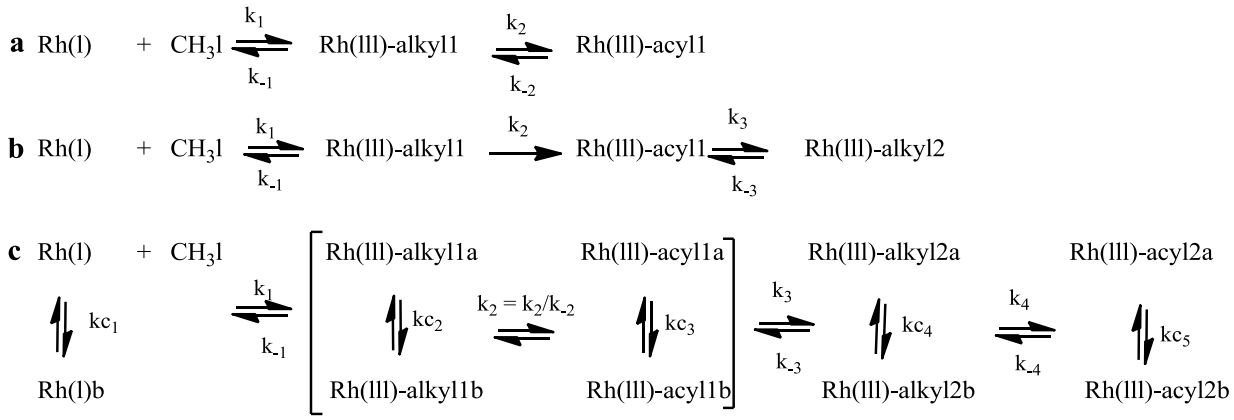

Scheme 3. 4. Different proposed mechanisms for the oxidative addition of CH_3I to rhodium(I) complexes. (a)[96] *Permission has been granted by Elsevier (1990)* (b)[97] (c)[98] *Permission has been granted by Elsevier (2007).*

3.4.1. Validation of Beer Lambert law and determination of extinction coefficients

Since this kinetic study will be conducted using UV/vis-spectroscopy, it is important to show that these complexes (**11, 14** and **15**) obey the Beer Lambert law. (**Figure 3. 10)** shows the UV/vis spectra of the rhodium(I) complexes $Rh(H_3CCOCHCOCH_3)CO(C_6H_5XPPh_2)$, where X = O (**11**), S (**14**) and NH (**15**), the spectral data are summarized in **Table 3. 6**. The linear relationship (**Figure 3. 11**) that exists between the absorbance values and different concentrations (from 0.0006 mol dm^{-3} to 0.001 mol dm^{-3}) of the rhodium(I) complexes **11, 14** and **15** in chloroform at 330 and 380 nm, validates that these three complexes obey the Beer-Lambert law: $A = \varepsilon c\ell$ with A = absorbance, ε = extinction coefficient, c = concentration

ℓ = path length.

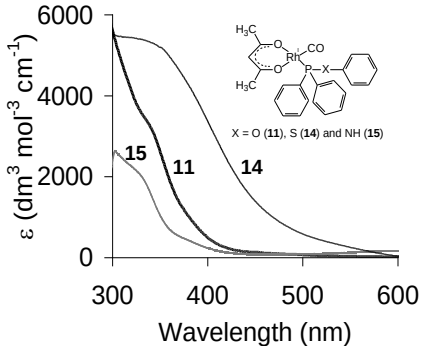

Figure 3. 10. UV/vis spectra of the rhodium(I) complexes $Rh(H_3CCOCHCOCH_3)CO(C_6H_5XPPh_2)$, where X = O (11), S (14) and NH (15) at 25˚C in chloroform.

Table 3. 6 Molecular extinction coefficients (ε) of the rhodium(I) complexes $Rh(H_3CCOCHCOCH_3)CO(C_6H_5XPPh_2)$, where X = O (11), S (14) and NH (15) at 25˚C in chloroform ($\lambda_{exp} = \lambda_{maks}$).

Rhodium(I) complexes	No.	λ_{exp} / nm	ε / $dm^3\ mol^{-1}\ cm^{-1}$
$Rh(H_3CCOCHCOCH_3)CO(C_6H_5OPPh_2)$	11	330	3591
$Rh(H_3CCOCHCOCH_3)CO(C_6H_5SPPh_2)$	14	330	5390
$Rh(H_3CCOCHCOCH_3)CO(C_6H_5NHPPh_2)$	15	330	2202

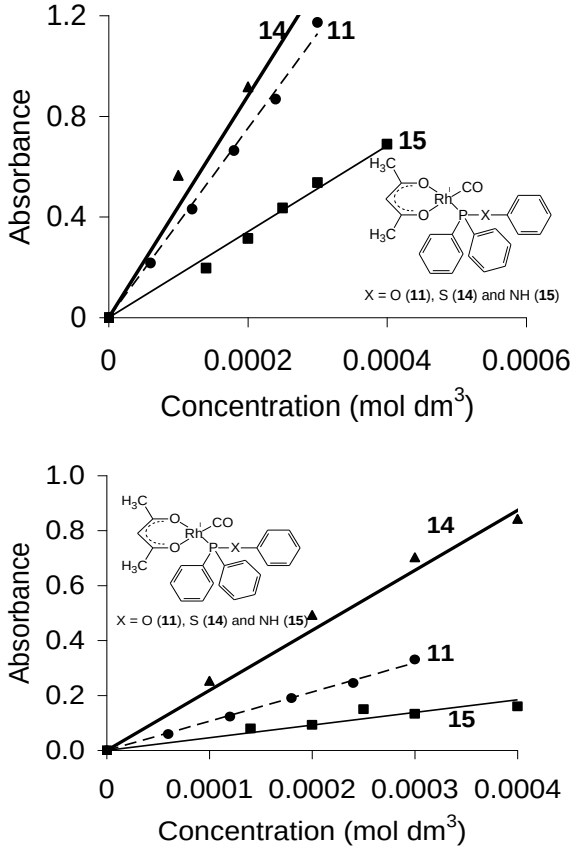

Figure 3. 11. Graph of absorbance *vs* concentration of 11, 14 and 15 at 25˚C in chloroform taken at λ_{exp} = 330 nm (left) and λ_{exp} = 380 nm (right) as indicated, used to validate the Beer Lambert law.

3.4.2. The oxidative addition of CH_3I onto $Rh(H_3CCOCHCOCH_3)CO(C_6H_5XPPh_2)$, where X = O (11), S (14) and NH (15) monitored by UV/Vis spectroscopy

The reaction between CH_3I and $Rh(H_3CCOCHCOCH_3)CO(C_6H_5XPPh_2)$, where X = O **(11)**, S **(14)** and NH (**15**) revealed only one reaction step when monitored by UV/Vis as shown in (**Figure 3. 12)** (**11** is shown as an example). Since the reaction was found to be first-order dependant on CH_3I, the sequence of the reaction is presumed to be as proposed in (**Scheme 3. 5**.). The observed change in the spectra corresponds to the simultaneous disappearance of the Rh(I) starting species and the formation of the Rh(III) alkyl species. A further reaction step to form an acyl species is not excluded, but within the time frame used for this reaction, no further reaction was observed.

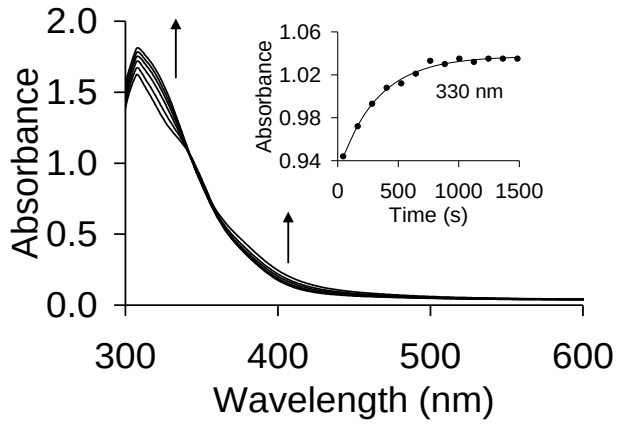

Figure 3. 12. Time based UV/Vis spectra for the first step in the oxidative addition CH_3I onto the Rh (I) metal center, using the time trace of $Rh(H_3CCOCHCOCH_3)CO(C_6H_5OPPh_2)$ (11) as an example. The insert shows the absorbance *vs* time graph measured at 330 nm.

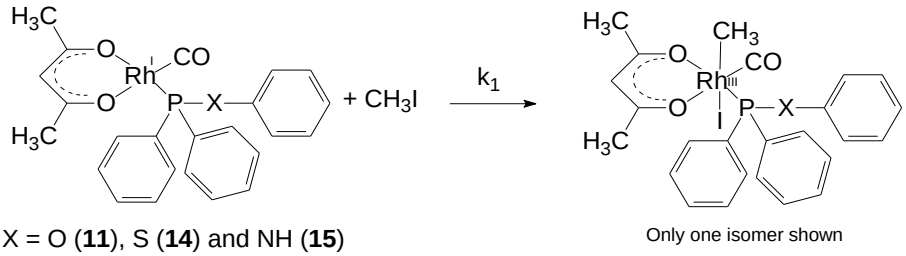

Scheme 3. 5. The presumed mechanism during the oxidative addition of methyl iodide on the $[Rh(H_3CCOCHCOCH_3)CO(C_6H_5XPPh_2)$, where X = O, S and NH.

The reaction between CH_3I and $Rh(H_3CCOCHCOCH_3)CO(C_6H_5XPPh_2)$, where X = O **(11)**, S **(14)** and NH (**15**), were followed at 330 and 380 nm for all three complexes, and the different wavelengths gave similar results, only the results for 330 nm will be presented. The dependence of the oxidative addition reaction between CH_3I and $Rh(H_3CCOCHCOCH_3)CO(C_6H_5XPPh_2)$, where X = O **(11)**, S **(14)** and NH (**15**) on temperature and the concentration of the methyl iodide as monitored by UV/Vis is illustrated

in (**Figure 3. 13)**. Rate constants obtained by UV/Vis are summarised in **Table 3. 7**

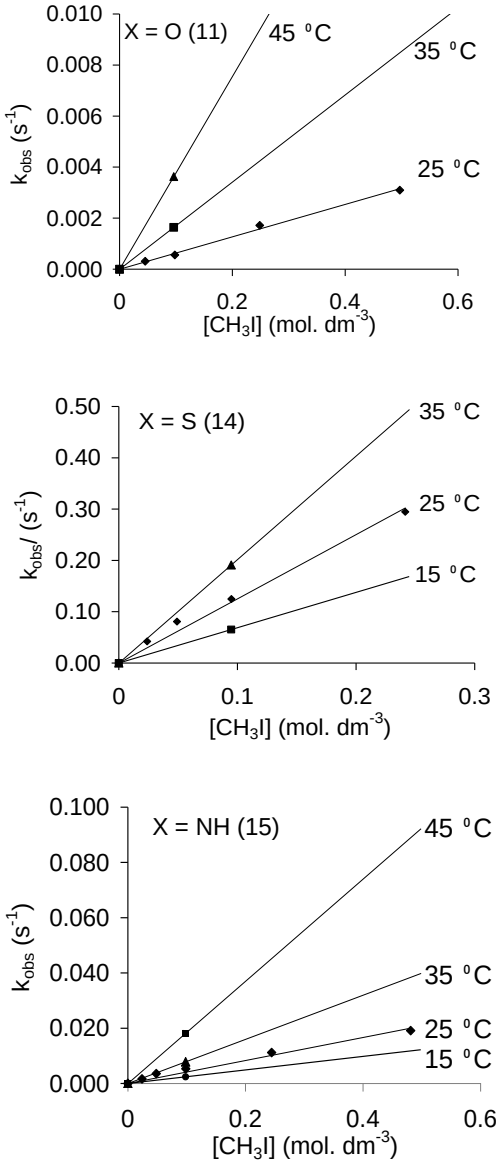

Figure 3. 13. The temperature and methyl iodide concentration dependence of the oxidative addition reaction between CH_3I and $Rh(H_3CCOCHCOCH_3)CO(C_6H_5XPPh_2)$, where X = O (11), S (14) and NH (15) as monitored by UV/Vis

Table 3. 7. Kinetic rate constants, activation parameters and Pauling electronegativity (χ_R) for the UV/Vis-monitored reaction between CH_3I and 11, 14 and 15.

No	X	χ_R	Temperature (°C)	k_1 (dm^3 mol^{-1} s^{-1})	ΔH* (kJ mol^{-1})	ΔS* (kJ mol^{-1} K^{-1})	ΔG* (kJ mol^{-1})
			25	0.0064	67 (3)	-60 (9)	17.9
11	O	3.44	35	0.0171			
			45	0.0378			
			15	0.6892	37 (2)	-118 (6)	35.2
14	S	2.58	25	1.2517			
			35	2.018			
			15	0.0245	48 (5)	-108 (15)	32.2
15	NH		25	0.0417			
		3.04	35	0.0798			
			45	0.1850			

The enthalpy (ΔH*) and the entropy (ΔS*) for the oxidative addition of CH_3I onto $Rh(H_3CCOCHCOCH_3)CO(C_6H_5XPPh_2)$, where X = O **(11)**, S **(14)** and NH (**15**), were determined from the least-square-fits (Scientist 3.0) of the first order rate constants (k_1) *vs* temperature (see **Figure 3. 14**) according to the Eyring equation:

$$\ln \frac{k_i}{T} = -\frac{\triangle H^*}{RT} + \frac{\triangle S^*}{R} + \ln \frac{R}{Nh}$$

where k_B is the Boltzmann's constant (1.38×10^{-23} $m^2.kg.s^{-2}.K^{-1}$), h is Planck's constant (6.62×10^{-34} $m^2.kg.s^{-2}$) and R is the universal gas constant (8.314 $J.K^{-1}.mol^{-1}$). The linear Eyring plots of $\ln(k_1/T)$ *vs* 1/T has a slope of $-\Delta H^*/R$ and an intercept of $\{\ln(k_B/h) + \Delta S^*/R\} = \{23.760 + \Delta S^*/R\}$. These linear relationships are illustrated in (**Figure 3. 14)**. The Gibbs free energy of activation can now be calculated from the equation $\Delta G^* = \Delta H^* - T\Delta S^*$.[99] The activation parameter ΔH*, ΔS* and ΔG* at 298 K are tabulated in **Table 3. 7**

The large negative entropy values ($\Delta S^* = -60$ (for **11**), -118 (for **14**) and -108 (for **15**) kJ mol^{-1} K^{-1}) confirms the associative mechanism of the CH_3I onto the Rh (I) center.

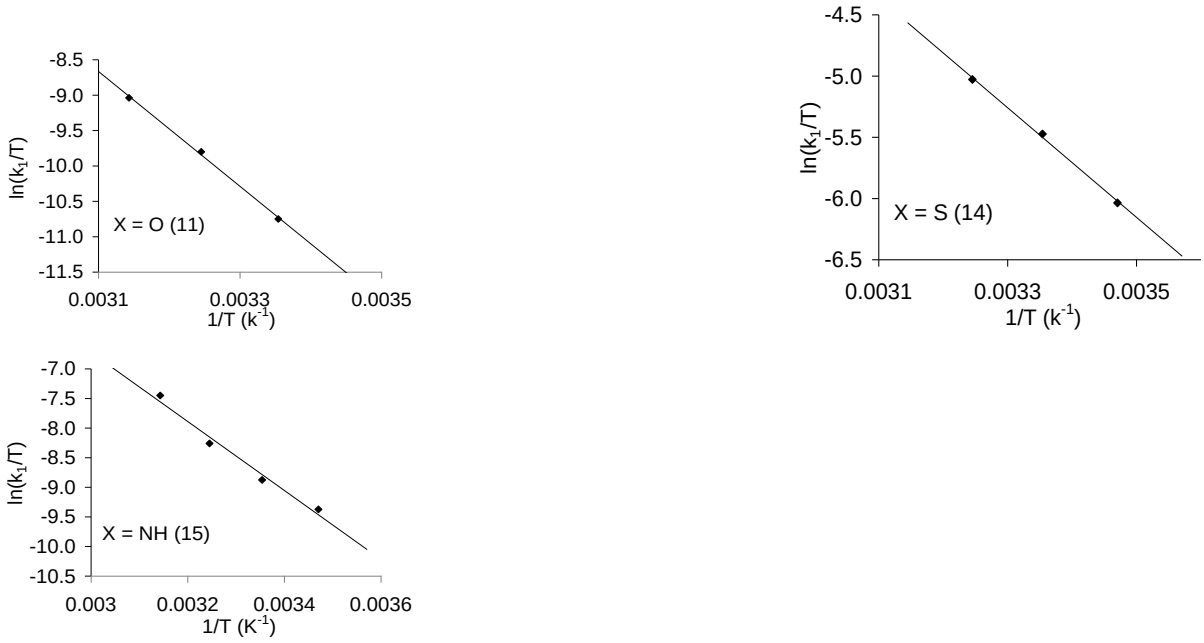

Figure 3. 14. Eyring plots of ln(k_1/T) vs 1/T for Rh($H_3CCOCHCOCH_3$)CO($C_6H_5XPPh_2$), where X = O (11), S (14) and NH (15) measured at temperatures ranging from 15 – 45°C.

Comparison of the Pauling group electronegativity of the oxygen, sulphur and nitrogen molecules in Rh($H_3CCOCHCOCH_3$)CO($C_6H_5XPPh_2$), where X = O **(11)**, S **(14)** and NH (**15**) and their first order rate constant measured at 25°C for the oxidative addition of methyl iodide are shown in (**Figure 3. 15**). A linear trend does not exist, however as the Pauling electronegativity of X increases (S < N < O), the first order rate constant (k_1) decreases. This implies that when electron density is moved away from the Rh(I) center, oxidative addition is more difficult. This is to be expected since during oxidative addition the oxidation state of the rhodium center changes from Rh(I) to Rh(III), which implies that the rhodium loses two electrons and when electron density is moved (pulled) away from the rhodium, it will be more difficult to be oxidised.

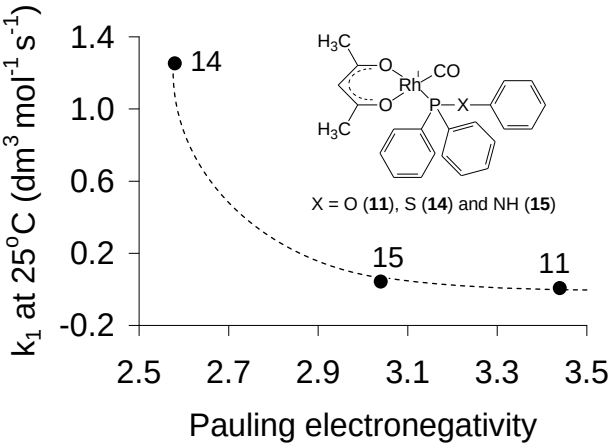

Figure 3. 15. Comparative graph between the Pauling electronegativity of O, S and N, and the first order rate constant at 25°C between CH_3I and $Rh(H_3CCOCHCOCH_3)CO(C_6H_5XPPh_2)$, where X = O (11), S (14) and NH (15) as monitored by UV/Vis.

3.4.3. The oxidative addition of CH_3I onto $Rh(H_3CCOCHCOCH_3)CO(C_6H_5XPPh_2)$, where X = O (11), S (14) and NH (15) monitored by IR spectroscopy

To confirm that the proposed sequence of reaction as shown (**Scheme 3. 5)** is correct, the reaction was studied in chloroform at 25 °C utilizing FTIR techniques. The reaction was performed using pseudo first-order kinetic conditions, with CH_3I concentrations of 100 to 1000 fold excess over the Rh(I) concentration (*ca*. 48 x 10^{-5} M). The reaction took place during the first 15 minutes. As with the UV/Vis data, the FTIR data revealed that only one reaction step is observed, see (**Figure 3. 16)** (**11** is shown as an example).there are two Rh(lll) species formed, a Rh(lll)**a** and Rh(lll)**b** species. These species can be can be identified by the FTIR spectrum, see (**Figure 3. 16)**. The disappearance of the Rh(l) signal occurs simultaneously and on the same time scale as the appearance of the two new Rh(lll)**a** and Rh(lll)**b** species. Since the two Rh(lll)-alkyl species appear at same rate, they appear to be in equilibrium. The next reaction step, which is normally the formation of the Rh(III)-acyl species is not excluded, but within the time frame used for this reaction no further reaction was observed.

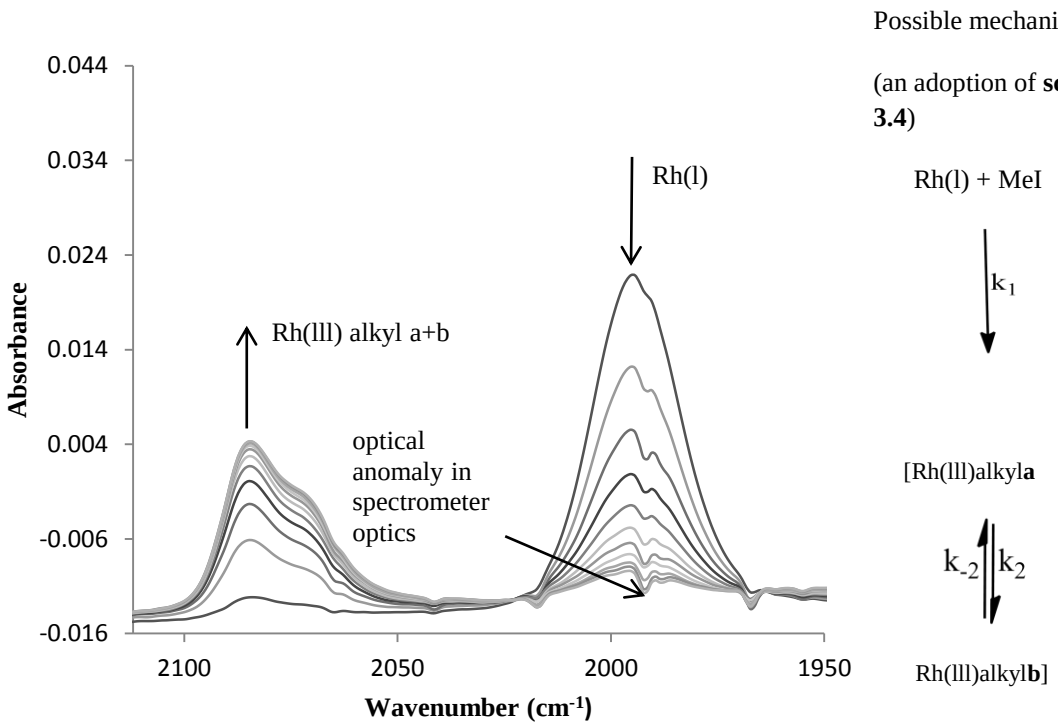

Figure 3. 16. Oxidative addition of CH_3I to the rhodium complex, $Rh(H_3CCOCHCOCH_3)CO(C_6H_5OPPh_2)$, 11, (shown as an example) monitored by infrared in chloroform at 25 °C. The change in absorbance (at 1995 and 2085 cm^{-1}) *vs* time was used to determine k_{obs}.

Because the ß-diketonato ligand $CH_3COCHCOCH_3$ is asymmetrical, the Rh(l) species cannot exist as a mixture of two isomers. Rather the shape of Rh(l) species peak above is considered to be the consequence of an electronic anomaly in the optics of the spectrometer. This can be clearly seen in the lowest amplitude scan of Rh(l) species where the optical anomaly is clearly identifiable.

The time trace of **11**, together with the graph showing the concentration dependence on methyl iodide is shown in (**Figure 3. 17)**. The kinetic rate constants determined for the oxidative addition of CH_3I onto $Rh(H_3CCOCHCOCH_3)CO(C_6H_5XPPh_2)$, where X = O **(11)**, S **(14)** and NH (**15**) is summarised in **Table 3. 8**

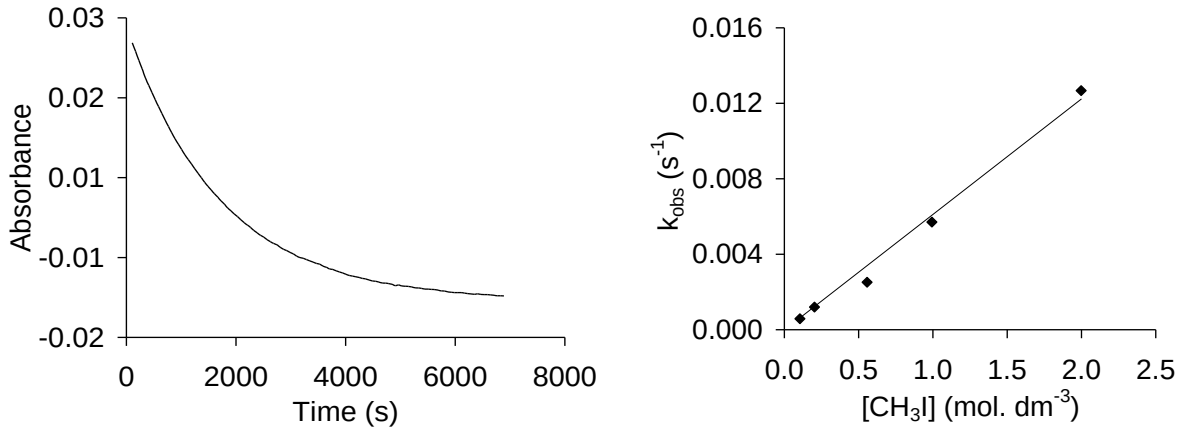

Figure 3. 17. Left: The absorbance *vs* time graph measuring the decrease in vibration height (2085 cm^{-1}) *vs* time was used to determine k_{obs}. Right: The methyl iodide concentration dependence of the oxidative addition reaction between CH_3I and $Rh(H_3CCOCHCOCH_3)CO(C_6H_5OPPh_2)$, (11), as monitored by FTIR

Table 3. 8. Kinetic rate constants and Pauling electronegativity (χ_R) for the FTIR-monitored reaction between CH_3I and 11, 14 and 15, measured in chloroform at 25°C.

No	X	χ_R	k_1 (dm^3 mol^{-1} s^{-1})
11	O	3.44	0.0061
14	S	2.58	1.22
15	NH	3.04	0.0444

The results from the FTIR study confirms that the proposed reaction scheme in (**Scheme 3. 5)**, is possible, that there is only one step present during the addition of methyl iodide onto the Rh(I) center without any carbonyl insertion. The FTIR data further shows that there are two different Rh(I) and two different Rh(III)-alkyl species present and that these two species are probably in equilibrium with each other.

3.4.4. Correlation of the kinetic rate constants of the reaction between CH_3I and $Rh(H_3CCOCHCOCH_3)CO(C_6H_5XPPh_2)$, where X = O (11), S (14) and NH (15) as obtained by various spectroscopic methods

A good correlation has been obtained for the kinetic rate constants of the oxidative addition of methyl iodide onto the Rh(I) center of $Rh(H_3CCOCHCOCH_3)CO(C_6H_5XPPh_2)$, where X = O (**11**), S (**14**) and NH (**15**) as determined from the data obtained by UV/Vis and FTIR spectroscopy see **Table 3. 9**, using chloroform as solvent at 25°C.

Table 3. 9. The kinetic rate constants of the oxidative addition of methyl iodide onto $Rh(H_3CCOCHCOCH_3)CO(C_6H_5XPPh_2)$, where X = O (11), S (14) and NH (15) as obtained by UV/Vis and FTIR spectroscopy.

No	Method	k_1 (dm^3 mol^{-1} s^{-1})
11	UV/vis	0.0064
	FTIR	0.0061
14	UV/vis	1.2517
	FTIR	- [a]
15	UV/vis	0.0417
	FTIR	0.0444

[a] stability of complex **14** was too low for reliable FTIR measurements.

3.4.5 Conclusion

This concludes the results and discussion of the research performed by the author. All goals as defined in Chapter 1 have been met. Chapter 4 gives all the experimental details that were adhered to in obtaining all the research described in this chapter while Chapter 5 summarizes compactly all the results of this study.

3.5 References

[89] L. Pauling, J. Amer. Chem. Soc. , 1932, **54**, 3570.
[90] E. Fourie, J.C. Swarts, *J. Organomet. Chem.*, 2014, **754,** 80.
[91] T.J. Hall, J.H. Hagis, *J. Org. Chem.*, 1986, **51**, 4185.
[92] E. Erasmus, *Inorg. Chim. Acta.*, 2011, **378,** 95.
[93] K.C. Kemp, E. Fourie, J. Conradie, J.C. Swarts, *Organometallics.*, 2008, **27**, 353.
[94] J. Conradie, J. Swarts, *Eur. J. Inorg. Chem.*,. 2011, 2439.
[95] J.J.C. Erasmus, J. Conradie, *Electrochim. Acta.*, 2011,**56,** 9287.
[96] J.G. Leipoldt, S.S. Basson, L.J. Botha, Inor. Chim. Acta., 1990, **168**, 215.
[97] S.S. Basson, J.G. Leipoldt, A. Roodt, J.A. Venter, T.J. van der Walt, Inorg Chim Acta, 1986, **35**,119.
[98] J. Conradie, G.J. Lamprecht, A. Roodt, J.C. Swarts, Polyhedron., 2007, **26,** 5075.
[99] P.W. Atkins, *Physical Chemistry*, 5th edition, Oxford University Press, Oxford, 1994, 939.

4 Experimental

4.1 Introduction

This chapter provides a description of the materials, equipment, techniques and experimental procedures giving the conditions for the synthesis of the ligands and complexes with certain modification of known procedures. Characterisation by spectroscopic and experimental procedures for electrochemical techniques and the kinetic study are also included.

4.2 Materials

Solid reagents (Merck, Aldrich and Fluka) employed for synthesis and liquid reagents (Merck and Aldrich) were used without further purification unless stated otherwise. Organic solvents were dried according to published procedures. For column chromatography silica gel 60 (Merck, grain size 0.040-0.063 mm) was used. Filtration and vacuum evaporation was performed with the aid of a water aspirator. Melting points were determined with the aid of an Olympus BX51 polarized microscope, fitted with a LINKAM THRM 600 heating stage (temperatures are uncorrected).

4.3 Spectroscopic measurements

^{1}H and ^{31}P Nuclear magnetic resonance (NMR) spectra were measured at 298 K on a Bruker Avance DPX 300 NMR spectrometer. All ^{1}H (NMR) chemical shifts are reported relative to

TMS ($Si(CH_3)_4$) at 0.00 ppm, whereas the ^{31}P (NMR) relative to 85 % H_3PO_4 (0 ppm) as external standards. Under these conditions, the $CHCl_3$ ^1H NMR signal in $CDCl_3$ was at 7.27 ppm, while traces of water in the $CDCl_3$ was measured at 1.60 ppm. All spectra have been provided in the appendix. The solid as well as the liquid phase FTIR adsorption spectra were measured using a Bruker Tensor 27 infrared spectrophotometer fitted with a Pike MIRacle single bounce diamond ATR crystal, running OPUS software (Version 1.1).

4.4 Electrochemistry

Cyclic voltammetry (CV) was carried out on a Princeton Applied Research PARSTAT 2273 advanced electrochemical workstation interfaced with a computer and recorded using PowerSuite (Version 2.58). A three electrode configuration was used, which consisted of a Pt auxiliary electrode, a glassy carbon working electrode and a platinum reference electrode. The glassy carbon working electrode (surface area 3.14 mm^2) was utilized after polishing on a Buhler polishing mat first with 1 micron and then with ¼ micron diamond paste. Measurements were conducted on *ca*. 0.2 mmol dm^{-3} solutions of the both the ligands and complexes in acetonitrile containing 0.2 mol dm^{-3} $[NnBu_4][B(C_6F_5)_4]$ as supporting electrolyte at 25°C. Experimental potentials were measured against a platinum reference electrode, but the results presented are referenced versus the ferrocene couple, FcH/FcH^+, as an internal standard as suggested by IUPAC.[100] To achieve this, each experiment was performed first in the absence of the ferrocene and then repeated in the presence of the ferrocene. Data were then manipulated on a Microsoft excel worksheet to set the formal reduction potentials of the FcH/FcH^+ couple at 0V. Ferrocene exhibited a formal reduction potential $E^{\circ\prime}$ = 70 mV *vs* platinum with a peak separation $\Delta E = \Delta E_{pa} - \Delta E_{pc}$ = 80 mV and i_{pc}/i_{pa} =1.00, under these experimental conditions.

4.5 Kinetic studies

The methyl iodide oxidative addition onto the various Rhodium complexes was studied by means of FTIR, at 25 °C in a KCl liquid cell connected to a water bath for temperature control, while monitoring the disappearance of the Rh(I) and formation of the Rh(III)

carbonyl peaks. This reaction was also followed using UV-Vis of the dilute rhodium complexes in quartz cuvettes on a Shimadzu UV/Vis spectrometer. At least three temperature ranges between 15-45 °C was monitored, from which the activation parameters ΔH^* and ΔS^* were obtained. Chloroform was used as solvent and passed through basic alumina just before use to make it acid free. All kinetic measurements were monitored under pseudo first-order conditions with a 500-2000 times molar excess of CH_3I over the concentration of the rhodium complex. Pseudo first-order rate constants, k_1, were calculated using MicroMath Scientist 2.0 program.

4.6 Synthesis

4.6.1 Synthesis of phosphinite ligands

Three of the phosphinite ligands; **6-8**, were prepared according to the same adopted procedure by Bedford *et al.*[101] while the other two organophosphate ligands, **9** and **10**, were prepared using the adopted procedure by Balakrishna *et al.*[102]

4.6.1.1 Phenyl diphenylphosphinite, $C_6H_5OPPh_2$, 6

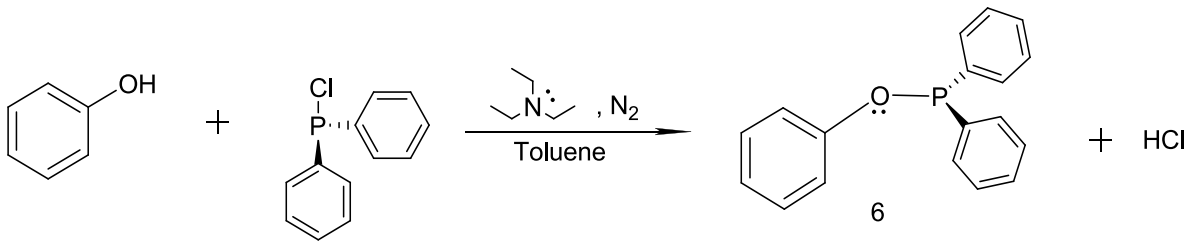

Phenol (2.0 g; 21.3 mmol) and chlorodiphenylphosphine (4 ml; 22.1 mmol) was dissolved in 40 ml toluene and the resulting solution was allowed to stir for 15 min. Triethylamine (4.2 ml; 30.1 mol) was added dropwise to the stirring solution; this resulted in the formation of a cloudy substance floating on the solution. The resulting reaction mixture was refluxed for 18 h. After cooling down to room temperature, the volatiles were removed by vacuum evaporation and the residue was extracted with THF (10 ml). The resultant solution was filtered through a celite plug. The solvent was removed from the filtrate under vacuum. The

colourless oil was purified by means of column chromatography using hexane: ethyl acetate 2:1 as the eluent to yield 1.19 g (20 %) of pure oily $C_6H_5OPPh_2$, R_f = 0.87 (hexane:ethyl acetate 2:1) ^{1}H NMR: δ_H (300 MHz, $CDCl_3$)/ ppm: 7.10 (1H, t, CH); 7.25 (2H, m, CH); 7.35 (2H, m, CH); 7.47 (6H, m, CH); 7.670 (4H, m, CH). ^{31}P NMR (CH_2Cl_2): δ (ppm) 110.67. See NMR spectra A1 and A11 in Appendix.

4.6.1.2 Bis(*P,P*-diphenyl)-*P,P*-1,4-phenylene ester. *para*-$Ph_2POC_6H_4OPPh_2$, 7

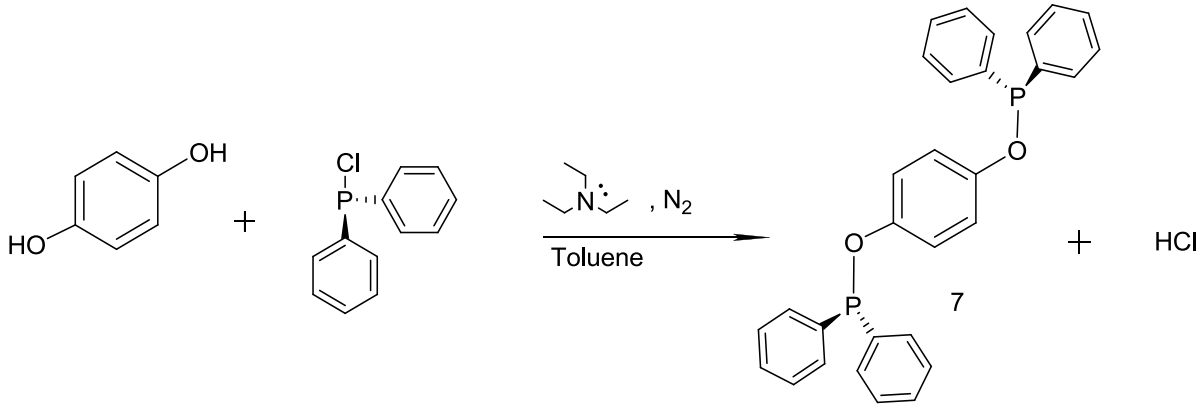

Hydroquinone (1.0 g; 9.08 mmol) and chlorodiphenylphosphine (3.4 ml; 19.07 mmol) were dissolved in 40 ml toluene. The resulting solution was allowed to stir for 15 min. Triethylamine (3.4 ml; 22.4 mmol) was added dropwise to the stirring solution; this resulted in the formation of a cloudy substance floating on the solution. The resulting reaction mixture was refluxed for 18 h. After cooling down to room temperature, the volatiles were removed under vacuum and the residue was extracted with THF (10 ml). The resultant solution was filtered through a celite plug. The solvent was removed from the filtrate under vacuum. The light yellow oil was purified by means of column chromatography using hexane: ethyl acetate 2:1 as the eluent to yield 0.89 g (20 %) of pure *para*-$Ph_2POC_6H_4OPPh_2$ as clear crystals. Melting point 130 °C, R_f = 0.87 (hexane:ethyl acetate 2:1) ^{1}H NMR: δ_H (300 MHz, $CDCl_3$)/ ppm: 7.03 (4H, s, CH); 7.41 (12H, m, CH); 7.61 (8H, m, CH) ^{31}P NMR [(CH_2Cl_2): δ (ppm) 112.38. See NMR spectra A2 and A12 in Appendix.

4.6.1.3. Bis(*P,P*-diphenyl)-*P,P*-1,3-phenylene ester, *meta*-$Ph_2POC_6H_4OPPh_2$, 8

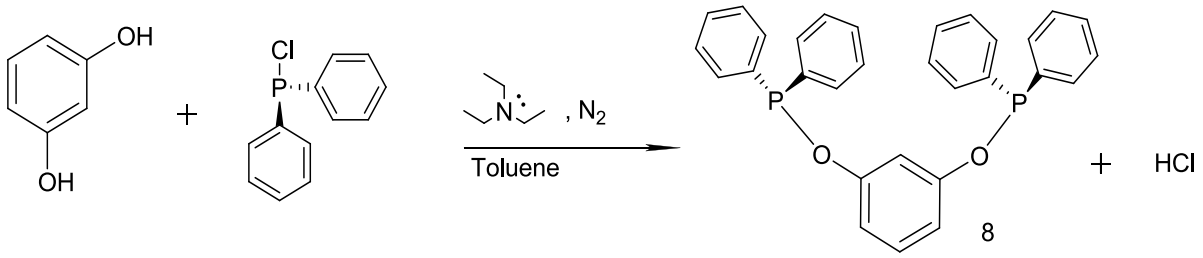

Resorcinol (1.0 g; 9.08 mmol) and chlorodiphenylphosphine (3.4 ml; 19.07 mmol) was dissolved in 40 ml toluene. The resulting solution was allowed to stir for 15 min. Triethylamine (3.2 ml; 21.1 mmol) was added dropwise to the stirring solution; this resulted in the formation of a cloudy substance floating on the solution. The resulting reaction mixture was refluxed for 18 h. After cooling down to room temperature, the volatiles were removed under vacuum and the residue was extracted with THF (10 ml). The resultant solution was filtered through a celite plug. The solvent was removed from the filtrate under vacuum to yield 2.54 g (58.3 %) of pure *meta*-$Ph_2POC_6H_4OPPh_2$ as white crystals. Melting point 61 ^{0}C, R_f = 0.9 (hexane:ethyl acetate 2:1) ^{1}H NMR: δ_H (300 MHz, $CDCl_3$)/ ppm: 6.88 (2H, d, CH); 7.03 (1H, s, CH); 7.18 (1H, t, CH); 7.42 (12H, m, CH); 7.60 (8H, m, CH) ^{31}P NMR (CH_2Cl_2): δ (ppm) 110.78. See NMR spectra A3 and A13 in Appendix.

4.6.1.4 Diphenylphosphinothious acid, $C_6H_5SPPh_2$, 9

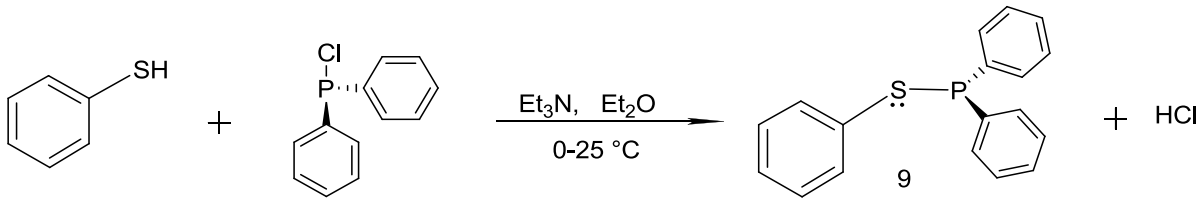

Chloro diphenylphosphine (3.8 ml, 21.2 mmol) dissolved in diethyl ether (10 ml) was added dropwise to mixture of thiophenol (2 ml, 19.5 mmol) and triethylamine (3 ml, 21.5 mmol) dissolved in 30 ml diethyl ether over a period of 15 min with constant stirring in an ice-bath. The ice-bath was removed and the reaction mixture was allowed to reach room temperature

and the stirring was continued for a further 18 h. The hydrochloride salt which formed was filtered off through a celite plug and all volatiles were removed under vacuum. The residue was recrystallized from ethanol to yield 3.49 g (60 %) of pure $C_6H_5SPPh_2$ as a white crystalline compound. Melting point 51 °C, R_f = 0.87 (hexane:ethyl acetate 2:1) ^{1}H NMR: δ_H (300 MHz, $CDCl_3$)/ ppm: 7.30 (3H, m, CH); 7.41 (6H, m, CH); 7.56 (2H, m, CH); 7.65 (4H, m, CH) ^{31}P NMR (CH_2Cl_2): δ (ppm) 41.60. See NMR spectra A4 and A14 in Appendix.

4.6.1.5 Diphenylphosphino amide $C_6H_5NHPPh_2$, 10

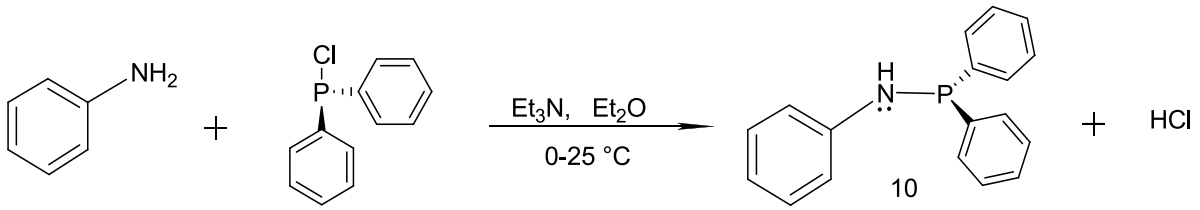

Chloro diphenylphosphine (4 ml, 22.3 mmol) dissolved in diethyl ether (10 ml) was added dropwise to mixture of aniline (2 ml, 21.9 mmol) and triethylamine (3.6 ml, 25.8 mmol) dissolved in 30 ml diethyl ether over a period of 15 min with constant stirring in an ice-bath. The ice-bath was removed and the reaction mixture was allowed to reach room temperature and the stirring continued for a further 18 h. The hydrochloride salt which formed was filtered off through a celite plug and all volatiles were removed under vacuum. The residue was recrystallized from ethanol to yield 2.05 g (33.7 %) of pure $C_6H_5NHPPh_2$ as a white crystalline compound. Melting point 72 °C, R_f = 0.9 (hexane:ethyl acetate 2:1) ^{1}H NMR: δH (300 MHz, $CDCl_3$)/ ppm: 4.42 (1H, d, NH); 6.75 (1H, t, CH); 7.12 (2H, d, CH); 7.34 (2H, t, CH); 7.45 (6H, m, CH); 7.57 (4H, m, CH) ^{31}P NMR (CH_2Cl_2): δ (ppm) 68.54. See NMR spectra A5 and A15 in Appendix.

4.6.2 Synthesis of the Rhodium complexes

All the rhodium complexes where prepared according to the same adopted procedure by Conradie *et al.*[103]

4.6.2.1 [Rh(acac)CO($C_6H_4OPPh_2$)], 11

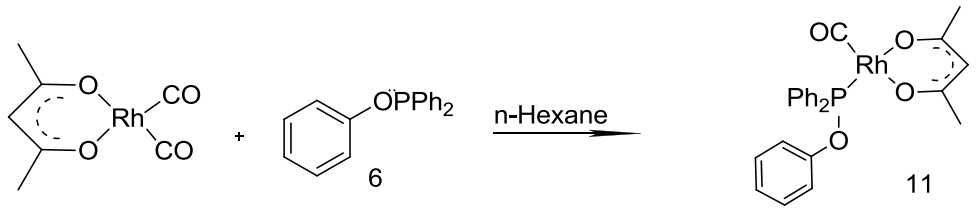

A solution of phenyl diphenylphosphinite (59 mg; 0.21 mmol) in 5 ml hot dry *n*-hexane was added dropwise to a boiling solution of dicarbonyl-acetylacetonato-rhodium (I) (50 mg; 0.19 mmol) in dry *n*-hexane (10 ml). This solution was allowed to boil for a further 5 min, followed by the filtration of the solution while still hot. Thereafter the volatiles where removed in *vacuo* to yield 84 mg (85%) of pure [Rh(acac)CO($C_6H_4OPPh_2$)] as a dark-brown product. Melting point 91 ^{0}C, *v* (CO) = 1987 cm^{-1} δ_H (300 MHz, $CDCl_3$)/ppm: 1.6 (3H, s, CH_3); 2.08 (3H, s, CH_3); 5.44 (1H, s, CH); 7.05-7.16 (1H, t, CH); 7.21-7.37 (4H, m, CH); 7.40-7.51 (6H, m, CH); 7.85-7.99 (4H, m, CH) ^{31}P NMR (CH_2Cl_2): δ (ppm): 137.26 - 138.87 (d, $^1J_{Rh-P}$ =205.40 Hz). See NMR spectra A6 and A16 in Appendix.

4.6.2.2 [(Rh(acac)CO($Ph_2POC_6H_4$-*p*-$OPPh_2$)], 12

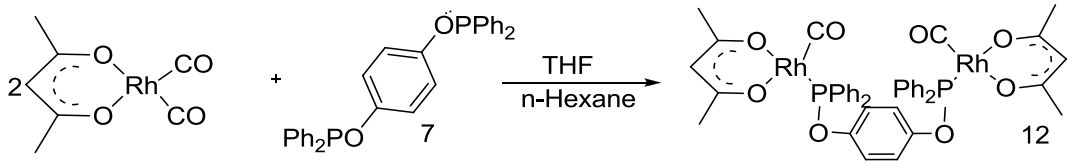

A solution of bis(*P*,*P*-diphenyl)-*P*,*P*-1,4-phenylene ester (47 mg; 0.19 mmol) in 10 ml hot dry *n*-hexane was added dropwise to a boiling solution of dicarbonyl-acetylacetonato-rhodium (I) (50 mg; 0.19 mmol) in dry *n*-hexane (10 ml). This solution was allowed to boil for a further 5 min, followed by the filtration of the solution while still hot. Thereafter the volatiles where removed in *vacuo* to yield 155 mg (84%) of pure [(Rh(acac)CO($Ph_2POC_6H_4$ *p*-$OPPh_2$)] as a yellow product. Melting point 79 ^{0} C, *v* (CO) = 1988 cm^{-1} (300 MHz, CDCl3)/ppm: 1.58 (3H, s, CH3); 2.08 (3H, s, CH3); 5.44 (1H, s, CH); 7.15 (2H, s, CH); 7.41-7.46 (6H, m, CH); 7.82-7.90 (4H, m, CH) 31P NMR (CH2Cl2): δ (ppm): 138.31 – 139.94 (d, 1JRh-P =197.15 Hz). See NMR spectra A7 and A17 in Appendix.

4.6.2.3 [(Rh(acac)CO($Ph_2POC_6H_4$-*m*-$OPPh_2$)], 13

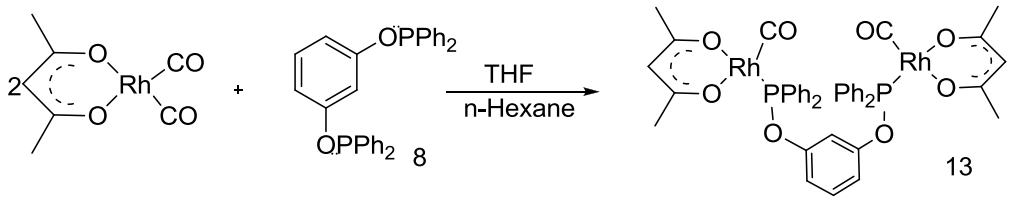

A solution of bis(*P*,*P*-diphenyl)-*P*,*P*-1,3-phenylene ester (47 mg; 0.19 mmol) in 10 ml hot dry *n*-hexane was added dropwise to a boiling solution of dicarbonyl-acetylacetonato-rhodium (I) (50 mg; 0.19 mmol) in dry *n*-hexane (10 ml). This solution was allowed to boil for a further 5 min, followed by the filtration of the solution while still hot. Thereafter the volatiles where removed in *vacuo* to yield 138 mg (76%) of pure [(Rh(acac)CO($Ph_2POC_6H_4$ *m*-$OPPh_2$)] as a yellow product. Melting point 107 ^{0} C, *v* (CO) = 1986 cm^{-1}. δ_H (300 MHz, $CDCl_3$)/ppm: 1.59 (3H, s, CH_3); 2.10 (3H, s, CH_3); 5.45 (1H, s, CH); 7.09 (1H, s, CH); 7.28 (1H, s, CH); 7.37-7.53 (6H, m, CH); 7.75-7.98 (4H, m, CH) ^{31}P NMR (CH_2Cl_2): δ (ppm): 137.48 - 139.10 (d, $^1J_{Rh-P}$ =205.40 Hz). See NMR spectra A8 and A18 in Appendix.

4.6.2.4 [Rh(acac)CO($C_6H_4SPPh_2$)], 14

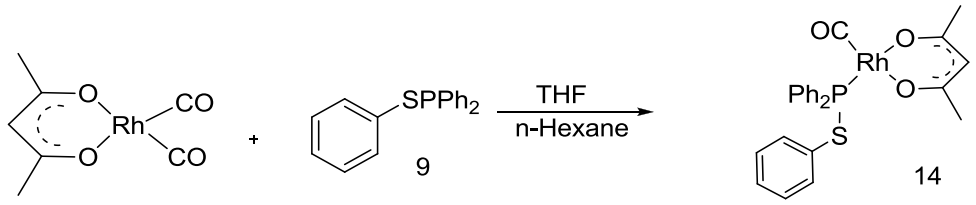

A solution of diphenylphosphinothious acid (47 mg; 0.19 mmol) in 5 ml hot dry *n*-hexane was added dropwise to a boiling solution of dicarbonyl-acetylacetonato-rhodium (I) (50 mg; 0.19 mmol) in dry *n*-hexane (10 ml). This solution was allowed to boil for a further 5 min, followed by the filtration of the solution while still hot. Thereafter the volatiles where removed in *vacuo* to yield 58 mg (58 %) of pure [Rh(acac)CO($C_6H_4SPPh_2$)] as a yellow product. Melting point 114 ^{0} C, *v* (CO) = 1981 cm^{-1} δ_H (300 MHz, $CDCl_3$)/ppm: 1.62 (3H, s, CH_3); 2.06 (3H, s, CH_3); 5.41 (1H, s, CH); 7.08-7.17 (2H, t, CH); 7.21-7.25 (1H,dd, CH); 7.30-7.44 (8H, m, CH); 7.73-7.84 (4H, m, CH) ^{31}P NMR (CH_2Cl_2): δ (ppm): 83.59-85.15 (d, $^1J_{Rh-P}$ =190.35 Hz). See NMR spectra A9 and A19 in Appendix.

4.6.2.5 [Rh(acac)CO($C_6H_4NHPPh_2$)], 15

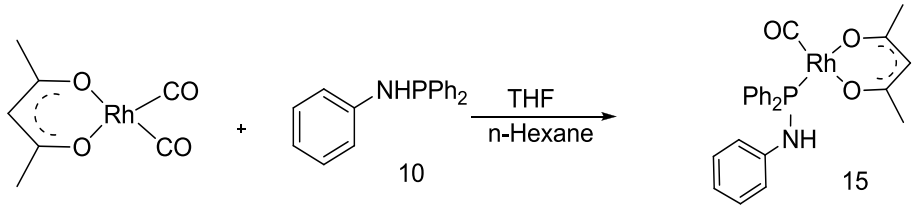

A solution of diphenylphosphino amide (41 mg; 0.15 mmol) in 5 ml hot dry *n*-hexane was added dropwise to a boiling solution of dicarbonyl-acetylacetonato-rhodium (I) (37 mg; 0.15 mmol) in dry *n*-hexane (10 ml). This solution was allowed to boil for a further 5 min, followed by the filtration of the solution while still hot. Thereafter the volatiles were removed in *vacuo* to yield 34 mg (44%) of pure [(Rh(acac)CO($Ph_2POC_6H_4$-*m*-$OPPh_2$)] as a brown/black product. Melting point 134 ^{0} C, *v* (CO) = 1986 cm^{-1} δ_H (300 MHz, $CDCl_3$)/ppm: 2.20 (3H, s, CH_3); 2.66 (3H, s, CH_3); 3.84 (1H, s, NH); 5.59 (1H, s, CH); 6.63-6.72 (2H, d, CH); 6.76-6.85 (1H, t, CH); 7.00-7.10 (2H, t, CH); 7.41-7.49 (6H, m, CH); 7.83-7.92 (4H, m, CH) ^{31}P NMR (CH_2Cl_2): δ (ppm): 67.31-68.72 (d, $^1J_{Rh-P}$ =171.56 Hz). See NMR spectra A10 and A20 in Appendix.

This concludes the experimental part of this study.

4.7 References

[100] G. Gritzner, J. Kuta, Pure Appl. Chem., 1984, **56,** 461.
[101] R. B. Bedford, S. M. Draper, P. N. Scully, S. L. Welch, New J. Chem., 2000, **24**, 747.
[102] M. S. Balakrishna, D. Suresha, P. Kumar, J. T. Mague, Journal of Organometallic Chemistry., 2011, **696**, 3616.
[103] J. Conradie, G.J. Lamprecht, S. Otto, J.C. Swarts, Inorganica Chimica Acta., 2002, **328**,192.

5 Summary and Future Perspectives

5.1. Summary

In this study, different organophosphorus ligands were synthesised, which included the phosphinites of the type, $C_6H_5OPPh_2$, *meta*- and *para*-$Ph_2POC_6H_4OPPh_2$, as well as other heteroatomic organophosphorus ligands of the type $C_6H_5XPPh_2$, where X = S and NH by means of a base catalysed reaction between chlorophenylphosphine and the desired phenyl substituent. An attempt was made to prepare *ortho*-$Ph_2POC_6H_4OPPh_2$, however this was unsuccessful. The carbonyl(acetyl acetonato)organophopshorus rhodium(I) compounds, [Rh(acac)CO($C_6H_4XPPh_2$)] where X = O, S and NH, as well as [(Rh(acac)CO($Ph_2POC_6H_4$-*m*-$OPPh_2$)] and [(Rh(acac)CO($Ph_2POC_6H_4$-*p*-$OPPh_2$)], were prepared by the reaction between [Rh(acac)$(CO)_2$] and the prepared phosphorus ligands.

The kinetics of the oxidative addition of methyl iodide to the rhodium(I) complexes of the type, [Rh(acac)CO($C_6H_4XPPh_2$)] where X = O, S and NH, were explored by means of UV/Vis and FTIR studies. The reaction scheme was found to exhibit only one stage, which is the oxidative addition, within the time frame of the reactions measured in this study. No carbonyl insertion to form the acyl species was observed and no other alkyl species was observed either. The reaction followed the first order rate law:

$R = k_1[CH_3I]$

with a first order dependence on the concentration of the methyl iodide. The activation parameters ΔH* and ΔS* were determined. The entropy of the reaction for the rhodium complexes, Rh(acac)CO($C_6H_4XPPh_2$)] where X = O, S and NH were ΔS* = -60, -118 and -108 kJ mol^{-1} K^{-1} respectively. This is a strong indication that the reaction takes place according to an associative mechanism. Comparison of the first order rate constants of the different rhodium complexes with the Pauling electronegativity of O, S and N, showed that there is an exponential increase in rate constant as the Pauling group electronegativity decreases.

A good correlation has been obtained for the kinetic rate constants of the oxidative addition of methyl iodide onto the Rh(I) center of Rh($H_3CCOCHCOCH_3$)CO($C_6H_5XPPh_2$), where X = O, S and NH as determined from the data obtained by UV/Vis and FTIR spectroscopy.

An electrochemical study in the form of cyclic voltammetry was conducted on all the synthesised organophosphorus ligands, $C_6H_5XPPh_2$ where X = O and NH, *meta*- and *para*-$Ph_2POC_6H_4OPPh_2$, as well as their associated rhodium complexes, [Rh(acac)CO($C_6H_4XPPh_2$)] where X = O, S and NH, [(Rh(acac)CO($Ph_2POC_6H_4$-*m*-$OPPh_2$)] and [(Rh(acac)CO($Ph_2POC_6H_4$-*p*-$OPPh_2$)]. The redox activity of organophosphorus ligands was found to be chemically and electrochemically irreversible and showed one oxidation and one reduction peak. The oxidation peak was allocated to the one-electron oxidation of the free electron-pair on the phosphorous moiety, while the reduction peak is assigned to the reduction of the radical cation back to the neutral form.

There are two oxidation peaks, one for the rhodium metal center the other for the phosphorus moiety. The first peak is for the rhodium and the second belongs to the phosphorus. The rhodium peak O1 for all the complexes is in the region of 400-530 mV and for the phosphorus, O2, in the region of the 700-1200 mV. Both these peaks are electrochemically and chemically irreversible.

5.2. Future perspectives

Future studies in the field could concern synthesising other related organophosphorus ligands of the types $PPh(XPh)_2$, $P(XPh)_3$, where X = O, S or NH as well as their associated Rhodium complexes, $[Rh(acac)CO(PPh(XPh)_2)]$ and $[Rh(acac)CO(P(XPh)_3)]$ where X = O, S or NH. Additional synthetic studies could even include substituting the phenyl ring with other cyclic groups like cyclohexene (ch), biphenyl (bipy), naphthalene (nap) to produce $PR_2(XR)$, $PR(XR)_2$ or $P(XR)_3$, where X = O, S or NH and R = ch, bipy or nap.

Since it is known that phosphite ligands has the ability to coordinate two ligands to the rhodium center, it would be interesting to find the binding modes of rhodium complexes prepared from the above mentioned organophosporus ligands.

The testing of these compounds for oxidative addition of methyl iodide should also be investigated to find whether they can undergo the next step of the Monsanto process, the carbonyl insertion to produce the rhodium(III)-acyl species.

Many Rh-β-diketonato complexes exhibit anti-neoplastic properties; the next step would be to study their anti-tumor activity.

--oo--oOo--oo--

A Appendix ^{1}H and ^{31}P NMR

^{1}H NMR spectra

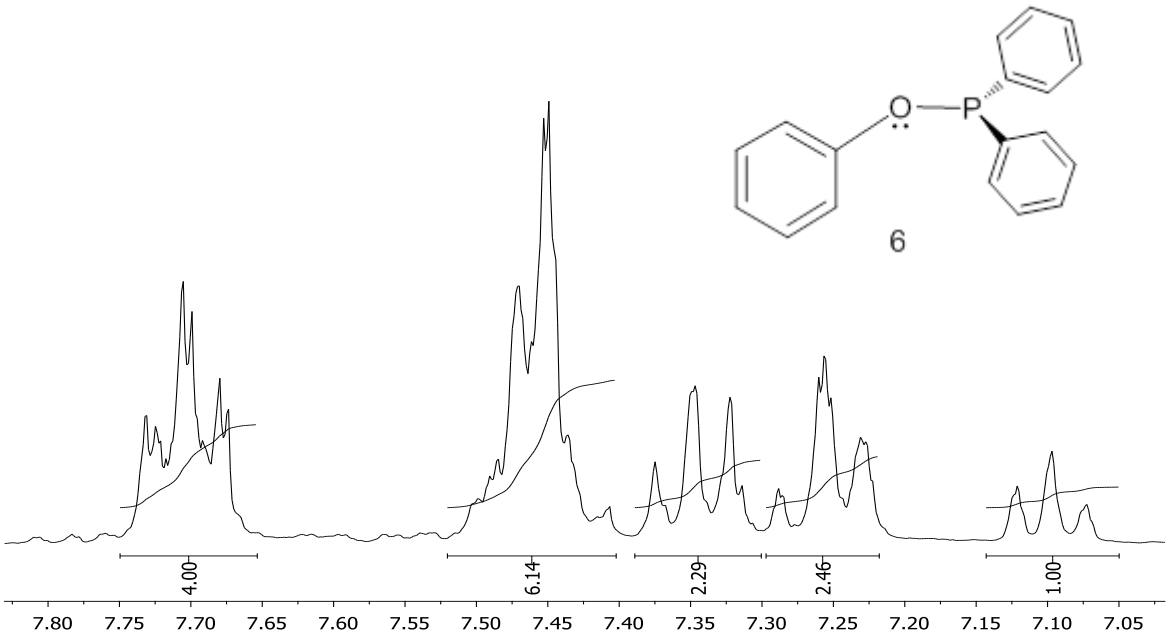

Spectrum A1: Phenyl diphenylphosphinite, $C_6H_5OPPh_2$, 6

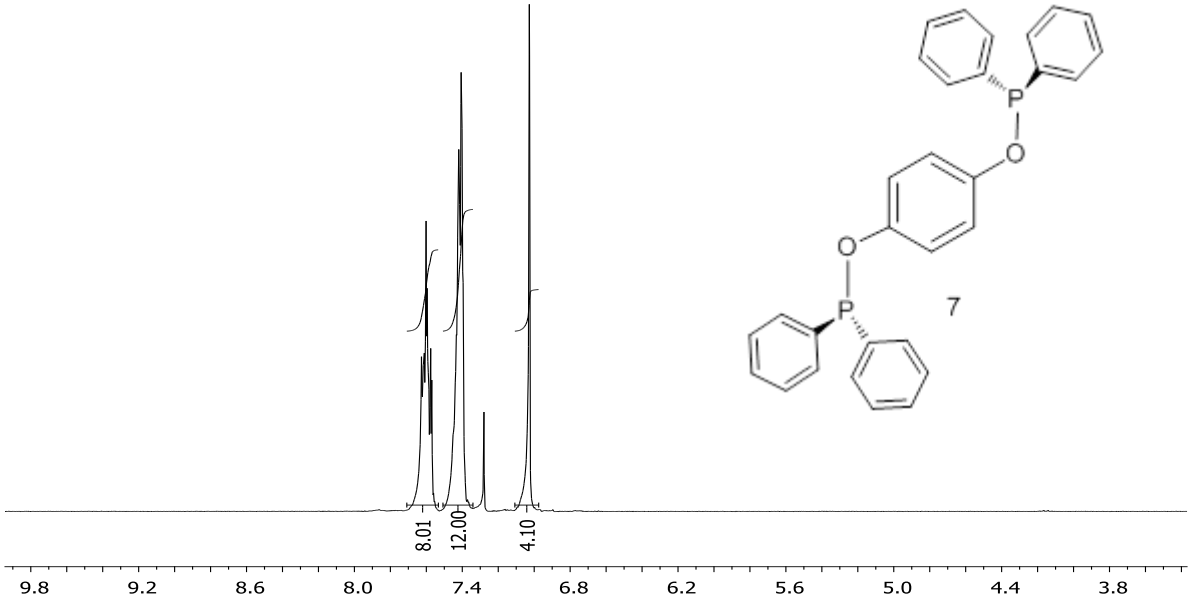

Spectrum A2: Bis(*P,P*-diphenyl)-*P,P*-1,4-phenylene ester. *para*-$Ph_2POC_6H_4OPPh_2$, 7

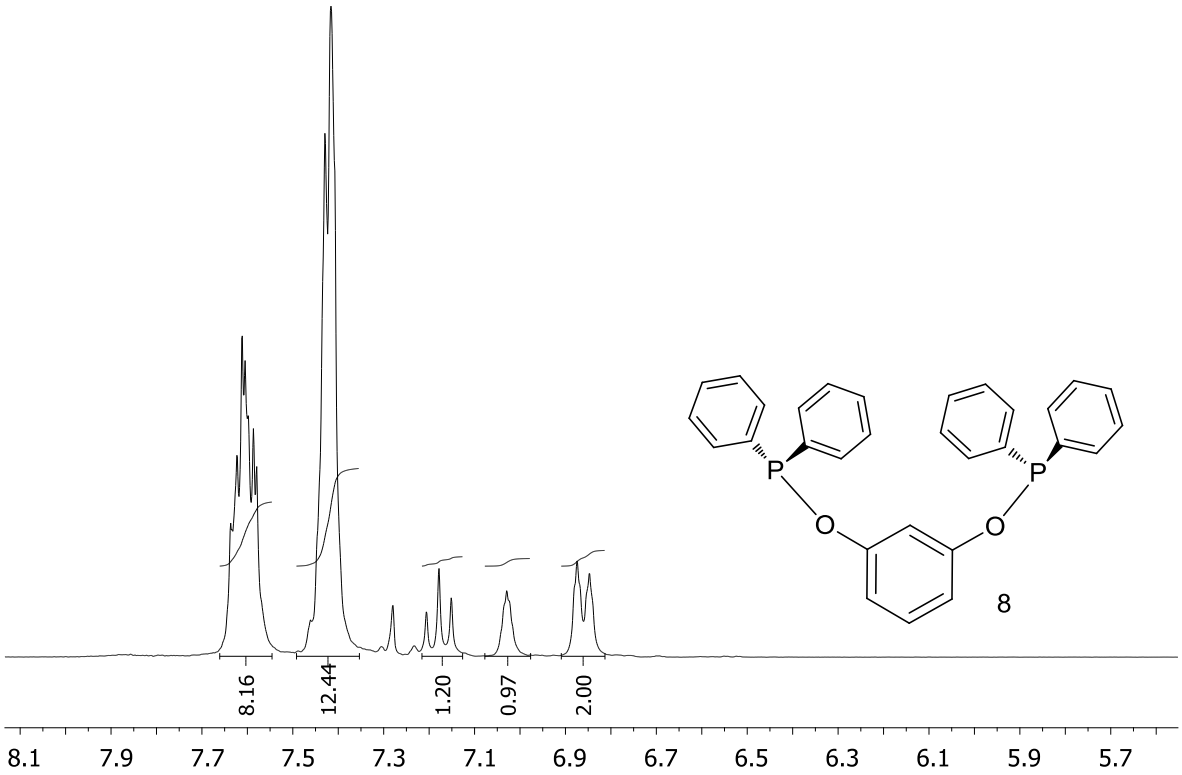

Spectrum A3: Bis(*P,P*-diphenyl)-*P,P*-1,3-phenylene ester, *meta*-$Ph_2POC_6H_4OPPh_2$, 8

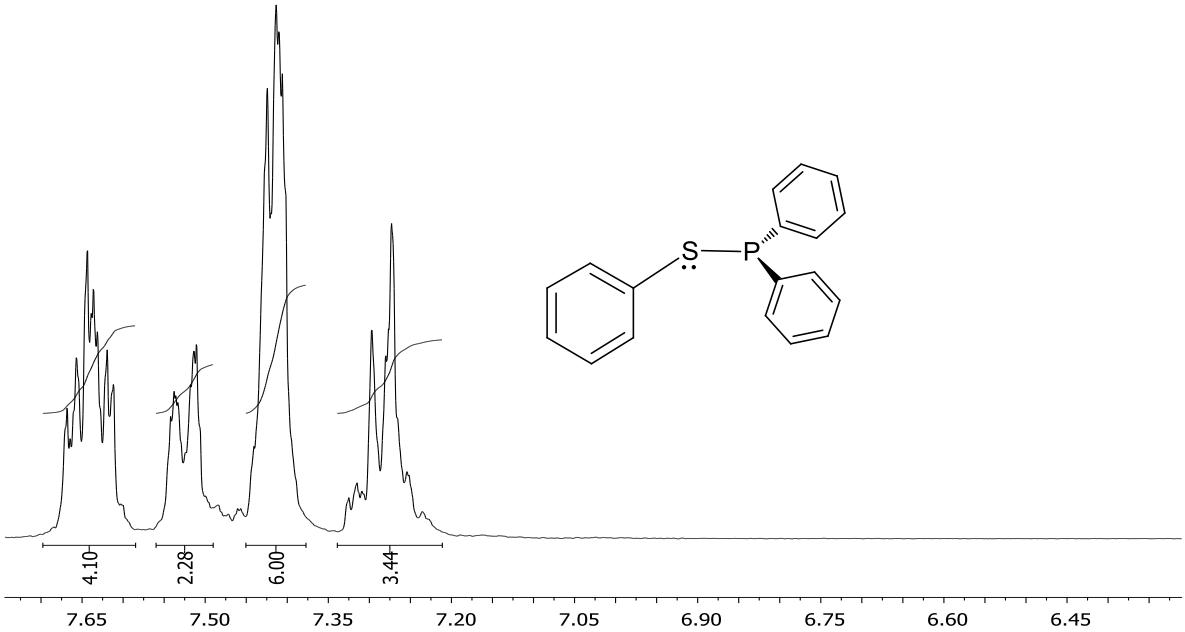

Spectrum A4: Diphenylphosphinothious acid, $C_6H_5SPPh_2$, 9

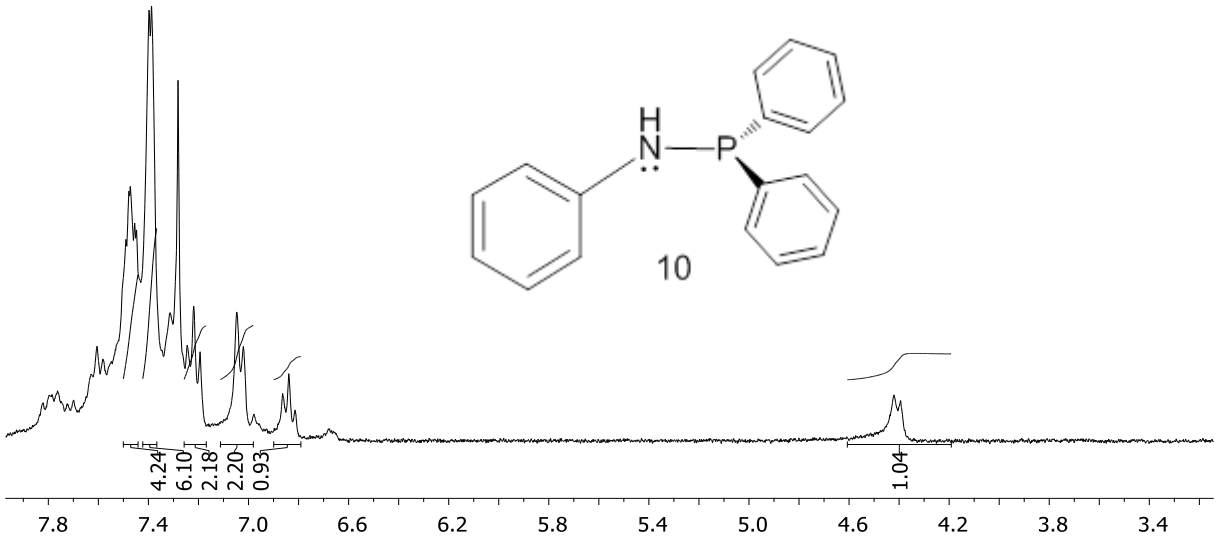

Spectrum A5: Diphenylphosphino amide $C_6H_5NHPPh_2$, 10

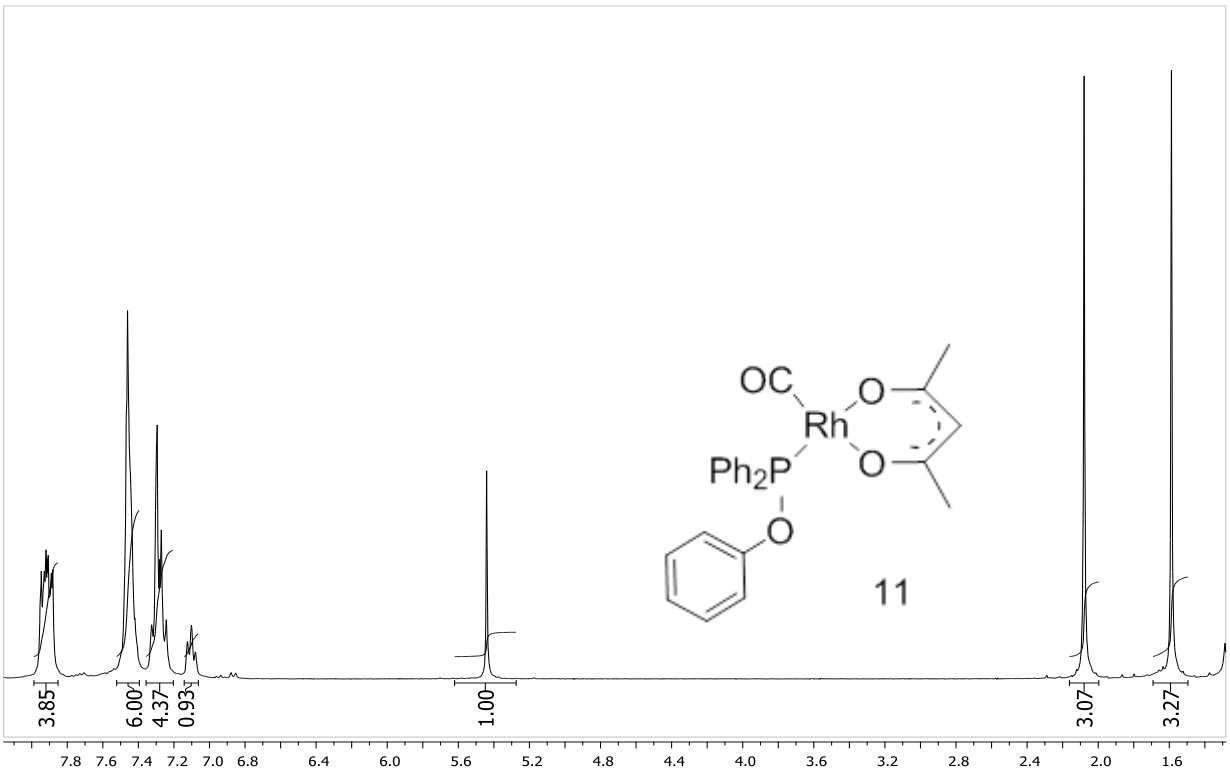

Spectrum A6: [Rh(acac)CO($C_6H_4OPPh_2$)], 11

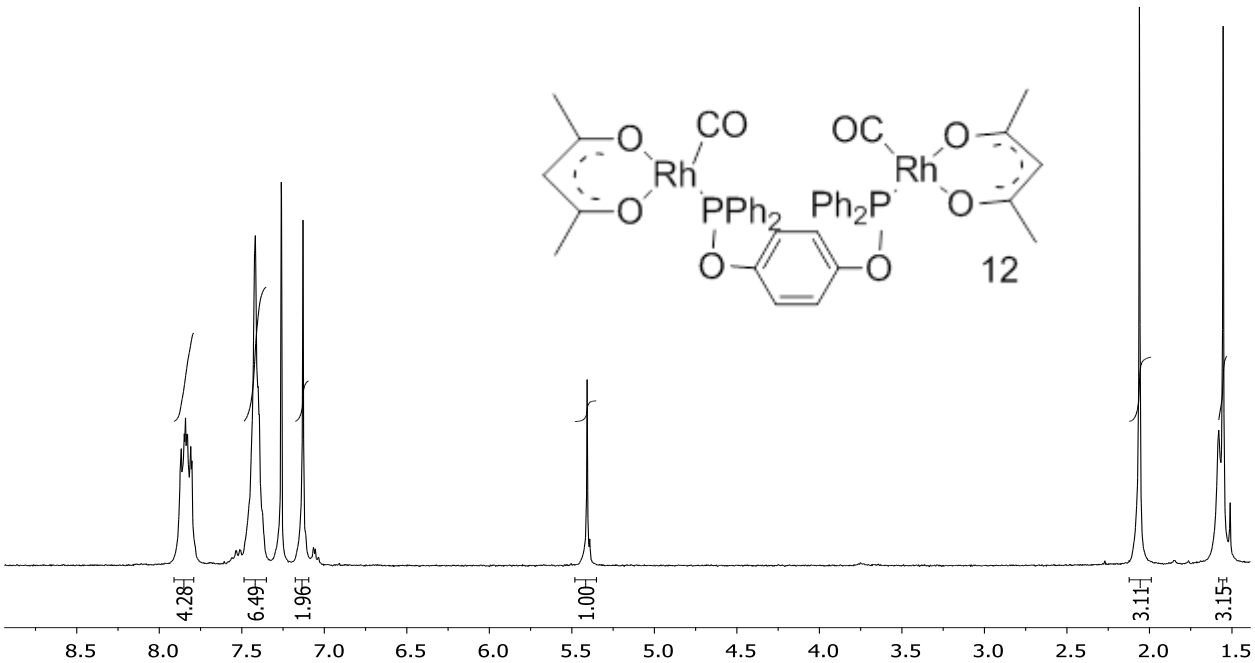

Spectrum A7: [(Rh(acac)CO($Ph_2POC_6H_4$*p*-$OPPh_2$)], 12

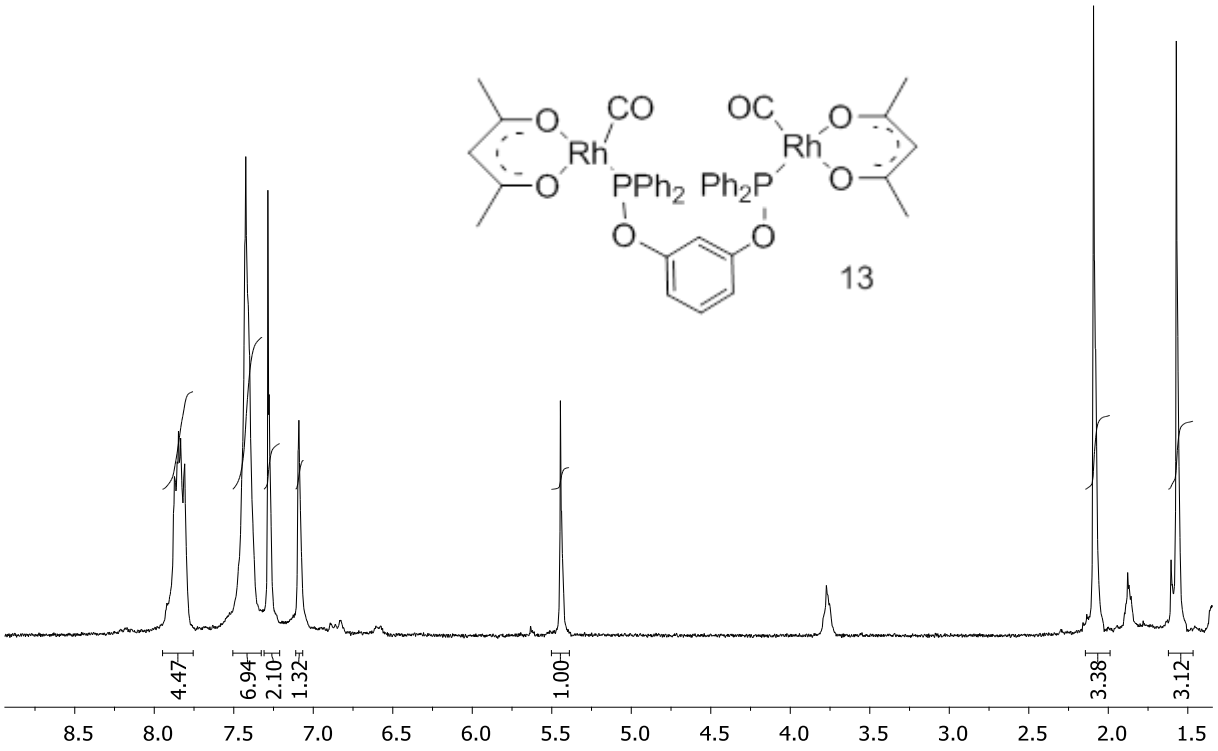

Spectrum A8: [(Rh(acac)CO($Ph_2POC_6H_4$-m-$OPPh_2$)], 13

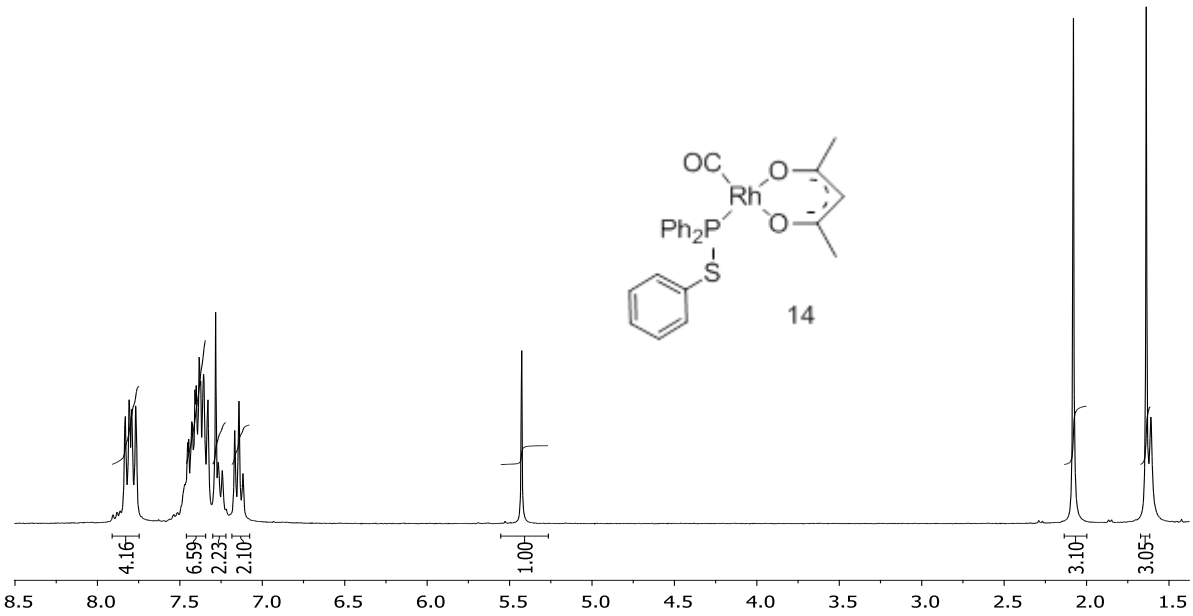

Spectrum A9: [Rh(acac)CO($C_6H_4SPPh_2$)], 14

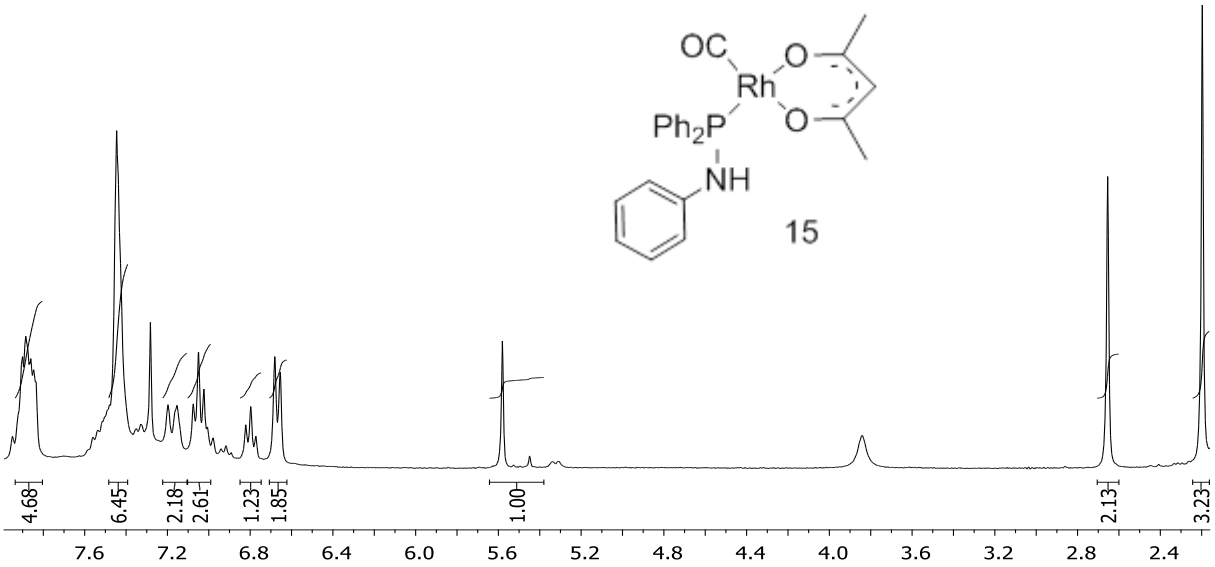

Spectrum A10: [Rh(acac)CO($C_6H_4NHPPh_2$)], 15

^{31}P NMR spectra

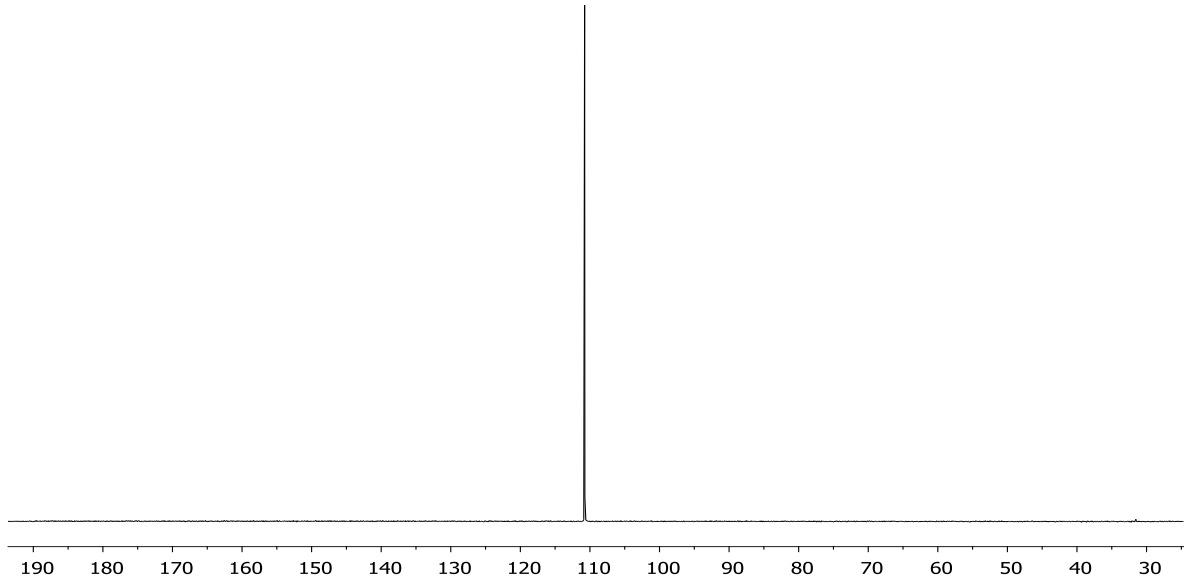

Spectrum A11: Phenyl diphenylphosphinite, $C_6H_5OPPh_2$, 6

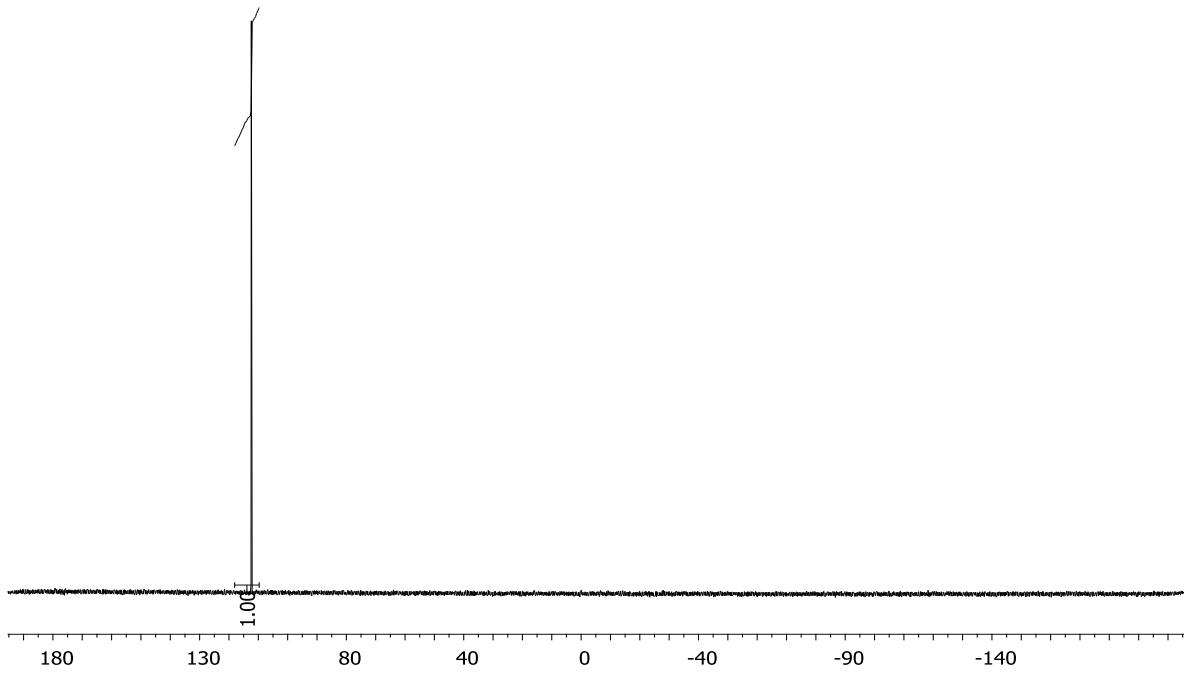

Spectrum A12: Bis(P,P-diphenyl)-P,P-1,4-phenylene ester. para-$Ph_2POC_6H_4OPPh_2$, 7

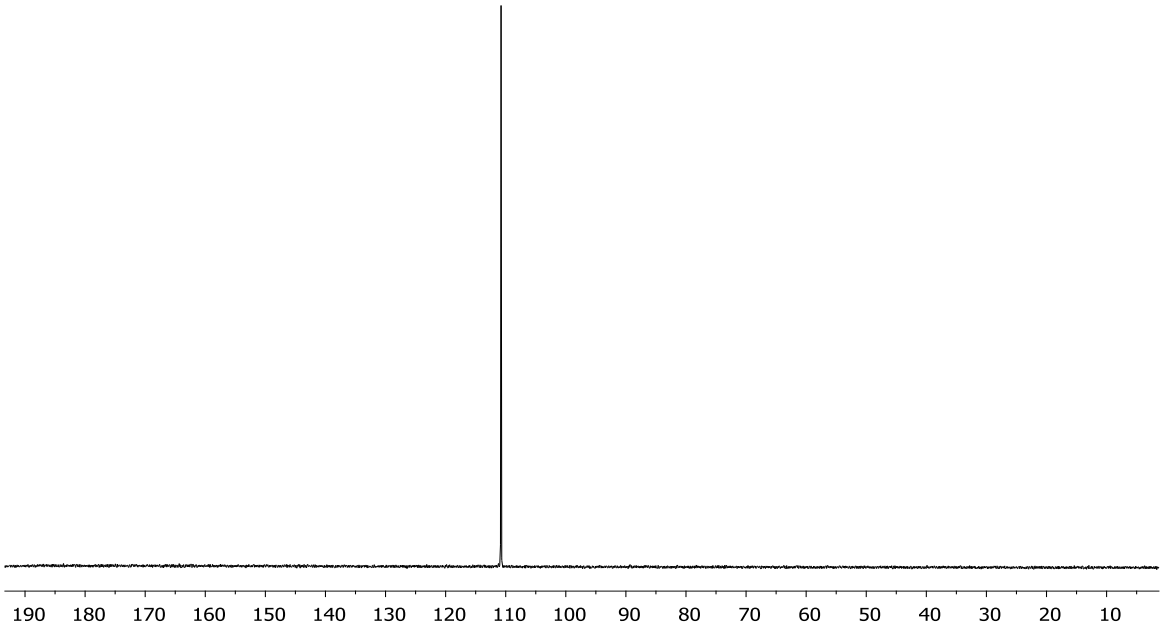

Spectrum A13: Bis(*P*,*P*-diphenyl)-*P*,*P*-1,3-phenylene ester, *meta*-$Ph_2POC_6H_4OPPh_2$, 8

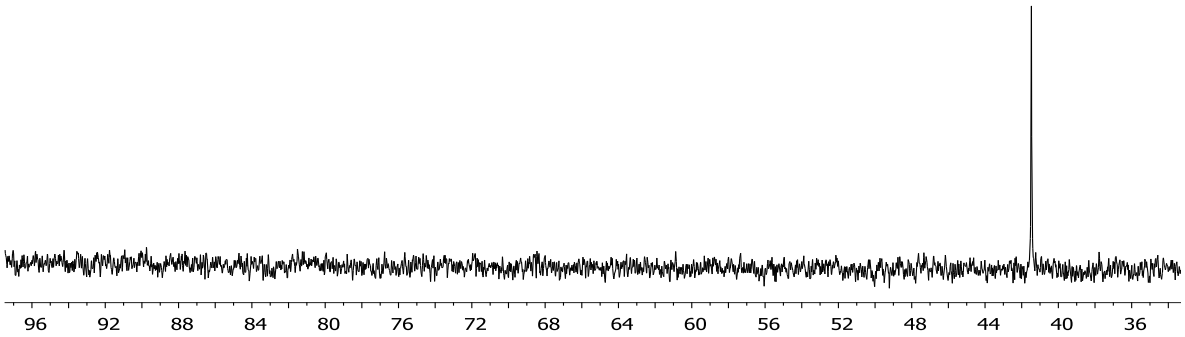

Spectrum A14: Diphenylphosphinothious acid, $C_6H_5SPPh_2$, 9

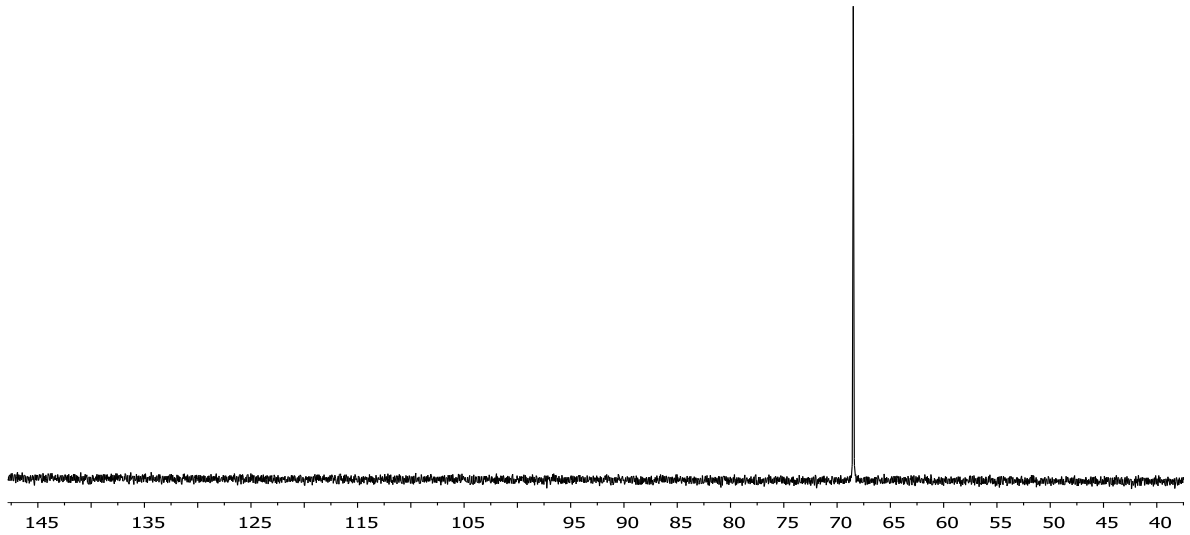

Spectrum A15: Diphenylphosphino amide $C_6H_5NHPPh_2$, 10

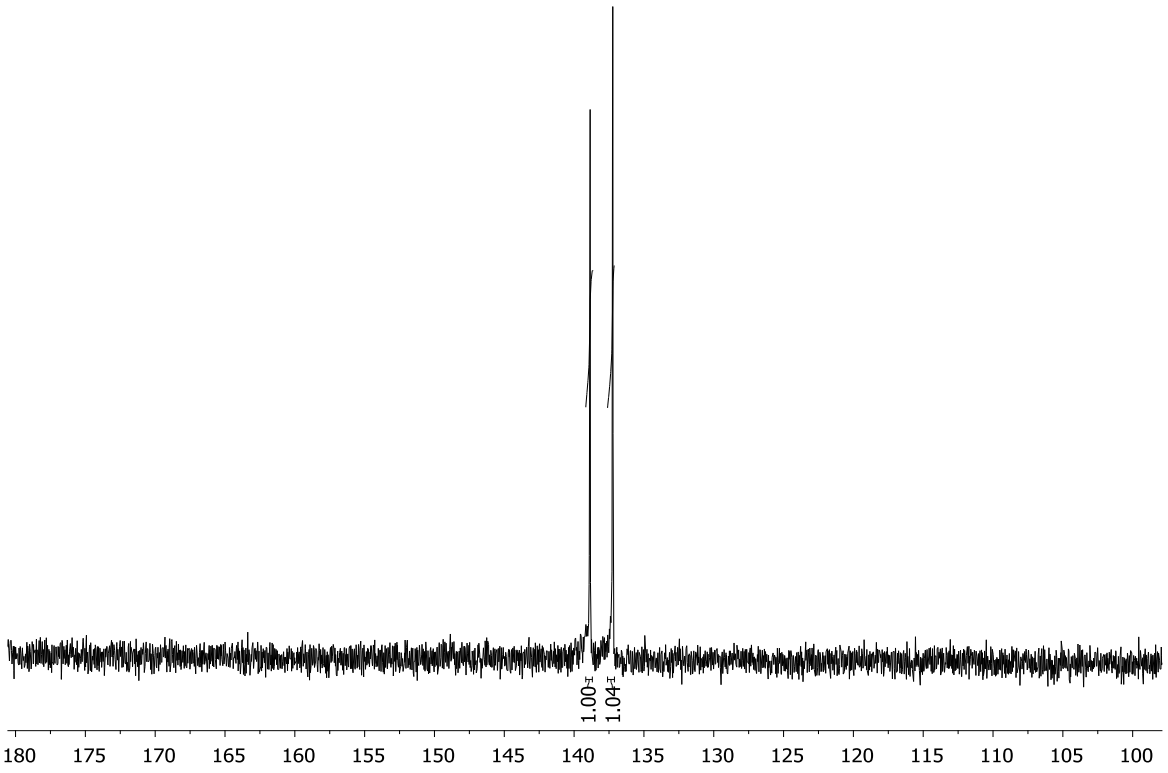

Spectrum A16: [Rh(acac)CO($C_6H_4OPPh_2$)], 11

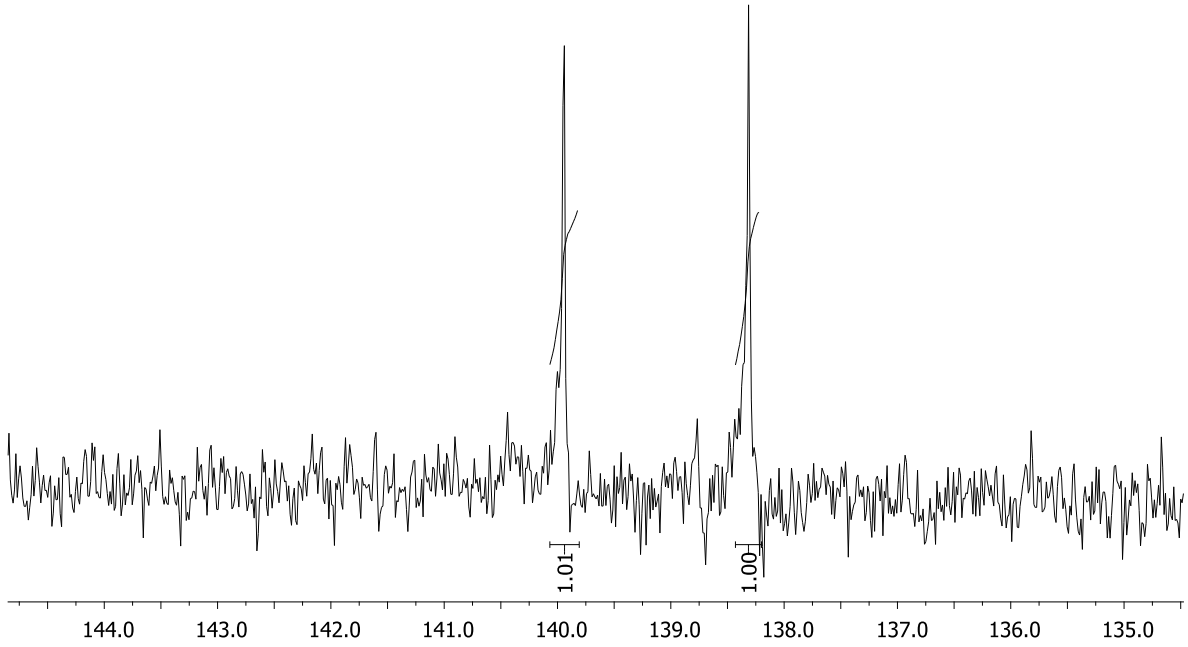

Spectrum A17: [(Rh(acac)CO(Ph_2POC6H_4-*p*-$OPPh_2$)], 12

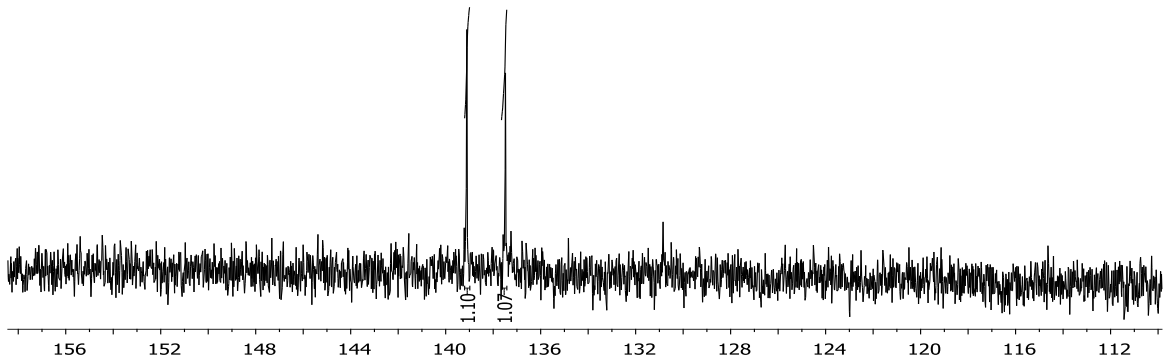

Spectrum A18: [(Rh(acac)CO($Ph_2POC_6H_4$-*m*-$OPPh_2$)], 13

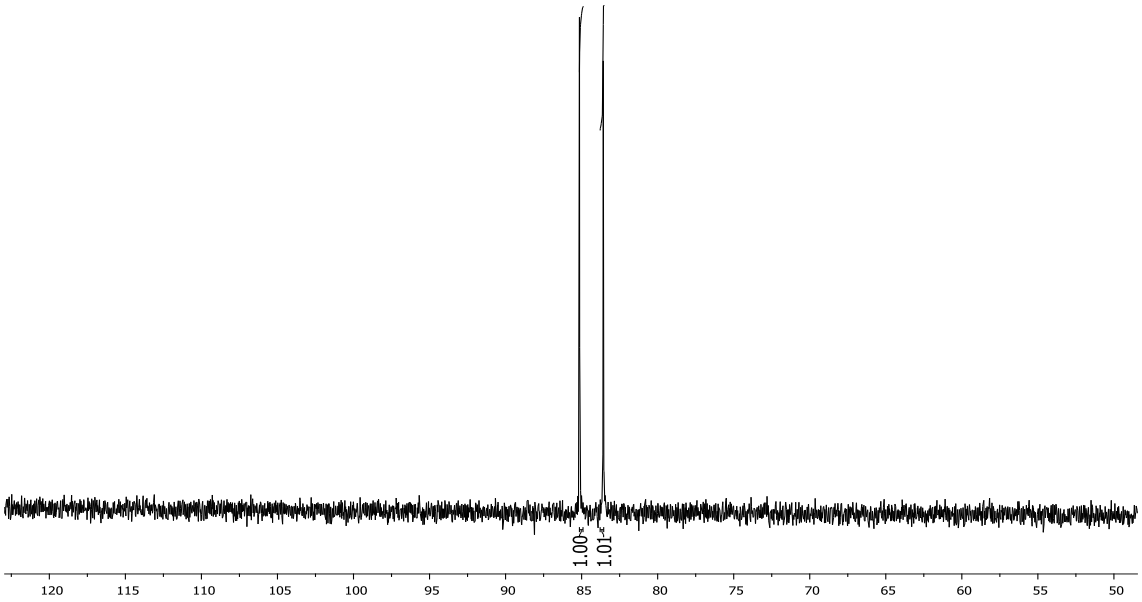

Spectrum A19: [Rh(acac)CO($C_6H_4SPPh_2$)], 14

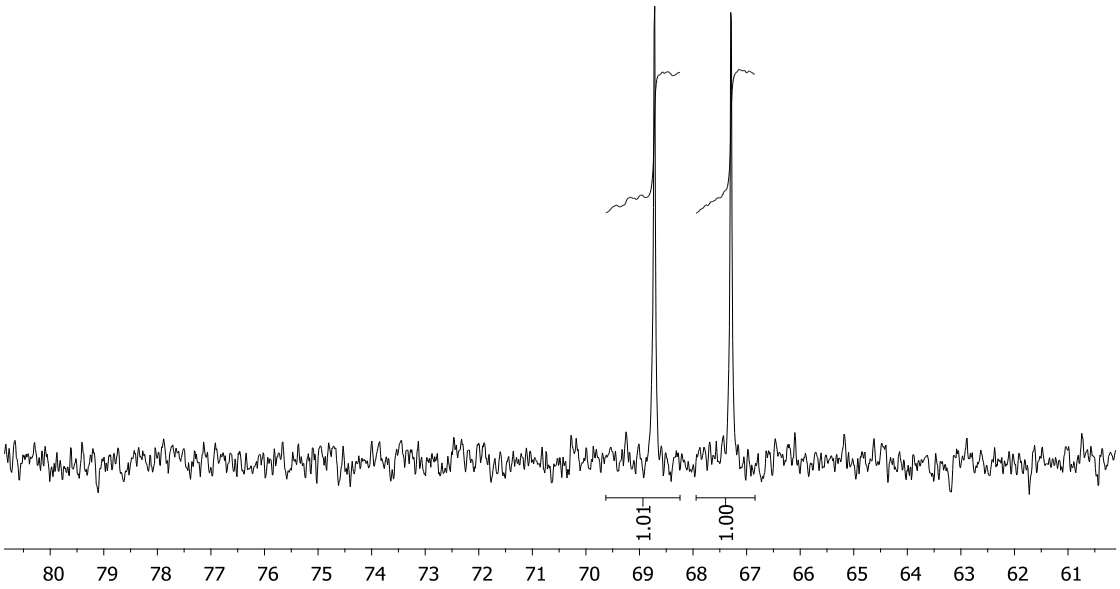

Spectrum A20: [Rh(acac)CO($C_6H_4NHPPh_2$)] 15

Abstract

Organophosphorus ligands of the type, $C_6H_5XPPh_2$, where X = O, S and NH, *meta*- and *para*-$Ph_2POC_6H_4OPPh_2$, were synthesised by the reaction between chlorophenylphosphine and the desired phenyl substituent in the presence of a base. The rhodium(I) complexess, [Rh(acac)CO($C_6H_4XPPh_2$)] where X = O, S and NH, as well as [(Rh(acac)CO($Ph_2POC_6H_4$-*m*-$OPPh_2$)] and [(Rh(acac)CO($Ph_2POC_6H_4$-*p*-$OPPh_2$)], were obtained by treating [Rh(acac)$(CO)_2$] with the appropriate organophosphorus ligands.

Kinetic results for the oxidative addition of methyl iodide to the rhodium(I) complexes of the type, [Rh(acac)CO($C_6H_4XPPh_2$)] where X = O, S and NH, revealed that the reaction exhibited only the oxidative addition. The reaction was found to be first order dependent on the concentration of the methyl iodide. The large negative activation entropy vales that were obtained, suggested an associative mechanism and no observable solvent pathway was found. It was found that as the Pauling electronegativity of O, S and N, increased, the first order rate constant of the oxidative addition decreased.

The cyclic voltammetry of the organophosphorus ligands, $C_6H_5XPPh_2$ where X = S and NH, *meta*- and *para*-$Ph_2POC_6H_4OPPh_2$, was found to be chemically and electrochemically irreversible. Only one oxidation and one reduction peak was observed and the oxidation peak was assigned to the one-electron oxidation of the free electron-pair on the phosphorous moiety, while the reduction peak was assigned to the reduction of the radical cation back to the neutral form.

The rhodium complexes to which the phosphorus ligand was bound, showed two oxidation peaks of which the first one, O1, was assigned to the rhodium metal center and the second, O2, to the phosphorus moiety. Similar to the ligands system, the rhodium complex system is both chemically and electrochemically irreversible. The reduction peaks (R1) and (R2) assigned reduction of the Rh(III) back to Rh(I) in a two electron process and the second reduction peak (R2), which is the reduction of the radical cation of the organophosphorus ligand back to the neutral form (with the free electron-pair on the phosphorous moiety), respectively.

***Keywords*:** Rhodium(I), phosphinites, oxidative addition, electrochemistry, organophosphorus ligands.

Opsomming

Organofosfaat ligande van die vorm, $C_6H_5XPPh_2$, waar X = O, S en NH, *meta*- en *para*-$Ph_2POC_6H_4OPPh_2$ is gesintetiseer deur die reaksie tussen chlorofenielfosfien en die gewenste feniel substituent in die teenwoordigheid van 'n basis. Die rodium (I) komplekse, [Rh(acac)CO($C_6H_4XPPh_2$)] waar X = O, S en NH, sowel as [(Rh(acac)CO($Ph_2POC_6H_4$-*m*-$OPPh_2$)] en [(Rh(acac)CO($Ph_2POC_6H_4$-*p*-$OPPh_2$)], is verkry deur die behandeling van [Rh(acac)$(CO)_2$] met die toepaslike organofosfaat ligande.

Kinetika resultate vir die oksidatiewe addisie van metiel jodied aan die rodium (I) komplekse van die formaat, [Rh(acac)CO($C_6H_4XPPh_2$)] waar X = O, S en NH, het aan die lig gebring dat die reaksie slegs oksidatiewe addisie ondergaan het. Daar is gevind dat die reaksie eerste orde afhanklikheid toon van die konsentrasie van die metiel jodied. Die groot negatiewe aktiverings entropie wat verkry is, stel 'n assosiatiewe meganisme voor en geen waarneembare oplosmiddel pad is gevind nie. Daar is gevind dat soos die Pauling elektronegatiwiteit van O, S en N, toegeneem het, die eerste orde tempo konstante van die oksidatiewe addisie afneem.

Die sikliese voltammetrie van die organofosfaat ligande, $C_6H_5XPPh_2$ waar X = S en NH, *meta*- en *para*-$Ph_2POC_6H_4OPPh_2$, toon aan dat hulle chemiese en elektrochemiese onomkeerbare redolsprosesse ondergaan. Slegs een oksidasie en een reduksie piek is waargeneem. Die oksidasie piek is aan die een-elektron oksidasie van die vrye elektron-paar op die fosfor groep toegeken, terwyl die reduksie piek aan die reduksie van die gesolveerde ontbinde radikaalkatioon toegeken kan word.

In die geval van die rodium komplekse is twee oksidasie pieke waargeneem waarvan die eerste een, O1, toegeskryf word aan die rodium metaal sentrum en die tweede, O2, aan die fosfor eenheid. Soortgelyk aan die ligande, was redolsprosesse van die rodium komplekse beide chemies en elektrochemies onomkeerbaar. Die reduksie piek R1 is toegeken aan die reduksie van ‘n Rh(III) spesie terug na Rh (I) in 'n twee-elektron oordrag proses en die tweede reduksie piek (R2) is die reduksie van die metal-gestabiliseerde radikaalkatioon van die organofosfaat ligand terug na die neutrale vorm (met die vrye elektron - paar op die fosfor eenheid), onderskeidelik.

Sleutelwoorde: Rodium (I), phosfinite, oksidatiewe addisie, elektrochemie, organofosfaat

I, Pholani Sakhile Manana, declare that the dissertation hereby submitted by me for the Magister Scientiae degree at the University of the Free State is my own independent work and has not previously been submitted by me at another university/facility. I therefore cede copyright of the dissertation in favour of the University of the Free State.

Signed Date